DEVELOPMENT OF CHROMATOGRAPHY-BASED PURIFICATION PROCESSES FOR CELL CULTURE-DERIVED INFLUENZA VIRUS PARTICLES

Dissertation

zur Erlangung des akademischen Grades

Doktoringenieur

(Dr.-Ing.)

Von Dipl. Biol (t.o.) Thomas Weigel

geb. am 19.02.1979

in Mülheim a.d. Ruhr

genehmigt durch die Fakultät für Verfahrens- und Systemtechnik
der Otto-von-Guericke-Universität Magdeburg

Promotionskommission: Prof. Dr.-Ing. Andreas Seidel-Morgenstern (Vorsitz)

Prof. Dr.-Ing. Udo Reichl (Gutachter)

Prof. Dr. Jürgen Hubbuch (Gutachter)

Dr. Egbert Müller (Gutachter)

eingereicht am: 27.08.2021

Promotionskolloquium am: 13.04.2022

Author rights

Most parts of this dissertation have been published as first author publications by the author (Weigel et al., 2014; Weigel et al., 2016; Weigel et al., 2019). It is confirmed that the usage of text passages, figures and diagrams of these three publications is in agreement with the publisher's guidelines. In addition, these publications are hereby fully acknowledged and text passages, figures and diagrams from these three publications are not further referenced in the following.

Index of content

Abbreviations

A/PR	virus strain A/Puerto Rico/8/34 (H1N1)
A/Wis	virus strain A/Wisconsin/67/2005, H3N2 (A/Wis)
AC	affinity chromatography
AEC	anion-exchange chromatography
B/Mal	virus strain B/Malaysia/2506/2004 (B/Mal)
BCA	bicinchoninic acid
bps	base pairs
BSA	bovine serum albumin
But	functional group: butyl
CAC	critical salt concentration inducing the formation of aggregates
Capto Core	Capto™ Core 700
Capto Q	HiTrap™ Capto™ Q
CDC	Centers for Disease Control and Prevention
CEC	cation-exchange chromatography
CFDA	Chinese Food and Drug Administration
CFZC	continuous flow zone centrifugation
CHO	Chinese hamster ovary
CIM-QA	convective interaction media® (monolith) – quaternary amine
CIP	cleaning-in-place
cond	conditioned
CV	column volume(s)
DBC	dynamic binding capacity
DEAE	HiTrap™ DEAE FF
dil	diluted
DLS	dynamic light scattering
DMEM	Dulbecco's minimal essential medium
DNA	deoxyribonucleic acid
DoE	design of experiments
dsDNA	double stranded deoxyribonucleic acid
DSP	downstream processing
EL	elution
ELISA	Enzyme-Linked Immunosorbent Assay

EMA	European Medicines Agency
Eth	functional group: ethyl
EV	extracellular vesicles
FCS	fetal calf serum
FDA	Food and Drug Administration
FPLC	fast protein liquid chromatography
FT	flow-through
GISRS	Global Influenza Surveillance and Response System
GMEM	Glasgow minimum essential medium
GMP	good manufacturing practice
HA	hemagglutinin
HAU	hemagglutination activity units (=HA-activity)
Hex	functional group: hexyl
HIC	hydrophobic interaction chromatography
I	ionic strength
IV	influenza virus
LCC	ligand-activated core chromatography
LOD	limit of detection
LOQ	limit of quantification
LRV	log reduction value
MDCK	Madin-Darby canine kidney
Me	functional group: methyl
$MgCl_2$	magnesium chloride
Min	minutes
MMC	mixed mode chromatography
MOI	multiplicity of infection
mRNA	messenger ribonucleic acid
MWCO	molecular weight cut-off
$(NH_4)_2SO_4$	ammonium sulfate
NA	neuraminidase
NaCl	sodium chloride
Na_2HPO_4/NaH_2PO_4	sodium phosphate
$Na_3C_6H_5O_7$	trisodium citrate
ND	not determined
NI	no information available

NS	non structural
PAGE	polyacrylamide gel electrophoresis
PBS	phosphate buffered saline
PEG	polyethylene glycol
PEI	Paul-Ehrlich-Institute
Ph. Eur.	European Pharmacopeia
Phe	functional group: phenyl
PicoGreen®	Quant-iT™ PicoGreen™
PPG	functional group: polypropylene glycol
PPRC	Pharmacopeia of the People's Republic of China
qPCR	quantitative real-time PCR (polymerase chain reaction)
RMPS	relative mean particle size
RNA	ribonucleic acid
RNP	ribonucleoprotein
rpm	revolutions per minute
RT	room temperature
SAM	self-amplifying mRNA
SBu	functional group: butyl ("SuperButyl": with smaller pore size)
SCM	sulfated cellulose membrane
SCMA	sulfated cellulose membrane adsorber
SD	standard deviation
SDS	sodium dodecyl sulfate
SEC	size-exclusion chromatography; unfunctionalized resin
sHTS	semi-high-throughput screening
SMB	simulated moving bed
SOP	standard operating procedure
SRID	single radial immunodiffusion (assay)
ssDNA	single stranded deoxyribonucleic acid
STMA	salt-tolerant membrane adsorber
SXC	steric exclusion chromatography
Threshold®	Threshold® Total DNA
TRIS	tris(hydroxymethyl)aminomethane buffer
UF	ultrafiltration
undil	undiluted
UV	ultraviolet

USP	upstream processing
VLPs	virus-like particles
WHO	World Health Organization
ZC	zonal centrifugation

Symbols

a_{HA}	hemagglutination activity (HA assay based) [kHAU/mL]
c_i	molar concentration of specific ion [M]
c_{in}	input concentration of virus particles or contaminant at a process step [kHAU/mL], [ng/mL] or [µg/mL]
c_{out}	output concentration of virus particles or contaminant at a process step [kHAU/mL], [ng/mL] or [µg/mL]
$DBC_{10\%}$	dynamic binding capacity at 10% breakthrough [kHAU/mL (resin)]
$DBC_{2\%}$	dynamic binding capacity at 2% breakthrough [µg (DNA)/mL (resin)]
DNA [%]	DNA recovery (based on PicoGreen®) [%]
DNA_{IN}	fraction of starting DNA concentration [%]
HA [%]	hemagglutinin recovery (based on SRID) [%]
HA [mg/mL]	hemagglutinin (based on SRID) [mg/mL]
hcDNA	host-cell DNA [ng/mL]
I	ionic strength [M]
IN	entering volume [mL] or concentration [kHAU/mL],[ng/mL] or [µg/mL] into step
LRV	log reduction value [-]
OUT	outgoing volume [mL] or concentration [kHAU/mL], [ng/mL] or [µg/mL] from step
protein [%]	total protein recovery [%]
U	activity units of nuclease Benzonase®
V_{in}	input volume of the process step [mL]
virus [%]	virus particle recovery (based on HA assay) [%]
V_{out}	output volume of the process step [mL]
z_i	charge number of specific ion

Abstract

The possibility to establish a chromatographic purification process for cell culture-derived influenza virus (IV) particles in the context of an influenza vaccine manufacturing process was tested here. The purification process was required to be as simple as possible but capable of achieving the required deoxyribonucleic acid (DNA) and protein contamination limits according to the European Pharmacopeia.

In total, three different purification processes were designed and tested, which were placed after the steps clarification and concentration at the beginning of the downstream process chain. Special focus was put on high virus yields in each step as well as on the depletion of DNA, the latter posing a significant challenge for most published processes, so far. In addition, IV strain dependency of the complete process or the process steps was tested using three different cell culture-derived IV strains (A/Puerto Rico/8/34, H1N1 (A/PR); A/Wisconsin/67/2005, H3N2 (A/Wis) and B/Malaysia/2506/2004 (B/Mal)). Furthermore, all three processes were tested for compliance with the requested limits of the European Pharmacopeia for cell culture-derived vaccines for human use.

The first process was designed as a completly flow-through based process in order to address the annual adaptation of multivalent influenza vaccines and emergence of new serotypes such as the bird flu H5N1. It avoids any virus-specific capture steps and reduces the requirement of specific elution buffers that potentially could have a negative impact on immunogenicity. At first, different anion-exchange chromatography (AEC) materials (strong and weak AEC) were tested regarding virus yields and DNA depletion. High virus yields (98–101% (of the column loaded virus material)) with DNA contents as low as 1.2% were achieved for the strong AEC. Additionally, a modern size-exclusion chromatography resin type with a ligand-activated core (ligand-activated core chromatography (LCC); Capto™ Core 700) was tested giving high virus yields of up to 94% and a residual total protein content as low as 37%. Furthermore, for a nuclease step the optimal concentration and the reaction endpoint were determined with 50 U/mL and about 13 h, respectively. Afterwards, a three-step process was established relying on the established AEC step, the nuclease step, and the LCC step. The complete process was tested with all three IV strains. It resulted in virus yields ≥68% with protein contamination levels fulfilling requirements of the European Pharmacopeia. DNA was depleted by ≥98.7% for all strains. The measured DNA concentrations per dose were close to the required limits of 10 ng DNA per dose set by the European Pharmacopeia. In subsequent experiments, detrimental effects of an added antibiotic as well as a suboptimal single radial

immunodiffusion (SRID) assay protocol causing an apparent virus yield decrease were found. The re-evaluation of the process data led to an estimated virus yield of ≥81% with a DNA content as low as 2.5–4.6 ng DNA per monovalent dose, which for two of the three tested IV strains complies with the limits of the European Pharmacopeia. In addition, it was shown that the added nuclease could be successfully removed by LCC from the product fraction.

The second process was set up as a completely membrane-based process in order to make full use of the high binding capacities, flow rates and productivities of membrane-based processes. In this context, a salt-tolerant membrane adsorber (STMA) was tested. As a starting point, a dual-salt strategy (with two polyvalent ions) was applied in a 96-well format screening for suitable STMA purification process conditions. After optimization at laboratory scale, a virus yield of up to 97% with a residual DNA level below 0.82% was achieved. In addition, the STMA was characterized regarding its dynamic binding capacity and the impact of flow rate on yields and contamination levels. Following, a process was established relying on only two unit operations. A pseudo-affinity membrane adsorber (sulfated cellulose; sulfated cellulose membranes adsorber (SCMA)) was applied for virus capture in a first chromatography step. The subsequent polishing step consisted of the STMA to bind residual DNA. For this presented process neither a buffer exchange step nor a nuclease step for further DNA digestion was required. Overall, the total virus yield for the tested influenza virus strain (A/PR) of this two-step membrane process was 75%, while the protein and the DNA contamination level could be reduced to 24% and at least to 0.5%, respectively. With 19.8 µg protein and 1.2 ng DNA per monovalent dose, this purity level complies with the limits of the European Pharmacopeia.

The third process was designed as an orthogonal process utilizing vastly different separation principles in order to achieve a high purity as well as a high adaptability of the process. At first, options for hydrophobic-interaction chromatography (HIC) for purification of influenza virus particles have been assessed using a 96-well-plate format in a semi-high-throughput approach. After optimization at laboratory scale, virus yields of up to 96% with a residual DNA level of about 1.3% were achieved. Based on this, a process relying on only two unit operations could be established. In a first process step, an AEC (using strong quaternary ammonium ligands) was applied for binding the DNA. Subsequently, HIC (with polypropylene glycol as functional group) was used to reversibly bind virus particles for capture and to remove residual contaminating DNA and proteins (flow-through). This two-step chromatographic process, which requires neither a buffer exchange step nor a nuclease step, resulted in a total virus particle yield for IV A/PR of 92%. The protein and the DNA contamination level could be reduced to 42% and at least to 1.0%, respectively. With 17.2 µg total protein and 2.0 ng

DNA per monovalent dose, this purity level complies with the limits of the European Pharmacopeia.

Overall, it could be shown for all three presented downstream processes that the required purity levels according to the European Pharmacopeia were achievable, while resulting in high virus yields. Therefore, they represent valuable alternatives to existing IV purification process schemes. Furthermore, the three processes only utilize off-the-shelf materials and represent simple as well as economic processes for IV particle purification. In particular, the flow-through process has the potential to serve as a simple, generic and economic platform technology for production of other cell culture-derived viruses and viral vectors.

Zusammenfassung

In dieser Arbeit wurde die Möglichkeit der Entwicklung eines chromatographischen Aufreinigungsprozesses für zellkulturbasierte Influenza-Viruspartikel im Rahmen eines Influenza-Impfstoff-Herstellungsprozesses untersucht. Der Aufreinigungsprozess sollte dabei so einfach wie möglich aber auch im Stande sein, die erforderlichen DNA- und Protein-Verunreinigungsgrenzwerte entsprechend dem Europäischen Arzneibuch zu erreichen.

Insgesamt wurden drei Aufreinigungsprozesse entwickelt und getestet, welche innerhalb der Produktaufarbeitungsprozesskette nach der Klärung und Konzentrierung lokalisiert sind. Besonderes Augenmerk wurde auf hohe Virusausbeuten in jedem Schritt als auch auf die Abreicherung der DNA gelegt, da Letzteres eine große Herausforderung für die meisten bislang publizierten Prozesse dargestellt hat. Darüber hinaus wurde die Influenza-Virusstamm-Abhängigkeit des gesamten Prozesses bzw. der Prozessschritte anhand von drei verschiedenen zellkulturbasierenden Virusstämmen (A/PR; A/Wis und B/Mal) überprüft. Auch wurden alle drei Prozesse bezüglich der Einhaltung der geforderten Grenzwerte des Europäischen Arzneibuches für zellkulturbasierte Impfstoffe zur humanen Verwendung geprüft.

Der erste Prozess war als ein vollständig durchflussbasierter Prozess konzipiert, um der jährlichen Anpassung von multivalenten Influenza-Impfstoffen und dem Auftreten neuer Serotypen wie der Vogelgrippe H5N1 Rechnung zu tragen. Er vermeidet jegliche virusspezifischen Anbindungsschritte und macht die Verwendung spezifischer Elutionspuffer obsolet, welche einen potenziellen negativen Effekt auf die Immunogenizität haben könnten. Zunächst wurden verschiedene Anionenaustauscher (AEC) Materialien (starke und schwache AEC) hinsichtlich der Virusausbeute und der DNA Abreicherung getestet. Mit dem starken Anionenaustauscher wurden hohe Virusausbeuten (98–101 % (des auf die Säule geladenen Virusmaterials)) mit DNA-Gehalten von bis zu 1,2 % erzielt. Darüber hinaus wurde ein moderner Größenausschluss-Chromatographie-Materialtyp mit einem liganden-aktivierten Kern (Liganden-aktivierter-Kern-Chromatographie (LCC); Capto™ Core 700) getestet. Er ergab hohe Virusausbeuten von bis zu 94 % und einen Restgesamtproteingehalt von bis zu 37 %. Des Weiteren wurden für einen Nuklease-Schritt die optimale Konzentration und der Reaktionsendpunkt mit 50 U/ml bzw. etwa 13 h ermittelt. Anschließend wurde ein dreischrittiger Prozess basierend auf dem etablierten AEC-, Nuklease- und LCC-Schritt aufgestellt. Der vollständige Prozess wurde jeweils mit allen drei Influenza-Virusstämmen getestet. Er lieferte Virusausbeuten ≥68 % zusammen mit Proteinverunreinigungswerten, welche die Anforderungen des Europäischen Arzneibuches erfüllten. Die DNA wurde für alle

Virusstämme um ≥98,7 % abgereichert. Die gemessene DNA-Konzentration pro Dosis lag nahe an dem vom Europäischen Arzneibuch geforderten Grenzwert von 10 ng DNA pro Dosis. In nachfolgenden Experimenten konnten sich nachteilig auswirkende Effekte des zugesetzten Antibiotikums als auch eines suboptimalen SRID Nachweisverfahrensprotokolls nachgewiesen werden, die zu einer scheinbaren Verringerung der Virusausbeute geführt hatten. Eine erneute Evaluierung der Prozessdaten führte zu einer geschätzten Virusausbeute von ≥81 % mit einen DNA-Gehalt von bis zu ≥2,5 ng DNA pro monovalenter Dosis, was für zwei der drei getesteten Stämme die Grenzwerte des Europäischen Arzneibuches erfüllte. Des Weiteren konnte gezeigt werden, dass die zugesetzte Nuklease erfolgreich durch die LCC aus der Produktfraktion entfernt werden konnte.

Der zweite Prozess war als vollständig membranbasierter Prozess ausgelegt, um die hohen Bindungskapazitäten, Flussraten und Produktivitäten von membranbasierten Verfahren im vollen Umfang auszunutzen. In diesem Zusammenhang wurde ein salztoleranter Membranadsorber (STMA) eingesetzt. Als Ausgangspunkt wurde eine duale Salzstrategie (mit zwei polyvalenten Ionen) in einem 96-Well-Screeningformat im Hinblick auf geeignete STMA Prozess-/Aufreinigungsbedingungen getestet. Nach Optimierung im Labormaßstab wurden eine Virusausbeute von bis zu 97 % und ein DNA-Restgehalt von unter 0,82 % erreicht. Darüber hinaus wurde der STMA hinsichtlich seiner dynamischen Bindungskapazität und dem Einfluss der Flussrate auf die Virusausbeute und den Verunreinigungsgehalt charakterisiert. Anschließend wurde ein Prozess etabliert, welcher lediglich aus zwei Operationseinheiten bestand. Ein Pseudoaffinitäts-Membranadsorber (sulfatisierte Zellulose; Sulfatisierte-Zellulose-Membranadsorber (SCMA)) diente zur Viruspartikelanbindung in einem ersten Chromatographieschritt. Der nachfolgende Feinreinigungsschritt bestand aus dem STMA zur Anbindung der restlichen DNA. Für diesen Prozess waren weder ein Pufferaustauschzwischenschritt noch ein Nuklease-Schritt zwecks weiteren DNA-Verdaus erforderlich. Insgesamt betrug die Virusgesamtausbeute beim getesteten Influenza-Virusstamm (A/PR) für den Zwei-Schritt-Membranprozess 75 %, während die Protein- und DNA-Verunreinigung auf 24 % bzw. mindestens 0,5 % reduziert werden konnte. Mit 19,8 µg Protein und 1,2 ng DNA pro monovalente Dosis erfüllt der Reinheitsgrad die Grenzwerte des Europäischen Arzneibuches.

Der dritte Prozess war als orthogonaler Prozess konzipiert, bei dem gänzlich unterschiedliche Aufreinigungsprinzipien zum Einsatz kamen, um eine hohe Reinheit und eine hohe Anpassungsfähigkeit des Prozesses zu erreichen. Zunächst wurden verschiedene Optionen der Hydrophoben-Interaktions-Chromatographie (HIC) zur Aufreinigung von Influenza-

Viruspartikeln mittels eines 96-Well-Platten-Formats in einem Semi-Hochdurchsatz-Ansatz untersucht. Nach Optimierung im Labormaßstab wurden Virusausbeuten von bis zu 96 % mit einem Rest-DNA-Gehalt von ungefähr 1,3 % erzielt. Basierend darauf konnte ein Prozess bestehend aus lediglich zwei Operationseinheiten etabliert werden. Im ersten Prozessschritt wurde ein Anionenaustauscher (mit starken quartären Ammonium-Liganden) zur DNA-Anbindung eingesetzt. Darauf folgend wurde die HIC (mit Polypropylenglykol als funktionelle Gruppe) zur reversiblen Viruspartikelanbindung und zur Entfernung der restlichen verunreinigenden DNA und Proteine (Durchfluss) verwendet. Dieser Zwei-Schritt-Chromatographie-Prozess, welcher weder einen Pufferaustausch- noch einen Nuklease-Schritt benötigt, erzielte für das Influenza-Virus A/PR eine Viruspartikelausbeute von 92 %. Der Protein- und DNA-Verunreinigungsgrad konnte auf 42 % bzw. mindestens 1,0 % reduziert werden. Mit 17,2 µg Gesamtproteingehalt und 2,0 ng DNA-Gehalt pro monovalenter Dosis erfüllt der Reinheitsgrad die Grenzwerte des Europäischen Arzneibuches.

Insgesamt konnte für alle drei vorgestellten Aufreinigungsprozesse gezeigt werden, dass die erforderlichen Reinheiten gemäß dem Europäischen Arzneibuch zusammen mit hohen Virusausbeuten erreichbar sind. Somit bilden sie wertvolle Alternativen zu bestehenden Influenza-Virus-Aufreinigungsprozess-Entwürfen. Des Weiteren verwenden alle drei Prozesse ausschließlich marktverfügbare Materialien und stellen sowohl einfache als auch ökonomische Prozesse zur Influenza-Viruspartikel-Aufreinigung dar. Insbesondere besitzt der Durchflussprozess das Potenzial, als einfache, generische und ökonomische Plattformtechnologie zur Produktion von anderen zellkulturbasierten Viren und viralen Vektoren zu fungieren.

1 Introduction and Objectives

Influenza virus (IV), the cause for seasonal epidemics (seasonal flu) and pandemic outbreaks (bird or swine flu), still remains a threat to mankind in the 21st century – in particular to infants and people of older age (Matthews, 2006). Especially, the high variability of the virus poses a problem. Both IV A and B lack a proof-reading activity during replication. Therefore, mutations occur in the HA (hemagglutinin) and NA (neuraminidase), which lead to antigenic drift. Over time, this results in an escape from the immune responses. Also, antigenic shifts occur through re-assortment resulting from a gene segment exchange between two or more strains, yielding a new subtype (Rajao et al., 2018).

Vaccination is still the most efficient measure to protect against IV infections (Nichol, 2008; WHO, 2021). Although the worldwide vaccine production capacity of about 1.5 billion doses per year for seasonal flu epidemics and 4.15–8.31 billion doses for potential pandemics should be sufficient, manufacturing processes still have significant limitations by mostly relying on egg-based production of the virus particles (McLean et al., 2016; Sparrow et al., 2021). Being still one of the most cost-effective production methods, egg-based production processes account for more than 80% of the market. As an alternative, cell culture-based influenza vaccines have been developed and licensed for many years as this technology has (1) a shorter lead time than the traditional approach, (2) allows to overcome potential capacity limitations in case of avian flu outbreaks affecting the availability of embryonated eggs, and (3) reduces the risk of sterility problems as all process steps can be performed in a completely aseptic environment (World Health Organization (1995) and A. M. Palache et al. (1997); Brands et al. (1999); Kistner et al. (1999); Tree et al. (2001); Voeten et al. (1999); Manini et al. (2017)). Since 2009, first cell culture-derived influenza vaccines have been commercially available. In addition, in 2013, the first recombinant influenza vaccine produced with insect cells was licensed in USA (M. M. Cox et al., 2011; FDA, 2013).

Introduction of new production methods, primarily utilizing continuous cell lines (i.e. immortal cell lines; closely related to cancer cells) from animals for virus particle production also involves significant challenges in downstream processing to comply with stringent specifications set by regulatory authorities and often resembles a bottleneck (Wolff et al., 2008; Gottschalk, 2013). Furthermore, there is a trend towards quadrivalent influenza vaccines requiring additional production capacities (Ray et al., 2017; Pérez Rubio et al., 2018). However, the high variability and diversity of IV renders the purification of IV in combination with the high purity demands a difficult task for downstream processing (DSP) of cell culture-based

influenza vaccines. Often, the same traditional downstream methods that are applied for traditional egg-based manufacturing are also used for cell culture-based manufacturing processes, just slightly modified. To this day, density gradient centrifugation with its drawbacks of being a laborious and difficult to scale-up technique is still applied in industry for IV purification (Reimer et al., 1967; Nestola et al., 2015). Meanwhile, chromatography processes have emerged as alternative tools for vaccine purification. They are cost-effective and scalable, providing high selectivity and usually apply moderate buffers. In addition, investment costs are low and the process setup is flexible. Finally, the product is not exposed to high shear stress (Präve et al., 1994).

At the beginning of this PhD project, previous attempts in the research community had not resulted in the establishment of a chromatography-based IV purification process for cell culture-derived IV particles capable of achieving the required contamination limits set by the European Pharmacopoeia. Consequently, the goal of this PhD thesis was the development of a working chromatography-based purification process capable of achieving deoxyribonucleic acid (DNA) and total protein contamination levels in agreement with the European Pharmacopeia. The scope was therefore directed towards the chromatographic purification steps in the DSP with the focus set on high yields, low DNA and total protein content levels. Also, the processes had to be transferable to industrial manufacturing processes. Therefore, the use of expensive special chromatographic materials or potentially toxic compounts should be avoided. Moreover, the purification chain was required to be set up as efficiently as possible, avoiding unnecessary steps (e.g., buffer exchanges).

Hence, new chromatography steps had to be established. Based on these requirements, three different chromatography downstream processes were designed and tested. Furthermore, multiple virus strains were used for testing, if required. In order to be able to compare the performance of the downstream processes with previously established chromatography methods for purification of IV vaccines in the research group, also serum-containing medium was used for the upstream process.

2 Theory and Background

2.1 Influenza virus and disease

IV belongs to the Orthomyxo viruses. It is membrane enveloped and contains a negative sense, single-stranded ribonucleic acid (RNA) genome (Figure 1). The genome consists of eight segments. IVs can be divided into four types: A, B, C and D, depending on their major antigenic differences. Influenza A virus (IV A) is further classified based on the antigenic properties of the viral surface glycoproteins hemagglutinin (HA) and neuraminidase (NA). While IV A and B are responsible for the annual human epidemics, IV A can be considered as the most relevant IV (Manini et al., 2017). IV C is known to infect humans and pigs, while causing usually milder symptoms in humans (Carroll et al., 2016; Thielen et al., 2018). IV D viruses primarily affect cattle and are not known to infect or cause illness in humans (WHO, 2021).

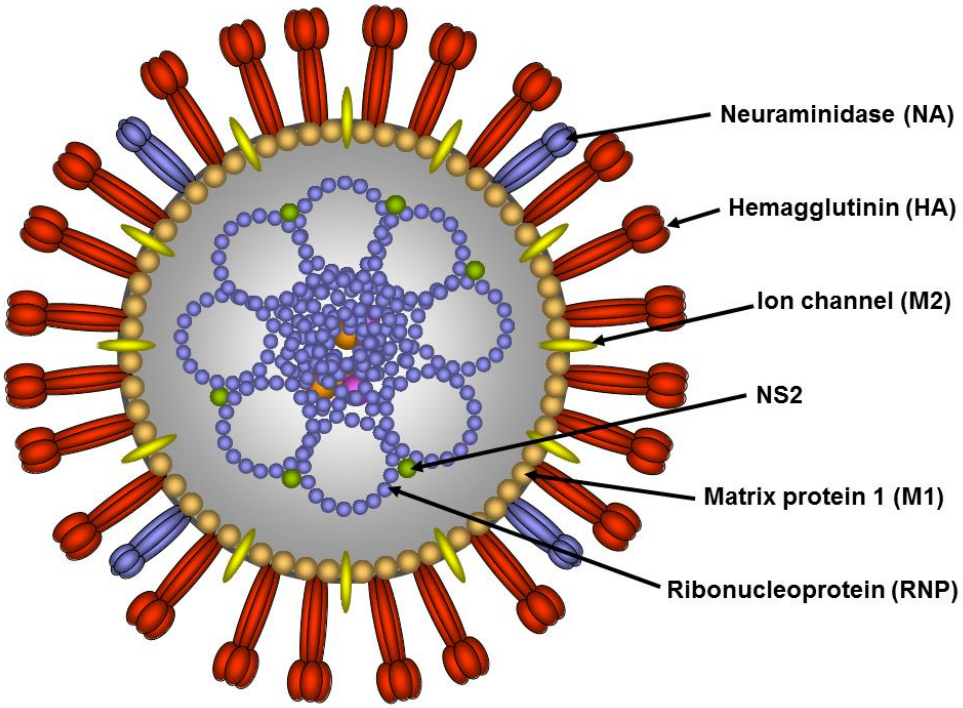

Figure 1: Schematic representation of an influenza A virus particle. Shown is a cross section of the IV particle with the viral proteins. NS2: nonstructural 2 protein. (With kind permission of Prof. M. Wolff, Institute of Bioprocess Engineering and Pharmaceutical Technology, Technische Hochschule Mittelhessen, Giessen, Germany).

So far, for IV A 18 HA (H1 to H18) and 11 NA (N1 to N11) subtypes have been identified, which can be further subdivided into two groups, which comprise different clades (Medina et al., 2011; P. S. Lee et al., 2015). Of the possible combinations, currently only H1N1 and H3N2 subtypes circulate in the human population (Rajao et al., 2018). Furthermore, H1 and H3 subtypes do circulate in various animals.

For IV B only a single subtype has been identified, which can be further subdivided into two antigenetically distinguishable virus lineages, B/Yamagata and B/Victoria, currently circulating (Wong et al., 2013a; Vijaykrishna et al., 2015; Kumar et al., 2018). Unlike IV A, IV B is usually restricted to humans and does therefore not pose a significant pandemic threat. Also, the mutation rate is lower than for IV A (Hay et al., 2001). Besides the proteins present in the IV A, a neuraminidase region B protein is located in the virus particle membrane of IV B virions (Rajao et al., 2018).

The HA and NA proteins are glycoproteins located at the surface of the influenza particles. The HA protein is a homo-trimer and responsible for receptor binding and fusion (Fields et al., 2007). During infection, it binds to the sialic acid residues of the epithelial cell surface (Wilks et al., 2012). It consists of a highly variable globular domain, responsible for the different HA-subtypes, and a conserved stalk domain (Kumar et al., 2018).

The NA protein is a homo-tetramer and relevant for different infection stages, such as the release of new virus particles from the host cell and the prevention of aggregation by cleavage of sialic acids from the mucin in the respiratory tract (Matrosovich et al., 2004; Moscona, 2005; Sylte et al., 2009).

Sialic acids are a rather diverse family of monosaccharides with a nine-carbon-backbone of various arrangements (branched and unbranched) and a variety of associated chemical groups. They are typically located at the end of glycan chains, which are an ubiquitous cell surface feature (Wilks et al., 2012).

Worldwide, seasonal epidemics are estimated to result in about three to five million cases of severe illness, and about 290,000 to 650,000 respiratory deaths (WHO, 2021). The annual attack rate is estimated to be 20–30% for children and 5–10% for adults (Manini et al., 2017). It is estimated that in developing countries 99% of deaths in children under five years of age are due to influenza related lower respiratory tract infections (Nair et al., 2011). According to the Centers for Disease Control and Prevention (CDC) the number of flu deaths in USA for the 2019/2020 season can be estimated with 22,000 (CDC, 2021).

IV constantly evolves through genome mutation (antigenetic drift) and re-assortment (antigenetic shift). This, together with the uncontrollable stock of wild hosts (e.g. wild water birds), makes the IV resistant to eradication due to continuous creation of new variants. In particular, pandemic outbreaks due to antigenic shift (caused by re-assortment of the segmented virus genome due to direct interspecies transmission or due to segment exchanges between two IVs infecting the same human) represent a high risk to humankind causing millions of deaths. Their threat lies in atypical clinical symptoms (including a high mortality) affecting also otherwise healthy people. Most infected by the Spanish flu have been people with 20–40 years of age. The Spanish flu alone caused 50–100 million deaths between 1918 and 1920 (Taubenberger et al., 2006). In comparison, the total number of deaths during the Second World War between 1939–1945 is estimated with 74.3 million dead soldiers and civilians worldwide ("Research Starters: Worldwide Deaths in World War II," 2021). It is assumed that since the 16th century at least 13 influenza pandemic outbreaks have struck the human population. The most recent IV pandemics in human history have been the “Spanish flu” (1918, caused by the H1N1 subtype), the “Asian flu” (1957, caused by H2N2), the “Hong Kong flu” (1968, caused by H3N2), the “Russian flu” (1977, caused by H1N1), and the “swine flu” (2009, caused by H1N1) (Rajao et al., 2018), which were caused by IVs with gene segments of animal origin (Taubenberger et al., 2009). Furthermore, besides the risk for humans, the financial damage attributed to animal influenza pandemics amounts to billions of dollars.

With the damage caused by the seasonal as well as by the pandemic influenza, a worldwide functioning vaccination strategy is of utmost importance, especially considering the effects of globalization.

2.2 Influenza vaccines

IV vaccines are the most widely used vaccines in the world (A. Palache et al., 2017). Inactivated influenza vaccines or live-attenuated influenza vaccines are still the most dominant vaccine types. They consist of a set of IV strains selected and suggested by the World Health Organization (WHO) every year based on the data of the Global Influenza Surveillance and Response System (GISRS) of the WHO. The strain selection process is based on antigenic data from ferret antisera, paired with serologic analysis of human samples, as well as virological surveillance data. In general, each vaccine strain is required to be updated every 2–3 years, leading to at least one strain update each year and therefore an annually altered vaccine (Rajao et al., 2018).

Currently, two influenza A subtypes (A/H1N1 and A/H3N2) and two influenza B lineages circulate worldwide each year (Ray et al., 2017). Although, the viral surface glycoproteins (HA and NA) lead to a strong humoral immune response, it is usually strain and subtype specific due to limited T-cell mediated immune response (R. J. Cox et al., 1999; Hoft et al., 2017; Saletti et al., 2018; Sycheva et al., 2018). Therefore, the vaccine effectiveness can vary strongly depending on the strain match each year as well as the patient (in particular the age). According to the US Flu Vaccine Effectiveness Network (coordinated by the CDC) the overall, adjusted vaccine effectiveness for influenza seasons from 2005-2016 can been estimated with 10–60% (Rajao et al., 2018).

So far, trivalent influenza vaccines, containing two influenza A strains and one influenza B strain, have been dominated the market. But it can be expected that they are soon going to be completely substituted by quadrivalent vaccines (containing the two influenza B virus lineages circulating globally) in many countries due to the limited cross-protection between both lineages (Ambrose et al., 2012; Ray et al., 2017; Pérez Rubio et al., 2018).

Three vaccine types have been approved by the Food and Drug Administration (FDA) for use in the human population so far: (1) inactivated influenza vaccines, (2) live attenuated influenza vaccines and (3) recombinant viral HA proteins (subunit vaccine) (Barberis et al., 2016). Among these, inactivated IV vaccines (split virus and virus subunit) are the most common vaccines due to their long manufacturing history, low production costs, and safety as well as effectiveness to a certain extend (Rajao et al., 2018; Blanco-Lobo et al., 2019). The virus particle related vaccines can be classified as shown in Figure 2. Additionally, nucleic acid vaccines represent an independent approach.

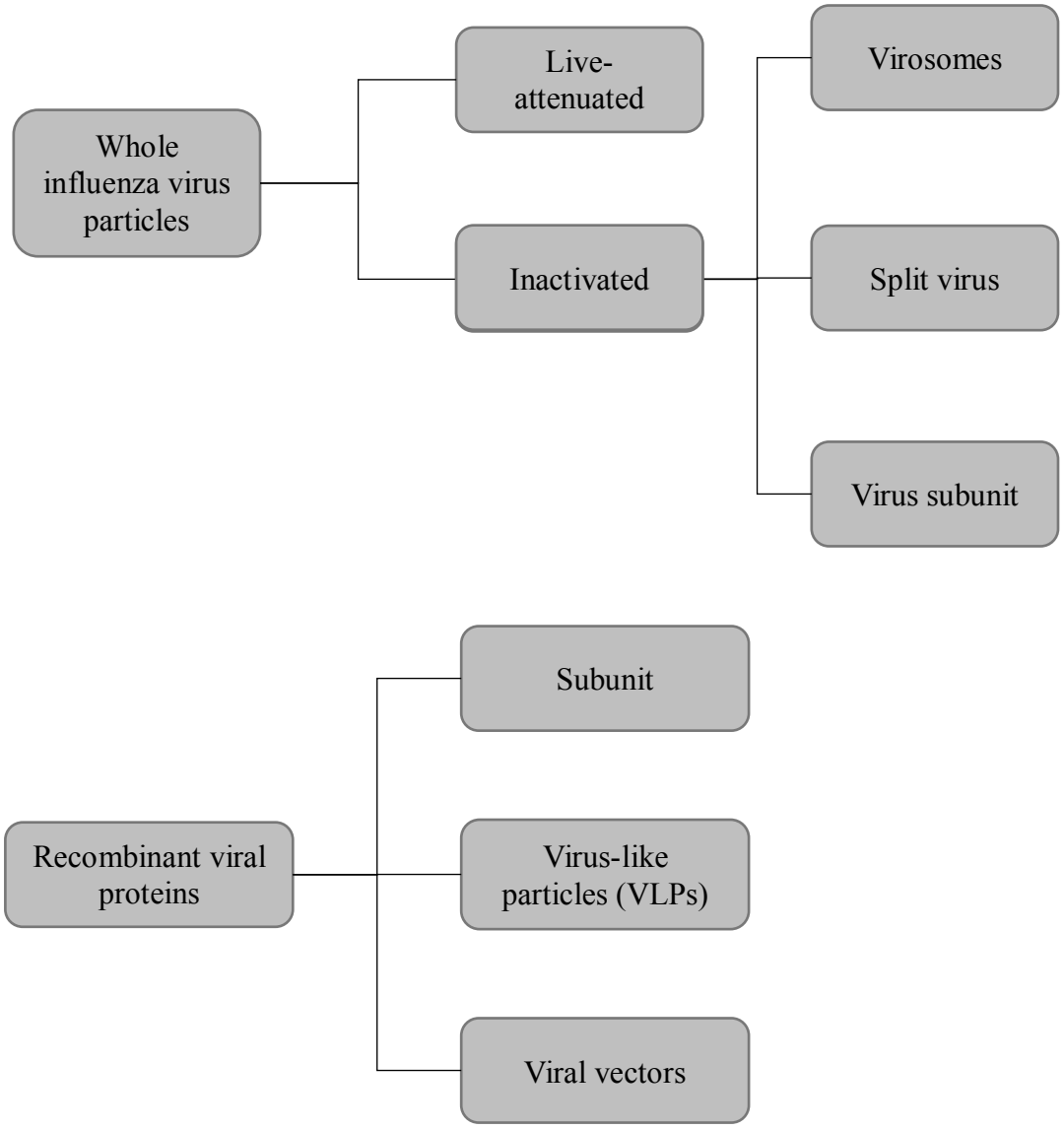

Figure 2: Classification scheme for different influenza vaccines. Classification based on the immunogenic active component of vaccine.

Inactivated whole IV vaccines have the advantage of low production costs. In general, these are prepared by inactivating the IV particles using chemicals (e.g., formalin or β-propiolactone) (Ellebedy et al., 2016; Sabbaghi et al., 2019). In fact, most conventional vaccine types (e.g. live-attenuated, split virus, etc.) originate process-wise from purified whole IV particles. The antibody response is typically influenza type specific. However, it can show high cross-reactivity resulting in cross-protection towards earlier and newer viral strains (Brokstad et al., 1995; Osterholm et al., 2012). Although showing a robust immunogenicity because of multiple pathogen-associated molecular patterns, due to association with side-effects in humans the

direct usage as vaccine is mostly limited to veterinary use (Beyer et al., 1998; Thacker et al., 2008; Ellebedy et al., 2016; Keshavarz et al., 2019). Hence, they play an important role in reducing the number of influenza infected pigs and poultry. Thus, the potential risk for antigenetic shift by interspecies transmission and thereby the risk for a pandemic is reduced (Thacker et al., 2008).

Virosomes, as well as virus-like particles (VLPs), are non-infectious particles which are devoid of genetic material, consisting mostly of protein multimers and the viral envelope. In particular, VLPs often display a high density of viral surface proteins, which might contribute to their frequently observed increased immunogenicity (Ellebedy et al., 2016). While structural and functional properties of virosomes and VLPs are mostly similar, they are characterized by their manufacturing methods: virosomes are assembled in vitro from lipids and viral envelope, while VLPs make use of an expression system and the self-assembly properties of viral components (Moser et al., 2013; Wong et al., 2013b).

Split and subunit IV vaccines are the most common IV vaccines. They are considered to have comparable immunogenicity but a reduced reactogenicity compared to whole IV vaccines (Wong et al., 2013b). They also seem to cause fewer local reactions upon injection (Agarwal et al., 2011). Split IV vaccines are produced by fragmentation of whole virus particles using mostly organic solvents (e.g., diethyl ether) or detergents (e.g., ammonium deoxycholate) in order to dissociate the viral lipid envelope, exposing all viral proteins (Laver et al., 1976). They contain mostly structural proteins (usually in changed proportions) and some lipids. In subunit IV vaccines additional purification steps are used to remove the nucleocapsid, the RNA and the lipids leaving mostly the surface viral proteins HA and/or NA.

In contrast to the above mentioned vaccines, live-attenuated IV vaccines employ deficient non-pathogenic IV particles, which can only replicate poorly in the human body. Attenuation is achieved by cold-adaptation, NS1 truncation, elastase-dependence, or rearranging the genome (Rajao et al., 2018). Live-attenuated IV vaccines induce wider and more robust immune responses including cellular and humoral responses in the mucosa, which is similar to a natural viral infection (Forrest et al., 2008; Hoft et al., 2011; Mohn et al., 2016). Most importantly, they can also provide immunity against heterosubtypic strains, including pandemic IVs (Blanco-Lobo et al., 2019). But the effectiveness of the live-attenuated IV vaccine varied over the last years with altered recommendations regarding the vaccine type (Grohskopf et al., 2018a), leading to the current opinion at the WHO, that none of the above mentioned vaccine types receives a preference (Grohskopf et al., 2018b; Blanco-Lobo et al., 2019).

Recombinant viral protein vaccines are characterized by using selected viral proteins as antigens and often making use of a different expression system. Usually they contain the main surface proteins (e.g., HA protein). They can be classified based on the presentation of the viral protein. They are considered as save and usually induce a humoral and cellular response. On the other hand, they often require appropriate adjuvants in order to compensate for the usually lower immunogenicity (Keshavarz et al., 2019).

Viral vector vaccines use not-influenza-related modified non-pathogenic viruses (replication-defective as well as replication-competent), such as adenovirus, poxvirus, or alphavirus, to express the IV antigens of interest (e.g., HA protein) in the (mostly) native state. Cell culture based production makes viral vectors an interesting alternative to other vaccine types.

Nucleic acid vaccines can be divided into DNA and RNA vaccines. Nucleic acid sequences encoding the antigen are delivered to the cells by using deficient non-pathogenic viral particles competent for entry in host cell, formulation with lipids or emulsions, or electroporation (Ulmer et al., 2012; Kumar et al., 2018). While the DNA requires to enter the cell nucleus making the delivery of the DNA to the designated cell location difficult, reaching the cell cytoplasm is sufficient for RNA vaccines to be translated (Rao et al., 2006; Saade et al., 2012). Currently, two different RNA vaccine-types are under development (but not yet approved): conventional non-amplifying mRNA (messenger ribonucleic acid) vaccines and self-amplifying mRNA (SAM) vaccines (Deering et al., 2014; Kumar et al., 2018). However, mRNA vaccines still raise safety-issues as seen with the Covid-19 vaccine of BioNTech. Also, the well-known instability of free mRNA and the required high amounts of synthetic mRNA material per dose (in case of non-amplifying mRNA) might limit the accessibility of vaccine in case of a pandemic (Keshavarz et al., 2019).

Besides the above mentioned mostly IV strain-specific vaccine approaches for the seasonal epidemics, new vaccine types (called “universal influenza vaccines”) are under development, which shall provide cross protection against all/most subtypes of IV, omitting the need for the vaccine adaptation each year (Keshavarz et al., 2019). They generally use the concept of inducing immune responses against conserved viral epitopes. Here, different approaches such as VLPs consisting of protein mixtures of different subtypes, chimeric antigens consisting of different subtypes, induction of cross-protective antibodies using designed highly reactive antigens, recombinant antibodies or induction of immune response towards more conserved viral proteins (e.g., NA, M2, NP, M1), polyvalent DNA vaccines, conventional non-amplifying

and self-amplifying mRNA vaccines and viral vectors are currently investigated (Kumar et al., 2018; Rajao et al., 2018).

Table 1 shows some of the approved vaccines sorted by vaccine type. As can be seen, the pharmaceutical industry is still mostly relying on split and subunits vaccines based on inactivated egg-derived IV particles. Often the downstream processes are not disclosed.

Table 1: Approved influenza vaccines for humans in USA and/or Europe. The monovalent strain products are marketed as pandemic influenza vaccines. Data comprised from the following resources: (Ellebedy et al., 2016; ECDC, 2018; FDA, 2018; Kumar et al., 2018; PEI, 2018, 2019)

Vaccine type	Trade name	Company	Production system	Primary purification method	Number of strains	Remarks
Whole virus						
- **Inactivated**	Daronrix	GlaxoSmithKline	Eggs	NI	1	
- **Live attenuated**	FluMist	MedImmune	Eggs	Centrifugation	3,4	
	Fluenz Tetra	Astra Zeneca	Eggs	NI	4	
	Pandemic influenza vaccine H5N1	Astra Zeneca	NI	NI	1	
Virosomes	Inflexal V	Crucell	Eggs	NI	3	
Split virus	Afluria	Seqirus/ Pfizer/ CSL	Eggs	Centrifugation (CFZC)	3	
	FluLaval	ID Biomedical	Eggs	Centrifugation	3,4	
	Fluarix (Alpahrix, Infflusplit)	GlaxoSmithKline	Eggs	Centrifugation (ZC)	3,4	
	Fluzone	Sanofi Pasteur	Eggs	Centrifugation (CFZC)	3,4	
	Vaxigrip	Sanofi Pasteur	Eggs	NI	3,4	
	IV vaccine H5N1	Sanofi Pasteur	Eggs	Centrifugation (CFZC)	1	
	Influenza A (H5N1)	ID Biomedical	Eggs	Centrifugation	1	
	Pandemrix (H1N1)	GlaxoSmithKline	Eggs	NI	1	
	Adjupanrix (H5N1)	GlaxoSmithKline	Eggs	NI	1	

Virus subunit	Celtura	Novartis	MDCK	NI	1	
	Flucelvax	Novartis	MDCK	NI	3,4	Successor of Optaflu
	Fluvirin	Novartis	suspension	Centrifugation (ZC)	3	
	Fluad	Novartis	Eggs	Centrifugation (ZC)	3	
	Agriflu	Novartis	Eggs	Centrifugation (ZC)	3	
	Influvac	Mylan Healthcare / Abbott Biologicals	Eggs Eggs	NI	3,4	
	Agippal, Fluad, Begripal	Sequirus	Eggs	NI	3,4	
	Xanaflu	Mylan Healthcare	Eggs	NI	3,4	
	Foclivia (H5N1)	Novartis	Eggs	NI	1	
Viral vectors	Not yet approved					
Recombinant viral proteins	Flublok	Sanofi	Insect cells	Chromatography	3,4	Baculovirus vector
Nucleic acids	Not yet approved*	CureVac				
Virus-like particles (VLPs)	Not yet approved					

Legend: CFZC=Continuous flow zone centrifugation; ZC=Zonal centrifugation; MDCK=Madin Darby canine kidney; NI = no information available to the author; * still in pre-clinical discovery phase; grey font color: not approved.

2.3 Vaccine manufacturing processes

The annual production capacity for seasonal influenza vaccines was estimated with 1.48 billion doses, while the production capacities for pandemic influenza vaccines were estimated between 4.15 billion doses (moderate estimation) and 8.31 billion doses (best estimation). Regarding the pandemic influenza vaccines production processes, 79% are egg-based while 21% are cell-based. In the best case scenario the first doses would be available after four to six months. Also, the above numbers illustrate that even at the best case scenario only half of the world population could be vaccinated (Sparrow et al., 2021).

Upstream processing

The most relevant approaches for production of IV vaccine (upstream) are shown in Figure 3. In Europe, most seasonal flu vaccine productions are still egg-based (Manini et al., 2017). Here, the IV is cultivated in the allantoic fluid inside the embryonated hen eggs, before harvest and purification. In case of a pandemic, these production facilities would be required to provide vaccines for the world-wide population in a matter of weeks, which is difficult to achieve using eggs as a starting source. So far, on average the production of IV vaccines requires about four to five months before release due to the long lead time in egg-base production processes (Jin et al., 2014). Also, the process quality control and scale-up of the egg-based production processes is difficult considering the space-requirement and a potential antigenetical change due to a native virus variant selection process, sometimes reducing the immunological efficacy (Schild et al., 1983; Skowronski et al., 2014). Furthermore, an occasionally difficult adaptation process of the human IV to hen eggs is required. Moreover, the “egg-producing” chickens can be infected with viruses, such as Rous sarcoma virus (tumor-inducing retrovirus), avian leukosis virus (retrovirus; can cause B-cell-leukemia in chickens and is known to infect other animal hosts), and reticuloendotheliosis virus (tumor-inducing retrovirus), which could potentially be introduced into egg-based vaccine manufacturing processes (Dormitzer, 2011). Overall, mammalian cell culture-based production can be considered to give higher virus particle yields, to have shorter production cycles and are easier to scale-up (Tree et al., 2001; Perdue et al., 2011; Manini et al., 2017).

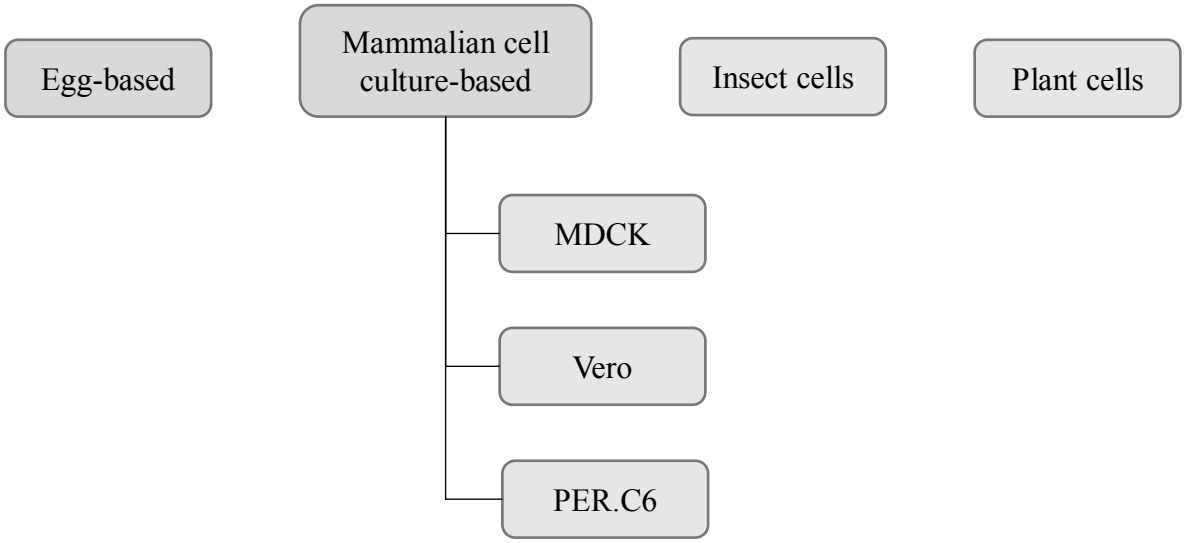

Figure 3: Approaches for IV vaccine production. Cell lines: MDCK (Madin-Darby canine kidney cells); Vero (Kidney epithelial cells from an African green monkey); PER.C6 (human retina-derived cells).

Therefore, mammalian cell culture-based production of influenza vaccines seems to be a valuable option. Although approved by the FDA in 2012, mammalian cell culture-based production processes are still not widely used in IV vaccine industry (Harding et al., 2018), yet already in development at some pharmaceutical companies (Manini et al., 2017). For cell culture-based manufacturing of IV vaccines, the WHO proposed three cell lines: (1) Madin-Darby canine kidney cells (MDCK), (2) Vero (kidney epithelial cells from an African green monkey), and (3) PER.C6 (human retina-derived cells) (Pérez Rubio et al., 2018). The cells can be grown either adherent (often on bead-carriers) or in suspension using serum-containing or serum-free media with different outcomes concerning the yields. While no PER.C6-based flu vaccine has entered the market so far, MDCK and Vero cell culture-based vaccines have already been successfully approved by the FDA (Manini et al., 2017).

Furthermore, a vaccine relying on production of plant-derived IV hemagglutinin (HA) virus-like particles (Medicago Inc.) is close to FDA approval (clinical phase III) (Pillet et al., 2016; Margolin et al., 2018).

Downstream processing

After production of virus particles (upstream), the manufacturing process is continued by the DSP. Over the past decades, advances in upstream processing (USP) have significantly increased the yields (e.g., by using high-density cell cultivations), while shifting the bottlenecks of the overall manufacturing process towards the DSP. Therefore, up to 70% of the total production cost for vaccines can be attributed to DSP, underlining the need for significant advances there (Morenweiser, 2005; Nestola et al., 2015).

Besides product concentration or change of the product medium, the goal of the DSP is to eliminate process and product-related contaminants, such as medium components (e.g., bovine serum albumin (BSA), antifoam, dye), nucleases, host cell DNA, host cell proteins, detergents, particulate matters, and leaching compounds (Nestola et al., 2015). Ultimately, process performance is usually a trade-off between purity and product recovery.

In general, the DSP for vaccines can be traditionally divided into the steps harvest, concentration, purification and formulation, while certain steps (e.g., purification and concentration) can sometimes be combined. A standard chromatography-based vaccine downstream process is shown in Figure 4 (the box (dotted line) representing the actual purification steps).

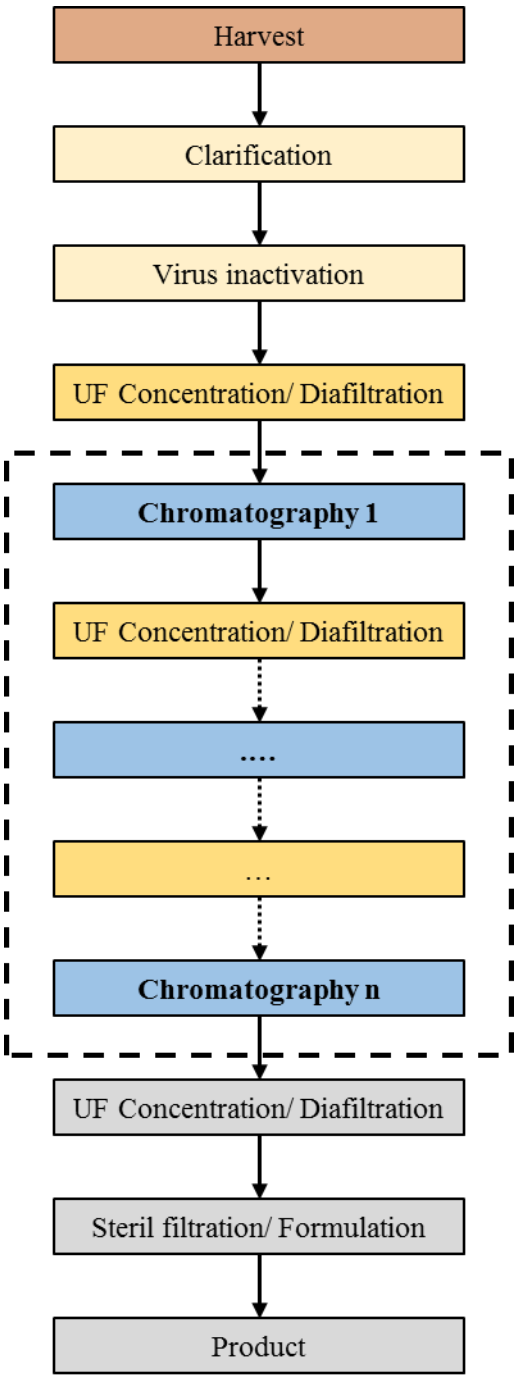

Figure 4: A chromatography-based generic viral vaccine downstream process scheme. UF: ultrafiltration.

While for the harvest often filtration (dead-end or crossflow) or centrifugation is applied, for concentration crossflow ultrafiltration (UF) is most common. For purification, chromatography can be applied, with the viral surface protein (HA and NA glycoproteins are the most abundant ones) often resembling the target for adsorption/binding steps. Between the purification steps, ultrafiltration/diafiltration steps are frequently required in order to exchange the buffer and/or

to concentrate the product fraction. Considering an average product loss of 5–10% for each step, the need for reduction of the number of steps becomes evident.

Chromatography can be categorized based on the backbone structure of the stationary phases into bead-, membrane- and monolith-based chromatography.

While mostly methods for adsorption/binding based on physico-chemical surface properties of either the target (capture-mode or positive mode) or, less frequently, the impurities (flow-through mode or negative mode) are used, methods utilizing virus particle size have also been applied (e.g., size-exclusion chromatography) in vaccine production (Nestola et al., 2015). Based on the physico-chemical binding modes, stationary phases can be further divided into anion exchange (AEC), cation exchange (CEC), hydrophobic interaction (HIC), mixed mode (MMC) and (pseudo) affinity chromatographies (AC). Besides chromatographic approaches, density-gradient centrifugation is another popular method. Zonal ultra-centrifugation has been traditionally used for the purification of egg-based vaccines (Reimer et al., 1966; Reimer et al., 1967). It combines concentration and purification in one step, but is expensive to scale-up and very laborious (Nestola et al., 2015).

Regarding the selection of appropriate methods, high purity demands – in particular due to the use of continuous cell-lines – as well as the requirement for easy scale-up forces new challenges onto the purification process. Moreover, the continuing antigenic drift of seasonal circulating IVs requires a process, which is robust and strain independent or at least quickly adaptable (in the limits given by good manufacturing practice (GMP)).

2.4 Regulatory requirements for influenza vaccines

For clinical use of vaccines the approval of the regulatory authorities (Table 2) is required. The regulatory requirements of each country are updated regularly. For veterinary use, the regulatory requirements are generally less strict (Meeusen et al., 2007).

Table 2: National and international regulatory offices/ institutes with their guidelines for vaccine manufacturing and purity demands.

Country	Regulatory office/institute	Regulatory guideline
USA	U.S. Food and Drug Administration* (FDA)	United States Pharmacopeia / Biologics Vaccine Standards
Europe	European Medicines Agency (EMA)	European Pharmacopoeia (Ph. Eur.)/ Vaccines for human use
Germany**	Paul-Ehrlich-Institute (PEI)/ European Medicines Agency (EMA)	European Pharmacopoeia (Ph. Eur.)/ Vaccines for human use
China	Chinese Food and Drug Administration (CFDA)	The Pharmacopoeia of the People's Republic of China (PPRC)

* in close collaboration with Centers for Disease Control and Prevention (CDC)
**vaccines for the market of European member states can either be approved by the national regulatory authorities (e.g., Germany: PEI) or by the European regulatory office (EMA). The PEI also refers to the European Pharmacopoeia.

Moreover, the purity requirements usually depend on the production system (egg-derived, cell culture-derived, etc.) and on the vaccine type (whole, split, subunit, etc.). Usually, for vaccine formulation, DNA and total protein contamination levels per dose are crucial. For example, for inactivated whole influenza virions prepared in cell cultures for each strain 15 µg HA are required, and the DNA amount must not be greater than 10 ng per dose in total. Regarding the total protein amount not more than 100 µg per virus strain and not more than 6 times the total HA amount (= 270 µg total protein per dose) are accepted for a trivalent influenza vaccine in Europe (European Pharmacopoeia, 2018).

Besides, except for recombinant IV vaccines, the presence and type of the neuraminidase antigen need to be confirmed in Europe (for the first three monovalent harvests from each working seed slot) (European Pharmacopoeia, 2018).

2.5 Process units

In this section, an overview of process units applied for vaccine purification is given. The used chromatography methods can be divided into bead- and membrane-based process units.

Using the bead structure as stationary phase, bead-based chromatographies are the most frequently used and proven designs. The bead resins are offered with the widest variety of

ligands and resin materials and are considered as rather affordable due to a reasonably large market. The beads usually consist of a rigid material (e.g., silica) to avoid compression and are generally highly porous to increase the surface area. The latter allows for high binding capacities and high resolution. On the other hand, bead-based chromatography often requires laborious packing and validation. The danger of bed compression often limits the flow rate and thus the productivity. Also, the applied samples should be free of a particulate matter in order to avoid clogging and back pressure increase. Due to the time-consuming bed packing and the sometimes expensive chromatography materials, multi-usage of a packed column is still chosen for some processes necessitating the establishment of cleaning-in-place (CIP) protocols – in particular for special affinity chromatography materials. Furthermore, axial scale-up is difficult, while the horizontal scale-up (increase of column diameter) is limited, if not using a radial-flow system. Moreover, the pores in the beads are usually of small diameter allowing only for slow pore-diffusion (Charcosset, 2006) and molecules up to a certain (globular) size to enter. While most globular molecules in solution can enter the pores, large protein aggregates, particle matter or long linear molecules cannot.

Therefore, for virus particle and virus-like particle purification, membrane adsorbers have emerged as well suited stationary phases. Due to their size, virus particles cannot enter the pores of most resin-based stationary phases, while membrane pores are larger allowing access to most of the membrane surface area (Figure 5). Membranes offer a significantly reduced mass transfer resistance compared to resin beads and virus particles are mainly transported by convective flow. Due to a low back pressure and a higher pressure stability compared to resins, they can be operated at higher flow rates increasing the productivity. In addition, they have a low void volume and do not suffer from channeling, which simplifies the operation. Also, membranes are reasonably scalable and can reduce the process costs substantially, since they are simple to manufacture allowing for a disposable use while avoiding CIP and validation procedures (Ghosh, 2002; Gagnon, 2009; Opitz et al., 2009b; Orr et al., 2013). However, compared to the bead-based materials, the surface area is still low and the availability of membrane adsorbers is still poor in terms of ligand variety.

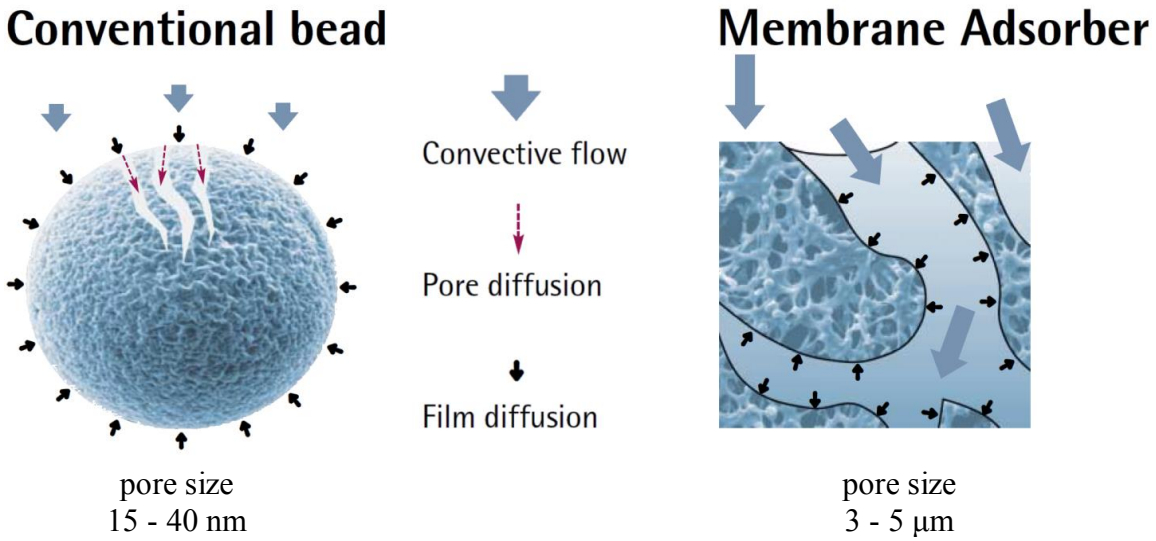

Figure 5: Schematic representation of a conventional bead and a membrane adsorber. Shown are the dominating transport mechanisms through a bead and a membrane (convective flow, pore diffusion, film diffusion). Convective flow is the most relevant transport mechanism for virus particles as well as the dominating transport mechanism through a membrane. Source: Fischer-Frühholz (2012); with kind permission of Sartorius AG, Göttingen, Germany.

2.5.1 Bead-based anion-exchange chromatography

Ion-exchange chromatography is considered to be the workhorse of bioseparations, including virus particle purifications (Gagnon, 2013). Generally, it can be subdivided into CEC, which ligands are negatively charged and bind positively charged solutes, and AEC, which ligands are positively charged and bind negatively charged solutes. The net charge on proteins and virus particle surfaces depends on the exposed amino acids as well as on post-translational modifications (e.g., glycosylation). Furthermore, the net charge strongly depends on the pK_a of the protein and the pH of the solution.

Looking at the source of charge of solutes, such as proteins, or virus particles (as whole target), the conservative concept of a net charge might not be adequate to describe, model or predict target binding to the resin. Rather a charge distribution, which can be uneven on the surface of the proteins or virus particles, should to be taken into account giving each protein (or virus particle surface protein) or even certain virus particles potentially a preferential orientation upon binding. This is in particular of relevance, when pH is changed since the preferred binding site might change as well altering the elution behavior (Gagnon, 2013).

IV particles (pK_a: about 5–5.3 (Miller et al., 1944; Zhilinskaya et al., 1972)) show only a small pH tolerance, with the optimal process operation window ranging between pH 7 and 7.5

(Kalbfuss, 2009). Therefore, AEC might not be the first choice for purification, since the common two control parameters in AEC, pH and salt concentration, are preferable reduced to the latter.

AEC resins are available in a wide variety. The resins can be classified according to their ligands into weak and strong AEC resins (Figure 6). The term does not refer to the strength of the binding force, but to the ability to maintain their charge over a wide range of pH (Gagnon, 2013):

- strong AEC resins (e.g., quaternary amines (Q, QA, …) → wide pH operation window
- weak AEC resins (e.g., diethylaminoethyl (DEAE)) → narrow pH operation window

(A) (B)

Figure 6: AEC ligand types: A) quaternary amine (Q, strong ligand), **B)** DEAE (weak ligand).

Traditionally, the AEC can be operated in capture mode (aim: binding of target (product)) or flow-through mode (aim: binding of contaminants). In capture mode, separation of the target and the contaminants can be achieved either during loading/adsorption by carefully adjusting the binding conditions or during elution using a gradient (e.g. linear or step gradient). Since IV particles and many contaminants (in particular DNA and a certain amount of the host cell proteins) are negatively charged at the given pH range, separation resembles a challenge, asking for a careful selection and fine tuning of conditions (in particular the salt concentration) and resins in order to achieve the best results.

Yet, in general the flow-through mode is to be preferred if the contaminant load is not too high since it usually leads to lower product losses. In the past, purification of IV particles has been achieved with promising results using AEC in the flow-through mode and different ligands (Kalbfuss et al., 2007b; GE Healthcare, 2010; He et al., 2011; Iyer et al., 2011; Iyer et al., 2012). Yet, the published processes have shown insufficient IV recoveries and contaminant depletion, suffered of insufficient data (in particular about the width of the tested conditions) or were missing a direct comparison of process data of different AEC resins using the same sample material, making a rational selection of an AEC resin and the best conditions difficult.

2.5.2 Bead-based ligand-activated core chromatography

Couple of years ago, ligand-activated core chromatography (LCC) resin types have been made available that offer several advantages over conventional chromatographic media (GE Healthcare, 2012a). With an unfunctionalized outer shell and a strong and multi-modal ligand (octylamine; Figure 8) in the bead core, only entities small enough to enter the particle (e.g., small proteins and other contaminants) are bound, while larger entities (e.g., larger proteins and virus particles) are excluded from the resin beads, simply pass by the unfunctionalized bead surface and are collected in the flow-through (Figure 7). Such resins are ideal for depletion of host cell proteins and removal of nucleases in one single step. Due to the spatial exclusion of virus particles from the binding sites (resin pore size: ~700 kDa; IV particle size: 75–120 nm (Lange et al., 1999)), high IV recoveries can be achieved. Moreover, this resin type does not suffer from typical size-exclusion chromatography (SEC) drawbacks such as low productivity due to limited loading capacity and could possibly replace a typical SEC step at the end of a purification train.

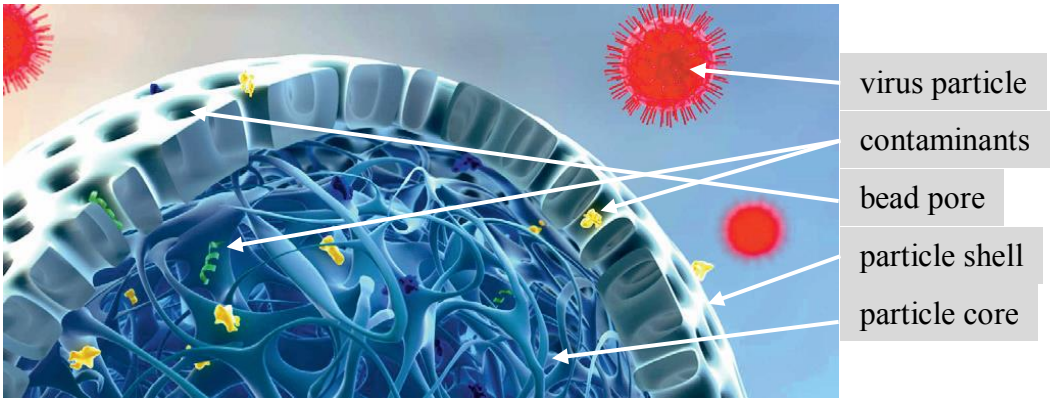

Figure 7: Schematic representation of a ligand-activated core (LLC) resin bead with contaminants (e.g., proteins and DNA fragments) and virus particles in solution. The cross section shows the unfunctionalized outer shell and the ligand activated core of the resin bead. Source: modified according to GE Healthcare (2012a).

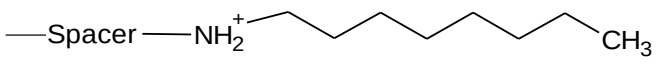

Figure 8: Multi-modal ligand (octylamine) in the LCC bead core.

2.5.3 Bead-based hydrophobic-interaction chromatography

Hydrophobic-interaction chromatography (HIC) offers an orthogonal approach to, e.g., AEC, CEC or SEC, (Gooding et al., 2002), which has not been tested for IV purification by other research groups yet (as to the authors knowledge). HIC exploits hydrophobic regions present on protein surfaces using hydrophobic resins and kosmotropic salts to modulate the polarity and surface tension of the mobile phase (Kennedy, 2001; Gooding et al., 2002; McCue, 2009). In addition, HIC can operate at high salt concentrations often found in product streams of other chromatographic steps, which renders HIC an ideal subsequent purification step after purification steps having high salt concentrations in their product fraction (e.g. AEC eluate) omitting the need for a buffer exchange. Moreover, targeting hydrophobic surface groups or regions for separation, HIC can be considered to be a relatively unspecific chromatography mode, which is potentially not much affected by changing virus strains. Nevertheless, HIC shows unique separation performance, e.g. the separation of native proteins from their aggregates as well as the separation of protein glycoforms (Shukla et al., 2006; Zolodz et al., 2010). So far, however, HIC-based processes have been rarely used for virus particle purification (Wolff et al., 2010; Li et al., 2015; Sviben et al., 2017). This is not only due to the applied high salt concentrations, which might potentially affect the virus particle integrity and activity (Utsunomiya et al., 2009; Nestola et al., 2015) or lead to precipitation (Gagnon et al., 1995b; Wu et al., 1996), but also due to its complexity and sensitivity regarding the choice and control of operating conditions (salt type, salt concentration, buffer type, temperature, pH, gradient choice, etc. …) (Gagnon et al., 1995b, 1995a; Gagnon et al., 1996b, 1996a; Wu et al., 1996; Lu et al., 2009). It also requires the need for extensive screening studies due to the lack of predictive models for process optimization (McCue, 2009). Furthermore, HIC resins require extensive and careful regeneration (Wu et al., 1996).

Nevertheless, HIC is one of the most powerful methods in preparative biochemistry regarding speed and resolution while still being a rather mild technique with good capacity (Gagnon et al., 1995b; Kennedy, 2001). Also, a wide selection of different ligands is available by most manufacturers (Figure 9).

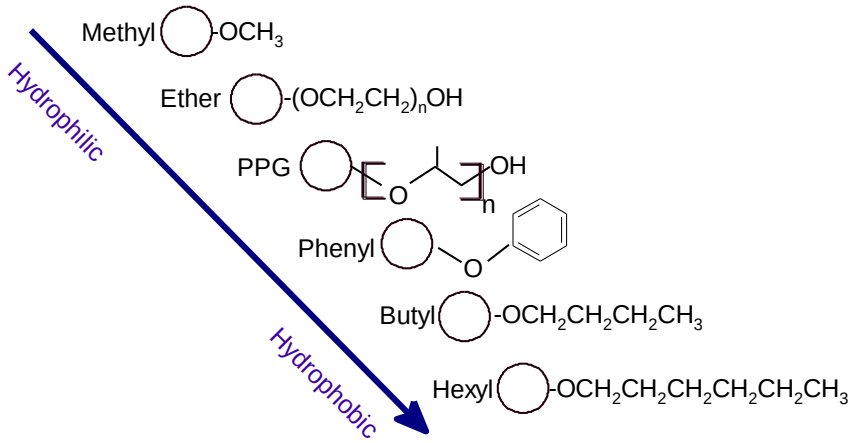

Figure 9: Hydrophobic order of selected HIC resin ligands (modified based on Tosoh Chromatographic Process Media Catalog 2010).

The effect of a salt in HIC equally depends on its concentration as well as on the salt itself. The cations and anions of the salts used for HIC can be ordered according to an empirical ranking based on their kosmotropic (destabilizing/salting-out) effect on egg globulin and isinglass (collagen) as well as some inorganic substances (colloidal ferric oxide and sodium oleate), the Hofmeister series (Lewith, 1887; Hofmeister, 1888). An excerpt of the most relevant salt ions for salting-out of proteins in DSP from Hofmeister is given in Figure 10.

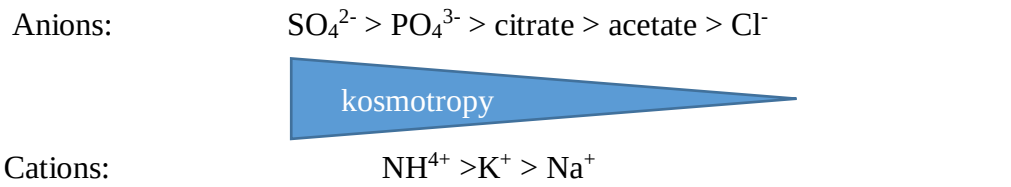

Figure 10: Kosmotropic series for selected salts (excerpt of the "Hofmeister series").

Magnesium does not follow a certain predictable trend in this series and was therefore excluded here. It needs to be mentioned here, that there are many so-called "Hofmeister series" published in literature, often with a different order or different salts. This even extends to reference literature sources such as encyclopedias (Ackermann et al., 1999; Spektrum, 2020). Hofmeister has published a series of six publications with various experiments regarding the salt effects. To the author's knowledge, he has not published a specific salt series called "Hofmeister-Serie". To add to the complexity, other researchers extended his work using altered experimental

conditions (e.g., benzene as salting-out target (McDevit et al., 1952)) further increasing the variety of “Hofmeister series”.

2.5.4 Membrane-based pseudo-affinity chromatography

The sulfated cellulose membranes adsorber (SCMA) consists of a cellulose backbone with sulfate groups, which are directly chemically bound to the sugar rings of the cellulose (Figure 11). At standard pH conditions (pH 7.4) used for IV purification the membrane surface is negatively charged. Due to the strong resemblance to the naturally on host cells occurring heparin, a glycosaminoglycan, it is considered to be a pseudo-affinity stationary phase for IV particles, which are known to bind to heparin. Pseudo-affinity chromatography (sulphated cellulose, Cellufine® sulphate) was successfully applied for vaccine purification by several research groups (A. M. Palache et al., 1997; Opitz et al., 2009b; He et al., 2011; Sakoda et al., 2012; Carvalho et al., 2018; Fortuna et al., 2018).

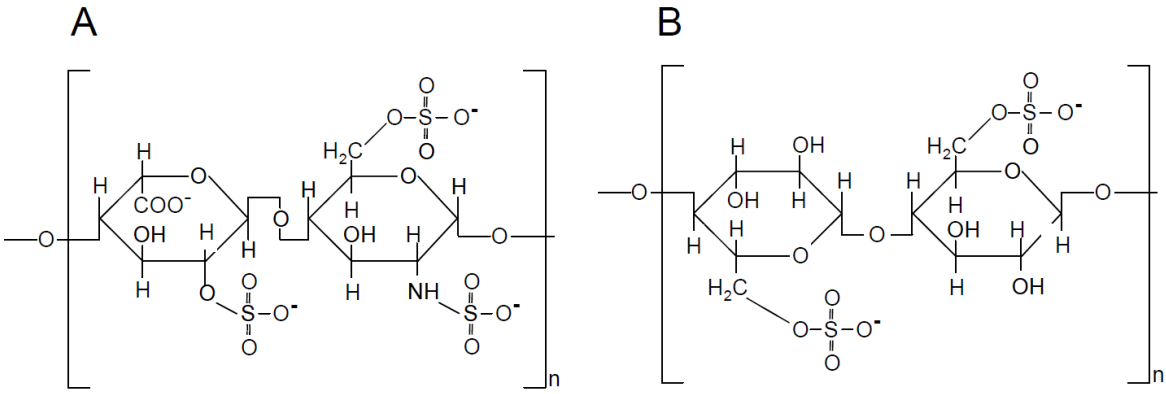

Figure 11: Comparison of chemical structure of relevant functional groups (disaccharides) of heparin (A; originally based on Rabenstein (2002)) and sulphated cellulose/cellufine sulphate (B; originally based on manufacturer’s application notes of cellufine sulphate (Chisso Corporation, Japan); Source: Opitz (2010)).

2.5.5 Membrane-based anion-exchange chromatography (salt-tolerant)

Salt-tolerant membrane adsorbers (STMAs) are specifically designed to be used at high salt concentrations to facilitate strong interaction with the target molecules. This is achieved, for example, by attaching free/primary amine ligands (anion exchanger) with a high ligand density to a macroporous membrane matrix leading to a high salt tolerance while maintaining a high binding capacity (Faber et al., 2009; Fischer-Frühholz et al., 2010) (Figure 12). That makes them an ideal candidate for polishing steps in purification processes. Besides Iyer et al. (2012),

who has tested a STMA (ChromaSorb™; discontinued) for influenza virus purification, other scientists have successfully tested STMAs for other tasks such as purification of monoclonal antibodies (Kang et al., 2013) or in viral clearance studies for removal of bacteriophages or minute virus of mouse (Faber et al., 2009; Riordan et al., 2009a; Riordan et al., 2009b).

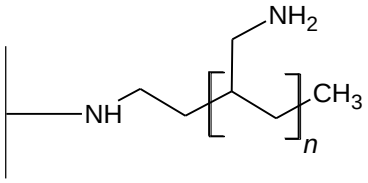

Figure 12: STMA ligand: primary amine (covalently attached).

2.5.6 Nuclease digestion

The majority of downstream processes for vaccines include a nuclease treatment step to achieve reliably accepted DNA contamination levels (Wolff et al., 2008). The aim is not only to meet the required levels of residual DNA, but also to reduce viscosity of virus-containing material and to provide an additional safety step regarding virus inactivation (FDA, 2012). With the expiration of patents for Benzonase® and the availability of new nuclease products, an enzymatic digestion step is now even more attractive for downstream processing of virus broths. However, the disadvantage is that the removal of nucleases can add to the complexity of downstream processing.

Nucleases are catabolic enzymes, which hydrolyze phosphodiester bonds of nucleic acids. Here, they catalyze either the cleavage of 3'- or 5'-bonds. The group of nucleases can be generally further subdivided into endo- (internal hydrolyses) and exonucleases (hydrolyses starts from the end of the nucleic acid chain). Often they show further specificity towards DNA or RNA, respectively single-strands or double-strands. But, for DSP an unspecific nuclease has advantages and is usually preferred. Here, the genetically engineered endonuclease Benzonase® produced with *E. coli*, originally isolated from the bacterium *Serratia marcescens*, was used: The 30 kDa nuclease degrades DNA and RNA, single-stranded as well as double-stranded nucleic acids, linear, circular as well as super-coiled nucleic acids. Furthermore, the resulting fragments are of small size (3–5 base pairs) and the nuclease shows a high enzymatic activity (4×10^5– 1×10^6 units/mg nuclease) reducing the required amount to a minimum. Finally, it is stable for up to 24 h giving the possibility for reducing the amount of used Benzonase® further by extending the process time (Martin, 1991).

Various criteria must be met for achieving an optimal digestion of nucleic acids. Most importantly, the DSP batch should be mostly free of proteases. Alternatively, proteases can be inhibited by using magnesium cations, while nuclease activity can be partially maintained. In addition, the pH-optimum of Benzonase® lies between pH 7.8–9.2, while it can be used in a range of pH 6–10. Furthermore, the temperature optimum is at 37°C, while operation at room temperature (RT) is unproblematic. But, Benzonase® is sensitive to monovalent cations such as Na^+, possibly requiring a dialysis of the starting material (Banta et al., 2007).

2.6 Analytical and sample preparation methods

2.6.1 Influenza virus quantification

The IV particles are commonly quantified by the Hemagglutination (HA) assay. It measures the hemagglutination activity (HA-activity, reported as kHAU/mL sample) of IV particles in the sample. The assay relies upon the cross-linking between erythrocytes and IV particles. The cross-linking is caused by the IV HA. Due to its spatial distribution on the virus particles (around 500 molecules per virus particle), it is able to cause a cross-linking, if the number of virus particles and erythrocytes is high enough. The cross-linking hinders the sedimentation of the erythrocytes, leading to an altered appearance of the sedimentation pellet. Adjusting the erythrocyte concentration to a certain level and using a serial dilution for the virus sample, a shift of the sedimentation appearance in the dilution series is detectable at a critical virus particle concentration. The negative logarithm of the corresponding dilution is defined as the logarithmic HA titer. The inverse of that dilution is defined as HA activity (HA units/100 µL) which is supposed to be proportional to the virus particle concentration in the sample (Mahy et al., 1996; Kalbfuss et al., 2008) and is used for mass balancing of IV particles in processes. Since the cross-linking activity relies upon the expression density and distribution of the HA protein on the virus particle, as well as on the phenotype of the erythrocytes, it can only represent an approximation for the number of virions and is not accepted by the authorities for product quantification. For the final vaccine product evaluation, the determination of the HA protein content (e.g., by single radial immunodiffusion (SRID) assay; refer to 2.6.3) is considered appropriate.

2.6.2 Protein quantification

Due to the high variety of composition of process samples, the protein quantification represents a certain challenge for DSP. Different types of analytical methods are commonly in use. The colorimetric quantification assays, such as Bradford, Lowry or bicinchoninic acid (BCA) assay are currently still the standard assays due to affordability, high capacities and simplicity in use.

In addition, spectroscopic methods (UV and fluorescence) are used frequently. Whether a dye-based or spectroscopic method is used, all suffer of certain drawbacks. The UV-based method is highly affected by the nucleic acid content in the sample. The fluorescence and UV method is strongly affected by the tryptophan content of the proteins. Furthermore, spectroscopic methods usually show lower sensitivities than colorimetric assays. While the detrimental effect of various sample components on the colorimetric assays, such as detergents or high salt concentrations, frequently present in laboratory samples, can be addressed by dialyzing the sample before analysis, a certain amino acid specificity cannot be resolved. In research often highly pure protein samples are used, so the protein standard can be selected in order to match the protein of the sample. The problem becomes apparently unsolvable when using a crude protein mixture, which might (and probably will) constantly change its relative composition during the IV vaccine downstream process. This makes mass balances to a certain extend imprecise, in disregard of the standard assay validation (often performed with pure "model" proteins or one sample mixture).

Although "objective" methods, i.e. amino acid-unspecific quantification methods, for proteins exist (quantitative amino acid analysis or weight determination of strongly purified protein samples), they are extremely laborious and require large amount of sample material. Moreover, losses during sample preparation for these methods cannot be accounted for. It is likely that even analytical methods, which are currently under development for protein quantification (e.g., mass spectrometry), will also be affected by sample preparation losses or amino acid-specificity to a certain extend.

For an excellent review on this topic, please refer to Lottspeich et al. (2018).

2.6.3 HA protein quantification

For IV vaccines the quantification as well as the immunogenicity testing is mainly based on the HA protein of the virus particle surface, which is also the most abundant protein of the IV. In order to have a comparable measure for the vaccine content, the immune reaction-based single radial immunodiffusion (SRID) assay is applied. It is based on an antibody-antigen (i.e. HA protein) precipitation circle in an agarose gel. After applying different dilutions and staining, the diameter of the precipitation circles is measured visually and the slope of these concentration-dependent diameters is used for quantification (by comparing it to the slope of a reference dilution series of known concentration). While being a very laborious, error prone and to a certain degree subjective assay format, it is still the preferred assay for the final IV vaccine dose quantification.

2.6.4 DNA quantification

For DNA quantification in DSP, different methods are available as well (Table 3). While the UV-based OD260nm method is most frequently used, with standard UV spectrophotometers it is limited by a limit of quantification (LOQ) of about 5 µg/mL. Also, there are many factors interfering with the UV measurements. Due to the low level of DNA contamination required for IV vaccines (<10 ng/dose; refer to 2.4), this method is inadequate for testing of the final product. For intermediate range DNA concentration measurements (1–1000 ng/mL), dye-based fluorescence methods are available, such as the Quant-iT™ PicoGreen™ (PicoGreen®) (Figure 13) or SYBR Green I assays. PicoGreen® is a fluorescence dye with a high binding selectivity towards double stranded deoxyribonucleic acid (dsDNA). The binding, which is based on intercalation and electrostatic interactions, results in a >1000-fold enhancement in its fluorescence (Dragan et al., 2010), and is supposed to enable quantification down to 50 pg/mL. In practice however, LOQs of about 5 ng/mL are achieved. While substances interfering with PicoGreen® assay are well studied, lower LOQs are often required due to dilutions during some DSP steps. In order to be able to detect DNA concentrations in the magnitude of picograms per milliliter, more sophisticated, costly and laborious methods are used, such as the DNA specific antibody-based Threshold® assay. Furthermore, recently, quantitative real-time PCR (qPCR) has emerged as the method of choice for DNA quantification.

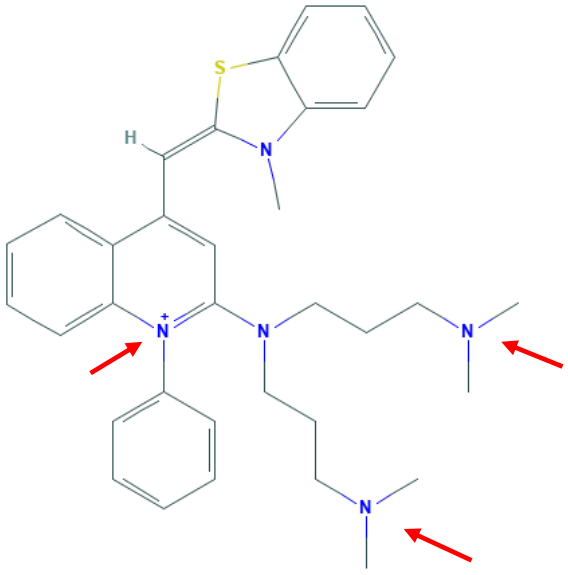

Figure 13: Structure of PicoGreen®. The arrows mark the interaction sites with the DNA. Source: NCBI PubChem; modified.

Table 3: Selected DNA quantification methods for DSP. Shown are the applicable quantification ranges according to the author's knowledge and the claimed LOQ by the manufacturer/literature.

DNA quantification method	Quantification range (applicable)	LOQ (claimed)
UV-spectroscopy (standard)	5–50 µg/mL	1 µg/mL
UV-spectroscopy (optimized devices; 96-well)	unknown	0.4 ng/mL*
PicoGreen® assay	5–250 ng/mL	50 pg/mL
Threshold® assay	50–200 pg/mL	2 pg/mL
qPCR (for mammalian host cell DNA)	unknown	1.5 pg/mL**/ 1.66 pg/mL***

*Thermo Fisher Scientific, Varioskan LUX
**Thermo Fisher Scientific, resDNASEQ™ Kit
***Bio-Rad, ddPCR™ CHO Residual DNA Quantification Kit

2.6.5 Dynamic light scattering and particle size determination

Dynamic Light Scattering (DLS) can be used for determination of the particle size and the particle size distributions of particular matter by measuring the Brownian motion of the particles. The translational diffusion coefficient depends on the particle size. In DLS, a beam of laser light is focused on the sample. In solution, particles move randomly due to collision with other particles and solvent molecules (Brownian motion). Therefore, the laser light is scattered by the particles in all directions. Due to the constant change in position of the particles and therefore the distance to the laser light source, a fluctuation of the scattered light intensity is detected. This is caused by a light phase shift resulting from the different distances. Since small particles diffuse faster, the light intensity fluctuation frequency is higher, while the light intensity fluctuation frequency of larger (and slower) particles is lower. From the light intensity fluctuation frequency, the translational diffusion coefficient can be determined using an autocorrelation function and various algorithms. A fitting function and the Stokes-Einstein equation than either yields the mean particle size or a distribution of the particle size (using the Mie theory) of the sample (Horiba Instruments, 2017; Malvern Instruments, 2017).

The light scattering technique is extremely sensitive to the presence of larger particles in a sample. Therefore, it is ideal for detecting the formation of aggregates (refer to 3.5.1). However, certain criteria need to be met in order to yield accurate data. First, the temperature needs to be constant. Furthermore, the viscosity and refractive index of the medium needs to be known.

In the scope of this study was the determination of the formation of aggregates using samples with increasing salt concentrations. Due to the changing solvent concentrations, the refractive index as well as the viscosity had to be accounted for using software algorithm parameter input options.

For the determination of the critical salt concentration (CAC) inducing the formation of aggregates, only the salt concentration was relevant, while the mean particle sizes were normalized to the reference samples giving the relative mean particle size (RMPS). Therefore, a significant increase in the RMPS gives the CAC.

2.6.6 Freeze drying - lyophilization

In order to preserve the activity of biopharmaceutical products after formulation for storage, lyophilization is usually the preferred drying method (Wang, 2000; De Jonge et al., 2007). Alternatively, spray-drying is also frequently used. In addition, lyophilization can be used for concentration of a sample due to the simplicity of the steps and the reduced risk of product losses, especially with small sample sizes and with low product concentrations. Here, lyophilization was mainly used for sample preparation for the SRID assay (concentration and storage).

Lyophilization is a process comprising of at least two steps: the freezing of the sample and the actual lyophilization for sample drying. The two steps as well as the following rehydration underly complex mechanisms and can strongly affect the stability of the target entity (e.g., protein or virus particle).

The freezing can either be performed slowly (e.g., by putting the sample into the freezer), or rapidly by using liquid nitrogen or dry ice, for example, yielding different frozen sample structures. It also strongly depends on the used buffers and the sample entities (e.g., protein composition). Also, in practice, the freezing process seldom follows the equilibrium phase diagram, is rather strongly sample-dependent and is based on rather complex principles (undercooling, nucleation, crystal growth, ...) (Singh et al., 2010). Moreover, the product can be exposed to different stresses (Bhatnagar et al., 2007): (I) cold denaturation (below 0°C), (II) freeze concentration by (i) concentration of solutes, (ii) crystallization of solutes, (iii) phase separation and (III) ice-induced denaturation (denaturation at the ice-aqueous interfacial area).

For example, due to the transition of liquid water to the solid state, concentration effects can occur for the remaining salts and proteins in solution during freezing, exposing the proteins to high salt concentrations. Furthermore, different solubility limits of the buffer salts of the solution and their crystallization can also lead to pH shifts (Arora et al., 2012).

The lyophilization (actual drying) is achieved by removing the water by sublimation (i.e. direct transition from solid to gas state without entering the liquid phase) from the frozen sample under low pressures. The drying process can be subdivided into a primary drying phase, where the ice formed during the previous freezing is removed, and an optional secondary drying phase, where the remaining adsorbed water molecules are removed. The reduction of the glass transition temperature during the removal of water can have adverse effects on the protein stability or integrity of the vaccine compound, since the protein structure shows higher flexibility above the glass transition temperature (Jiang et al., 1998; Bakaltcheva et al., 2000; Hinrichs et al., 2001; Amorij et al., 2007).

For the protection of the product during the freezing and lyophilization, strategies can imply the control of freezing and/or lyophilization (parameters: speed, temperature, vacuum pressure) as well as the addition of cryoprotectants (protective during freezing step) and lyoprotectants. Cryoprotectants, such as some organic/inorganic salts, polymers (polyethylene glycol (PEG)), sugars or amino acids, are used due to their protein stabilizing effect by preferential exclusion (Carpenter et al., 1988; Mohammed et al., 2007). Lyoprotectants, in particular disaccharides, are often able to form an amorphous structure (glass/glass state/glass matrix) once the temperature falls below the glass temperature during lyophilization. By steric stabilization of proteins through hydrogen bonds, the increase of the glass transition temperature of the proteins/the system and the immobilization in the amorphous glass matrix the native protein structure can be maintained (Bakaltcheva et al., 2000; Hinrichs et al., 2001). Since the effect of both protectants can often not be clearly distinguished from each other in the following both will be addressed together by the term lyoprotector (if not citing a publication).

2.7 Calculations

2.7.1 Log reduction value

Virus particle and contamination depletion is described by giving the log reduction value (LRV). LRV is calculated as shown below:

$$LRV = \left| Log_{10} \left(\frac{c_{out} \times V_{out}}{c_{in} \times V_{in}} \right) \right| \qquad \text{Eqn. 1}$$

with: c_{in} = input concentration of virus particles or contaminant at the process step

V_{in} = input volume of the process step

c_{out} = output concentration of virus particles or contaminant at the process step

V_{out} = output volume of the process step

2.7.2 Ion strength

Ion strength was calculated as shown below:

$$I = \frac{1}{2}\sum_i c_i z_i^2 \qquad \text{Eqn. 2}$$

with: I = ion strength

c_i = molar concentration of specific ion

z_i = charge number of specific ion

3 Materials and Methods

In this section the production of the used virus particles, the pre-processing of the harvest, the screening and chromatography methods, and the applied analytics are described. For each of the three developed processes a separate subsection is dedicated.

3.1 Influenza virus production, harvest and pre-processing

For all processes the virus material was prepared identically. Three human influenza strains have been used for this work: A/Puerto Rico/8/34, H1N1 (A/PR) (Robert Koch Institute, Berlin, Germany), A/Wisconsin/67/2005, H3N2 (A/Wis) (#06/112, National Institute for Biological Standards and Control, London; UK), and B/Malaysia/2506/2004 (B/Mal) (#06/104, National Institute for Biological Standards and Control, London; UK). As host cells, adherent MDCK cells (#841211903, European Collection of Cell Cultures, Salisbury, UK) were cultivated in a bioreactor with serum-containing Glasgow minimum essential medium (GMEM) (#22100-093, Life Technologies, Carlsbad, USA) supplemented with fetal calf serum (FCS, 10% (v/v) #10270-106, Invitrogen/Gibco™, Karlsruhe, Germany) and peptone (2.0 g/L, (#MC33, International Diagnostic Group, London, UK) as described by Genzel et al. (2004), except that 2.0 g/L microcarrier (Cytodex™ 1, GE Healthcare, Freiburg, Germany) were used. Accordingly, after four days of cell cultivation, the FCS containing culture medium in the bioreactor was replaced by fresh serum-free GMEM medium and the cells were infected with virus seed at a multiplicity of infection (MOI) of 0.025.

Culture broths were harvested about 70 h after the infection with a 5.0 µm and a 0.65 µm depth filter (#CFAP0508YY, #CFAP9608YY, GE Water & Process Technologies, Trevose, USA) in sequence, followed by a chemical inactivation with β-propiolactone (#33672.01, Serva Electrophoresis, Heidelberg, Germany; final concentration: 3 mM, 37°C, 24 h). Subsequently, the broths were processed by a 0.45 µm membrane filter (#CMMP9408YY, GE Water & Process Technologies, Trevose, USA).

Finally, the clarified broths were concentrated about 10-fold by crossflow filtration using polysulfone hollow-fiber UF membrane modules (total membrane area 840 cm^2, molecular weight cut-off (MWCO): 750 kDa; UFP-750-E-4MA, GE Healthcare, Uppsala, Sweden) as described by Kalbfuss et al. (2007a) and stored at -80°C. This clarified, inactivated and concentrated material was used for all shown experiments and will be called 'virus material' hereafter. An overview of the harvesting and pre-processing is shown in Figure 14.

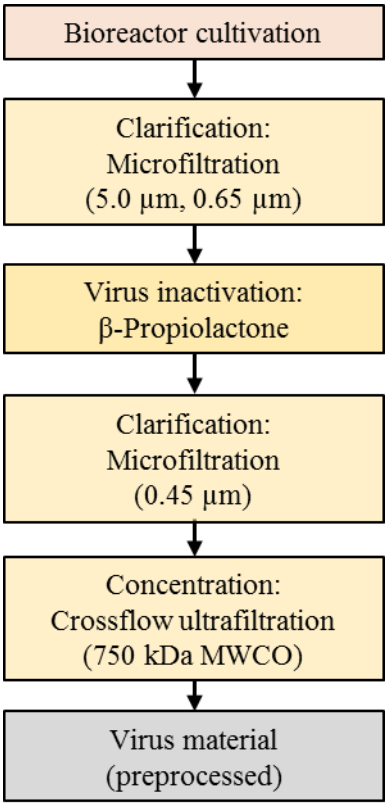

Figure 14: Overview of the harvest and pre-processing steps for preparation of the virus material for the following chromatographic purification processes.

3.2 General chromatography setup and process specifications

All chromatographic experiments were performed with an ÄKTAexplorer 100 (GE Healthcare, Uppsala, Sweden). Virus fractions were collected based on the in-line signal of a static light scattering detector (BI-MwA, Brookhaven Instruments Corporation, Holtsville, USA). After thawing and immediately prior usage in the chromatographic experiments the virus material was centrifuged at 9,000 x *g* for 10 min to eliminate potential precipitates from the freeze-thaw cycle. All steps involving dialysis (e.g., buffer exchanges, preparation of samples for analytics) were performed with 3,500 Da or 14,000 Da cut-off dialysis membranes (#132720, Spectrum

Labs, Los Angeles, USA; #0653.1, Carl Roth, Karlsruhe, Germany) at 4°C overnight (also called pre-dialyzed virus material hereafter). If buffer was added to virus material or sample in order to adjust the salt concentration, the ratio is given with 1:X, where X describes the manifold amount of buffer with respect to virus material or sample. Such an adjustment of buffer/salt-concentration is called "conditioning to/conditioned" in the following. For all experiments, the A/PR virus strain was used, if not stated otherwise.

3.3 Flow-through process development

Here, the methods used for the development of a flow-through purification process for IV particles consisting of an AEC, a nuclease and a LCC step are described.

3.3.1 Screening & process steps characterization

Screening of AEC and LCC

For the AEC step, a weak and a strong anion-exchanger were tested and compared: 1 mL HiTrap™ DEAE FF (DEAE) columns (#28-9165-37, weak anion-exchanger, GE Healthcare, Uppsala, Sweden) and 1 mL HiTrap™ Capto™ Q (Capto Q) columns (#11-0013-02, strong anion-exchanger, GE Healthcare, Uppsala, Sweden). The AEC matrices were tested at flow rates of 0.2–2.0 mL/min. Before loading onto columns, the virus material was dialyzed against the corresponding loading buffer (50 mM Tris (tris(hydrodymethyl)aminomethane buffer), pH 7.4, 50–500 mM NaCl (sodium chloride)). Two mL of dialyzed virus material were loaded. Elution was performed with 2 M NaCl, 50 mM Tris, pH 7.4 (data for the eluate fraction (waste fraction) not shown).

LCC prototype material (resin: Capto™ Core 700 (Capto Core) was tested using a self-packed 1 mL column (#28-4064-08, GE Healthcare, Uppsala, Sweden). Prior loading the virus material was conditioned (1:0.25) to 150 mM NaCl, 50 mM Tris, pH 7.4 (in case of nuclease usage: addition of magnesium chloride ($MgCl_2$) (2 mM final concentration)) or dialyzed over night against 500 mM NaCl, 50 mM Tris, pH 7.4, respectively. Twenty column volumes (CV) conditioned (corresponds to 16 CV virus material) or dialyzed virus material were loaded onto a 1 mL column. A flow rate of 0.33–2.4 mL/min was set. For residence time experiments with 0.4, 1 and 3 min, the DNA of the starting material was digested with Benzonase® (300–500 U/mL for 1–2 h; #101656, Merck, Darmstadt, Germany) before loading. Virus particles were collected in the flow-through fraction based on the in-line scattered light signal.

Determination of dynamic binding capacities

For DEAE, 40 CV dialyzed virus material (dialysis against: 50 mM Tris, 250 mM NaCl, pH 7.4; corresponds to 25.6 CV undialyzed virus material) were loaded onto a 1 mL column (#28-9165-37) at a flow rate of 0.33 mL/min.

For Capto Q, 40 CV of conditioned virus material (conditioned 1:0.33 to 500 mM NaCl, 50 mM Tris, pH 7.4; corresponds to 30 CV virus material) were loaded onto a 1 mL column (#11-0013-02) at a flow rate of 1 mL/min.

For LCC, the virus material was conditioned (1:0.1) to 150 mM NaCl, 50 mM Tris, pH 7.4 and 49 CV (corresponds to 44.6 CV virus material) were loaded onto a 1 mL Capto™ Core column (resin: Capto™ Core 700 prototype; self-packed; column: #28-4064-08) at a flow rate of 0.33 mL/min.

Nuclease endpoint determination

The nuclease Benzonase® with a purity >90% was used for all experiments. Virus material (A/PR) was dialyzed against 150 mM NaCl, 50 mM Tris, 2 mM $MgCl_2$, pH 7.4 (in case of i) and ii) in Figure 18) or conditioned (1:2.33) to 150 mM NaCl, 50 mM Tris, 2 mM $MgCl_2$, pH 7.4 (in case of iii) in Figure 18; according to the later process conditions). Gentamycin (#15710049, Life Technologies, Carlsbad, USA) with a final concentration of 0.1 mg/mL was added. Benzonase® with a final activity of 50 and 300 U/mL was applied, respectively. The nuclease digestion was performed at 37°C under moderate stirring. The digestion was stopped by heat-denaturation at 72°C for 10–12 min, followed by freezing at -80°C. Residual DNA content at different time points was analyzed by PicoGreen® assay.

3.3.2 Flow-through process

The process consisted of three consecutive steps: first, an AEC step, second a nuclease step and finally a LCC step (Figure 15). After the first step, the salt concentration of the product fraction of the AEC step was adjusted by adding a high concentration salt buffer solution.

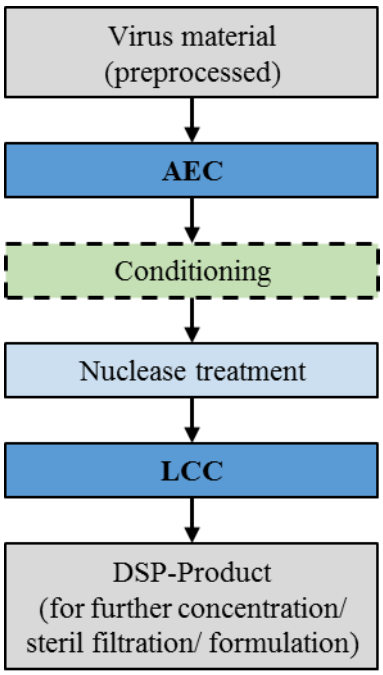

Figure 15: Overview of the flow-through process for IV purification.

Step 1: AEC

A 1 mL Capto Q column (#11-0013-02) was equilibrated with 500 mM NaCl, 50 mM Tris, pH 7.4. Virus material was conditioned (1:0.33) accordingly and 25 CV (corresponds to 18.75 CV virus material) were loaded at 1 mL/min. Elution was performed with 2 M NaCl, 50 mM Tris, pH 7.4 (data for the eluate fraction not shown).Virus particles were collected in the flow-through based on the in-line scattered light signal.

Step 2: Nuclease treatment

The flow-through product fraction from the AEC step was conditioned (1:2.33) to 150 mM NaCl, 50 mM Tris, 2 mM $MgCl_2$, pH 7.4. Gentamycin (0.1 mg/mL final concentration) and Benzonase® (applied: 50 U/mL of sample material; purity >90%) were added and incubated for 13 h at 37°C under moderate stirring.

Step 3: LCC

A 1 mL Capto Core column (resin: Capto™ Core 700 prototype; self-packed; column: #28-4064-08) was equilibrated with 150 mM NaCl in 50 mM Tris, pH 7.4 and 35 CV from the preceding process step were directly loaded onto the column at 0.33 mL/min. Virus particles were collected in the flow-through based on the in-line scattered light signal.

3.4 Membrane-based process development

Here, the methods used for the development of a membrane-based purification process for IV particles that comprises a SCMA step followed by a STMA step are described.

3.4.1 SCMA fabrication

The SCMAs were fabricated according to Wolff M. W. (2008). In short, a sulfating solution was generated by adding slowly 1.2 mL chlorosulfonic acid to 20 mL pyridine on ice. After heating to 65°C and further addition of 10 mL pyridine all precipitates were dissolved. For functionalization, unmodified reinforced cellulose sheets (pore size >3 µm, cut to discs of 2.5 cm in diameter; Sartorius Stedim Biotech GmbH, Goettingen, Germany) were incubated in that solution for about 12 h at 37°C, washed with Milli-Q® water and stored in 20% ethanol.

3.4.2 Screening & process step characterization

Since the SCMA step has been sufficiently established in the group before yielding satisfying results (Opitz et al., 2009b), the focus was put on the optimization of the STMA step.

STMA – 96-well-plate screening

Virus material (concentrated and unconcentrated) was dialyzed with 14,000 Da cut-off dialysis membranes (#0653.1) (refer to 3.2). The pre-dialyzed virus material was then adjusted to the tested buffer concentrations (refer to 4.2.1) and four times a volume of 400 µL/well was loaded onto equilibrated Sartobind STIC® PA 96-well-plates (#99STPA42GC) by centrifugation. After collecting the flow-through and washing the membranes, the bound material was eluted with increasing concentrations of sodium phosphate (Na_2HPO_4/NaH_2PO_4; pH7.4) and NaCl (up to 100 mM Na_2HPO_4/NaH_2PO_4, 2 M NaCl with 20 mM Tris, pH 7.4 or up to 350 mM Na_2HPO_4/NaH_2PO_4, 1 M NaCl with 20 mM Tris, pH 7.4) by centrifugation. All centrifugation steps were conducted at 1,000 x *g* for 2 min (centrifuge: Heraeus Multifuge 1S-R, rotor: #75002000, Thermo Scientific, Massachusetts, USA).

STMA – Preparative chromatography optimization (single-step)

Pre-dialyzed virus material was conditioned (1:2) to the required buffer concentration and 3 mL (37.5 CV) were loaded onto Sartobind STIC® PA modules (0.08 mL bed volume, pore size >3 µm, 2.9 cm^2 membrane area; #92STPA42DD-11, Sartorius Stedim Biotech GmbH, Goettingen, Germany).

For buffer optimization experiments, a range of 0-300 mM Na_2HPO_4/NaH_2PO_4 (with 600 mM NaCl, 20 mM Tris, pH 7.4) and a flow rate of 0.5 mL/min were used for loading. For flow rate optimization experiments, the pre-dialyzed material was conditioned (1:2) to 100 mM

Na_2HPO_4/NaH_2PO_4, 600 mM NaCl, 20 mM Tris, pH 7.4 and loaded with flow rates between 0.25–1.7 mL/min.

Virus particles were collected in the flow-through fraction. Elution was performed with 150 mM Na_2HPO_4/NaH_2PO_4, 2 M NaCl, 20 mM Tris, pH 7.4 at 1.3 mL/min (data for eluate fraction not shown). The modules were regenerated with 1 M sodium hydroxide and stored in 20% ethanol.

STMA strain-dependent single-process step robustness

Pre-dialyzed virus material was conditioned (1:2) to 100 mM Na_2HPO_4/NaH_2PO_4, 600 mM NaCl, 20 mM Tris, pH 7.4 and 3 mL (37.5 CV) were loaded onto a 0.08 mL Sartobind STIC® PA module (pore size >3 µm, 2.9 cm^2 membrane area; # 92STPA42DD-11) at 0.5 mL/min (A/PR) or 1.5 mL/min (A/Wis, B/Mal).

Virus particles were collected in the flow-through fraction. Elution was performed with 100 mM Na_2HPO_4/NaH_2PO_4, 2 M NaCl, 20 mM Tris, pH 7.4 at 1.5 mL/min (data for eluate fraction not shown). The modules were regenerated with 1 M sodium hydroxide and stored in 20% ethanol.

STMA – Determination of dynamic binding capacity

Pre-dialyzed virus material was conditioned (1:2) to 100 mM Na_2HPO_4/NaH_2PO_4, 600 mM NaCl, 20 mM Tris, pH 7.4 and 93 mL (1162 CV) were loaded onto a 0.08 mL Sartobind STIC® PA module (pore size >3 µm, 2.9 cm^2 membrane area; # 92STPA42DD-11) at 1.5 mL/min. The flow-through fractions were collected and analyzed for DNA content. The dynamic binding capacity (DBC) for DNA was determined at 10% breakthrough ($DBC_{10\%}$).

3.4.3 Membrane-based process

The process consisted of two consecutive membrane steps: first, a pseudo-affinity step (SCMA) and second, a salt-tolerant anion-exchange step (STMA) (Figure 16). Between both steps, the salt concentration of the product fraction of the SCMA step was adjusted by adding a high concentration salt buffer solution.

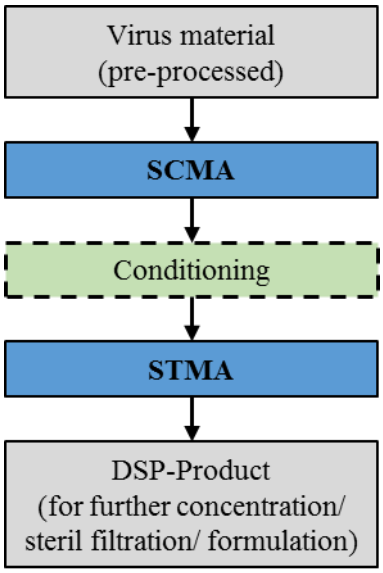

Figure 16: Overview of the membrane-based process.

Step 1: SCMA

A stainless steel housing (#1980 002, Whatman GmbH, Dassel, Germany) was packed with 10 SCMA membrane sheets (2.5 cm in diameter) and equilibrated with 50 mM NaCl, 10 mM Tris, pH 7.4. The virus material was conditioned (1:2) with 10 mM Tris buffer, pH 7.4 and 68 mL of conditioned virus material were loaded onto the SCMA module at 1.5 mL/min. Elution was performed step-wise with 2 M NaCl, 10 mM Tris, pH 7.4 at 30% (corresponding to 0.6 M NaCl, 10 mM Tris, pH 7.4) and 100% at 0.5 mL/min. Virus particle fractions were collected in the first elution step at 30% (0.6 M NaCl). Afterwards, the SCMA module was first regenerated with 1 M hydrochloric acid/1 M NaCl followed by 1 M sodium hydroxide/1 M NaCl and stored in 20% ethanol.

Step 2: STMA

The SCMA product fraction was conditioned (1:2) to 150 mM Na_2HPO_4/NaH_2PO_4, 600 mM NaCl, 20 mM Tris, pH 7.4 and 23 mL were loaded onto a 0.08 mL Sartobind STIC® PA module (pore size >3 µm, 2.9 cm^2 membrane area; # 92STPA42DD-11) at 1.5 mL/min. The loading/equilibration buffer was 150 mM Na_2HPO_4/NaH_2PO_4, 600 mM NaCl, 20 mM Tris, pH 7.4. Elution was performed with 150 mM Na_2HPO_4/NaH_2PO_4, 2 M NaCl, 20 mM Tris, pH 7.4 at 1.5 mL/min. Virus particle product fractions were collected in the flow-through. Afterwards, the STIC® PA module was regenerated with 1 M sodium hydroxide and stored in 20% ethanol.

3.5 Orthogonal process development

Following, the methods used for the development of an orthogonal chromatographic purification process (consisting of an AEC step followed by a HIC step) for IV particles are described.

3.5.1 Screening & process step characterization

Screening and process optimization was not required for the AEC step, since the conditions from section 3.3.1 (flow-through process development) could be used. Therefore, here the focus was put on the HIC step.

Critical salt concentration for virus aggregation

Undialyzed virus material (A/PR) was conditioned (1:2) with concentrated salt solutions to the tested salting-out salt concentration to identify the critical virus particle aggregation concentration (CAC). Additionally, the salt solution was adjusted to 150 mM NaCl and 20 mM Tris, pH 7.4; in case of NaCl as salting-out salt, buffers were only adjusted to 20 mM Tris, pH 7.4. Aggregation was detected by monitoring particle size distributions using a dynamic light scattering measuring device (LB-550, Horiba, Kyoto, Japan). Changes in viscosities and the refractive index due to different salts and salt concentrations were approximated (section 3.6.7). After salt addition, samples were incubated for 20 min at RT. Relative mean particle size (RMPS) was used for evaluation of aggregation for IV particles. Accordingly, all mean particle diameters were normalized to the mean particle diameter of the reference sample (150 mM NaCl and 20 mM Tris) of each samples set yielding a RMPS. A salt concentration was defined as CAC when a significant increase of mean diameter was observed. Samples were measured in duplex with a relative standard deviation ≤15.7%.

HIC – 96-well-plate screening

The method was partially based on the protocol published by Coffman et al. (2008). Each well of a 96-well filter plate (pore size: 10 µm, membrane: melt blown polypropylene, #7700-2817, Whatman, GE Healthcare, Chicago, USA) was loaded with 300 µl of the following chromatography resins (40% slurry in 20% ethanol): SEC-HW 65 C (SEC) (#21481, Tosoh, Tokyo, Japan), Methyl HIC Support Macro Prep (Me, Methyl) (#158-0080, Bio-Rad Laboraties, Hercules, USA), Ether-650M (Eth, Ether) (#19805, Tosoh, Tokyo, Japan), PPG-600M (PPG) (PPG: polypropylene glycol groups, #21301, Tosoh, Tokyo, Japan), Phenyl-650M (Phe, Phenyl) (#19818, Tosoh, Tokyo, Japan), Butyl-650M (But, Butyl) (#19802, Tosoh, Tokyo, Japan), Super-Butyl-550C (SBu, Super-Butyl) (#19955, Tosoh, Tokyo, Japan), and Hexyl-650C (Hex, Hexyl) (#44465, Tosoh, Tokyo, Japan). Ethanol was removed by

centrifugation at 1,200 x *g* for 3 min. Next, each well of the filter plate was equilibrated with 400 µl of water and twice with 400 µl loading buffer containing a concentration of salting-out salt according to section 4.2 (ammonium sulfate ($(NH_4)_2SO_4$), trisodium citrate ($Na_3C_6H_5O_7$), NaCl, or $MgCl_2$). Additionally, the loading buffer contained 150 mM NaCl and 20 mM Tris, pH 7.4 (in case of NaCl as salting-out salt, the loading buffer contained only 20 mM Tris, pH 7.4, in addition). Following, 400 µl of conditioned virus material (A/PR, 1:2 conditioned with loading buffer) was added into each well, mixed at 1,300 rpm for 15 min and centrifuged at 1,200 x *g* for 3 min. Next, three washing steps were performed. For each washing step 400 µl of loading buffer was added into each well, mixed at 1,300 rpm for 5 min and centrifuged at 1,200 x *g* for 3 min. Following, four elution steps were performed with an elution buffer containing 150 mM NaCl and 20 mM Tris at pH 7.4. For each elution step 400 µl of elution buffer was added into each well, mixed at 1,300 rpm for 5–10 min and centrifuged at 1,200 x *g* for 3 min. All mixing was performed with a thermomixer (Eppendorf, Hamburg, Germany). The flow-through of the sample loading, the washing and the elution steps were collected and dialyzed with 14,000 Da cut-off dialysis membranes (#0653.1) against 50 mM NaCl, 20 mM Tris, pH 7.4 at 4°C overnight. Virus particle quantification was performed by HA assay (section 3.6.1) and DNA was quantified by Quant-iT™ PicoGreen™ assay (PicoGreen®, section 3.6.3). All experiments were performed in duplicates.

HIC – General conditions for preparative chromatography

Virus material was conditioned (1:2) to the required buffer concentration and loaded onto equilibrated pre-packed 1 mL HIC columns (ToyoScreen® HIC Mix Pack, #21398, Tosoh, Tokyo, Japan) at a flow rate of 1 mL/min (if not stated otherwise). Salt concentrations of the loading buffer and the conditioned virus material as well as the used HIC columns and the amount of the loaded (conditioned) virus material used, are described below. In general, virus particles were collected in the eluate fraction (product fraction). Elutions were performed with 150 mM NaCl, 20–50 mM Tris, pH 7.4 at 1.0 mL/min using a linear gradient of 10 column volumes (CV). The columns were regenerated with water and 0.5 M sodium hydroxide and stored in 20% ethanol.

For "HIC – Preparative chromatography and optimization (single-step)" experiments a range of 0.45–1.6 M $(NH_4)_2SO_4$ (with 150 mM NaCl, 20 mM Tris, pH 7.4) and 10 CV of conditioned virus material (A/PR) was used for loading onto the Ether, PPG or Phenyl columns.

In “HIC – Salt performance based on ion strength” experiments 3 CV of virus material (A/PR) conditioned in a range of 0–1.04 M $(NH4)_2SO_4$, 0.15–3.27 M NaCl and 0–0.61 M $Na_3C_6H_5O_7$, and a 1 mL Phenyl HIC column was used.

For “HIC – Flow rate dependencies” experiments a 1 mL Phenyl HIC column was loaded with 10 CV of conditioned (1:2) virus material at a flow rate of 0.3–1.3 mL/min. A concentration of 0.928 M $(NH_4)_2SO_4$, 0.15 M NaCl, 50 mM Tris, pH 7.4 was used for equilibration and loading. Elutions were performed with 150 mM NaCl, 50 mM Tris, pH 7.4 with a linear gradient at the corresponding flow rate.

In “HIC – Salt effects on HA protein recovery” experiments 1.15 M $(NH_4)_2SO_4$ with 150 mM NaCl, 50 mM Tris, pH 7.4, and 18 CV of conditioned virus material (A/PR) was used (PPG column).

For “HIC – Effects of process conditions adaptation” experiments 1.063 M $(NH_4)_2SO_4$ with 0.41 M NaCl, 50 mM Tris, pH 7.4, and 18 mL of conditioned virus material (A/PR) was used (PPG column).

In “HIC – Influenza virus strain dependency/single-process step robustness” experiments loaded amount of virus material was adjusted based on the DBC determined at 10% breakthrough ($DBC_{10\%}$) for A/PR virus material for the corresponding conditions. Consequently, 18 CV (A/PR), 10.9 CV (A/Wis) or 4 CV (B/Mal) of conditioned virus material with 1.15 M $(NH_4)_2SO_4$, 150 mM NaCl, 50 mM Tris, pH 7.4 was used for loading onto a PPG column.

HIC – Determination of dynamic binding capacities

Virus material (A/PR) was conditioned (1:2) to 0.5–1.15 M $(NH_4)_2SO_4$, 0.15–1.8 M NaCl, 50 mM Tris, pH 7.4, and 50 CV were loaded onto a pre-packed 1 mL Phenyl-650M or PPG-600M column (ToyoScreen® HIC Mix Pack, #21398) at 1.0 mL/min. The flow-through fractions were collected and analyzed for virus particle content (HA assay). The DBC for virus particles was determined at $DBC_{10\%}$.

3.5.2 Orthogonal process

The process consisted of two consecutive chromatographic steps: first an AEC step and second a HIC step (Figure 17). Between both steps, the salt concentration of the product fraction of the AEC step was adjusted by adding highly concentrated salting-out salt buffer solution (conditioning).

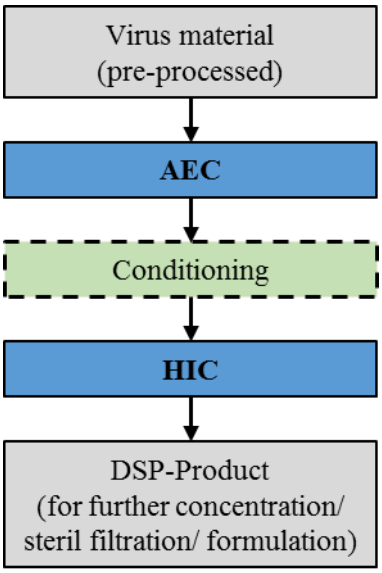

Figure 17: Overview of the orthogonal process.

Step 1: AEC

A 5 mL AEC HiTrap™ Capto™ Q column (#11-0013-03, GE Healthcare Life Science, Freiburg, Germany) was equilibrated with 500 mM NaCl, 50 mM Tris, pH 7.4. Virus material was conditioned (1:0.33) accordingly, and 16 CV of conditioned virus material (corresponds to 12 CV virus material) were loaded at 5 mL/min. Elution was performed with 2 M NaCl, 50 mM Tris, pH 7.4 (data for eluate (waste) fraction not shown). Virus particles were collected in the flow-through based on the online scattered light signal.

Step2: HIC

The AEC product fraction was conditioned (1:1.25) to 1.063 M $(NH_4)_2SO_4$, 0.41 M NaCl, 50 mM Tris, pH 7.4, and 18 CV were loaded onto a 5 mL PPG-600M column (ToyoScreen® HIC Mix Pack, #21399, Tosoh, Tokyo, Japan) at 5 mL/min. The loading/equilibration buffer was 1.063 M $(NH_4)_2SO_4$, 0.41 M NaCl, 50 mM Tris, pH 7.4. Elution was performed with 150 mM Na_2HPO_4/NaH_2PO_4, 50 mM Tris, pH 7.4 at 1.0 mL/min with a linear gradient (10 CV). Virus particles were collected in the eluate based on the online scattered light signal.

3.6 Analytical methods

Several analytical methods have been applied for this work. The used standard operation procedures (SOPs) are listed below in Table 4. Furthermore, relevant deviations from or improvements of the SOPs are stated in the text sections.

Table 4: SOPs used for the assays.

Assay	SOP title	Version/date
Hemagglutination assay	HA assay	2.1/30.11.06
Total protein assay	Protein estimation in microtiter plates	2.2/07.03.08
DNA – intermediate range	dsDNA estimation in microtiter plates	2.3/07.03.08
DNA assay – low range	Threshold® assay for DNA-Quantification	1.0/not specified
Single radial immunodiffusion assay	Single-Radial-Immunodiffusion (SRID)-assay	1.3/12.01.2011

Prior use in assays, samples were dialyzed against 150 mM NaCl, 20–50 mM Tris, pH 7.4 or against 15 mM NaCl, 5 mM Tris, pH 7.4 (in case of following lyophilization) with 3,500 Da cut-off membranes or 14,000 Da cut-off dialysis membranes (#132720; #0653.1) at 4°C overnight. All assay standards were prepared in the dialysis buffer corresponding buffer.

3.6.1 Hemagglutination assay (HA assay)

The hemagglutination (HA) assay measuring hemagglutination activity (HA-activity, reported as kHAU/mL sample) was used for virus particle quantification as described by Kalbfuss et al. (2008), originally reported by Mahy et al. (1996). Briefly, serial dilutions of the virus-containing samples in 100 µL phosphor buffered saline (PBS) were incubated with chicken erythrocytes (100 µL $2*10^7$ cells/mL) in 96-well-plates over night at RT. The 96-well-plates were scanned photometrically at 700 nm (Infinity M200 Pro, Tecan, Männedorf, Switzerland) and the inflection point (red-blood-cell settlement to the agglutinated blood cells) was automatically detected by applying a Boltzmann sigmoid fit to the data (data plotted against the negative logarithm of the dilution factor d; evaluation between the HA-activity titer of –log d = 1 and 3 corresponding to 10 and 1000 HAU/100 µL, respectively). The specific dilution factor at this point was defined as the amount of hemagglutination activity units (HAU, HA-activity) per 100 µL. The HA-activity values were used for determining the corresponding virus recoveries (i.e. ratio of HA-activity in the eluate or flow-through fraction per HA-activity in the virus material loaded onto the column or into the well, given in %) for all experiments. For 96-well-plate screening experiments and determination of dynamic binding capacities, single measurements were made. For all other experiments, samples were measured in duplicates with a relative standard deviation ≤10.7%.

3.6.2 Total protein assay

The total protein content (proteins from cell culture medium, host-cells and virus particles) was determined with a Bio-Rad assay (#500-0006, Bio-Rad Laboratories, Hercules, USA). Seven standard concentrations of BSA (#A3912, Sigma–Aldrich, St. Louis, USA) in a range of 5–40 µg/mL was used for assay calibration. After thermomixer incubation of 200 µl standard or sample with 50 µl of Bio-Rad assay dye reagent at 1000 rpm and RT, the 96-well-plates were scanned at 595 nm (Infinity M200 Pro). For the calibration curve a sigmoid fit was used. Samples were measured in triplicates and concentrated by lyophilization, if required. The relative standard deviation of independent sample dilutions was ≤11.7%.

3.6.3 DNA assay – intermediate range

As a first and fast control of DNA concentrations, a PicoGreen® assay (#P7581, Life Technologies, Carlsbad, USA) was used as described by Wickramasinghe et al. (2005) and Kalbfuss et al. (2007a). In short, 200 µL of each sample was mixed with 50 µL of a 1/60 TE-buffer (200 mM Tris, 20 mM EDTA, pH: 7.5) diluted PicoGreen® working solution in a 96-well-plate. After mixing at 1000 rpm for 5 min on a thermomixer, the fluorescence signal was measured (Infinity M200 Pro). For the standard curve, Lambda DNA (#D1501, Promega; Madison, USA) in a range of 4–1,000 ng/mL with a sigmoidal fit was used. Samples were measured in duplicates and concentrated by lyophilization, if required. The relative standard deviation of independent sample dilutions was ≤8.7%. The limit of detection (LOD) was given with 0.66 ng/mL. The LOQ was given with 2.36 ng/mL. The PicoGreen® assay was used for all DNA quantifications, if not stated otherwise.

3.6.4 DNA assay – low range

For accurate determination of DNA impurity levels for dose estimations, the DNA concentrations of the final product fractions were measured using a Threshold® system (MDS Analytical Technologies, Sunnyvale, USA) and a Threshold® Total DNA Assay Kit (Threshold® assay) (#R9009; MDS Analytical Technologies, Sunnyvale, USA) as described by Wolff et al. (2010). Due to its LOQ and its high reliability the Threshold® assay has been commonly used in industry and generally accepted by regulatory authorities.

In short, after protease treatment and DNA extraction using a DNA extractor kit (Cat.# 295-58501; Wako Chemicals GmbH, Neuss, Germany) the samples were adjusted to 500 mL with Zero Calibrator solution and heat denatured at 105°C for 15 min. Next, 1 mL of the supplied Threshold® Kit labeling reagent (containing biotin-conjugated, single-stranded DNA binding protein, streptavidin, and urease-conjugated monoclonal antibody) were added and incubated

for 1 h at 37°C. The samples were transferred to the Threshold workstation and mixtures were filtered through biotin-coated nitrocellulose membrane adsorber by vacuum. Next, the membrane adsorbers were transferred to the Threshold reader. Using a 5 M urea substrate solution (containing 0.05% NaN_3), the change in pH was measured – caused by the hydrolysis performed by captured urease in the DNA–protein complexes. For the standard curve, calf thymus DNA in a range of 6.2–400 pg/mL was used. For estimation of assay signal recoveries according to the manufacturer's recommendation, a second set of three samples was spiked with 50 pg of calf thymus DNA. Samples were measured in triplicates. The relative standard deviation of the assay was ≤10% according to the manufacturer.

3.6.5 Single radial immunodiffusion assay (SRID)

Mainly for estimation of the antigen input per dose, the virus HA protein content of the final product fraction was quantified by an SRID assay (Wood et al., 1977). Virus HA protein content is reported as "HA protein". For the virus strain A/PR an in-house produced HA standard was used, while the A/Wis and B/Mal standards as well as the anti-HA sera for all strains were purchased from National Institute for Biological Standards and Control (#06/120, #06/126, and #05/236, #03/242, #07/184, London, UK). All samples were dialyzed against 15 mM NaCl, 5 mM Tris, pH 7.4. After adjusting a final concentration of 1% sucrose as freeze-/lyoprotector the samples were lyophilized (remark: for the initial flow-through process characterization (4.1.3), no freeze-/lyoprotector was used). The following resuspension resulted in an up to 20-fold concentration of the sample according to the HA assay value. A 1% agarose gel containing 13 µL (for A/PR), 8 µL (for A/Wis) or 15 µL (for B/Mal) antiserum per mL gel was used as SRID diffusion matrix, respectively. The assay standard deviation of technical replicates was determined with ±8.2%. All samples were measured in duplicates.

The in-house standard was produced by purifying virus material with SCMA and lectin affinity chromatography (Opitz et al., 2008; Opitz et al., 2009b). The HA protein content was quantified by Bradford assay in combination with gel densitometrical quantifications. For the latter, the sample was treated with 100 U PNGase F/µg total protein at 37°C for 3 h (#P0704S New England Biolabs, Massachusetts, USA) before loading onto a sodium dodecyl sulfate-polyacrylamide gel electrophoresis (SDS-PAGE) gel (remark for the flow-through process characterization: A/PR standard batch without applying PNGase was used in the HA protein quantification.)

3.6.6 Benzonase® ELISA (Enzyme-Linked Immunosorbent Assay)

For determination of residual Benzonase® concentration the final product fractions were analyzed by the Benzonase® ELISA Kit II (#101681, Merck, Darmstadt, Germany). A standard curve between 0.2–25 ng/mL Benzonase® was prepared. Samples were dialyzed against PBS (pH 7.2) and diluted at least 1/2 with this buffer containing 1% Tween20 according to the manufacturer's instructions. One hundred µL of sample was incubated for 2 h at RT in antibody-coated 96-well-plates. After washing, 100 µL of 1/100 diluted horse radish peroxidase conjugated antibody was incubated in the wells for 1 h at RT. After further washing, 60 µL 3,3',5,5'-tetramethylbenzidine was added and incubated for 15 min at RT. The enzymatic reaction was stopped by adding 140 µL of 0.2 M sulfuric acid. The absorbance was measured at 450 nm using a plate reader (Infinity M200 Pro). The LOD was 0.2 ng/mL and the relative standard deviation (precision) of the assay was 20% according to the manufacturer. All samples were measured in triplicates.

3.6.7 Mean particle size analysis

Mean particle size determination for detection of aggregation was performed using a dynamic light scattering measuring device (LB-550, Horiba). For all measurements, by approximation a particle refractive index of 1.440 (Liposomes) was chosen. For the salt-buffer solutions, refractive indexes and viscosities were approximated by using reference data for salt-water-systems (Lide et al., 2009) and a salt-specific polynomial fitting function (annex section 9.1.3/Figure 39). As reference, virus material conditioned in the ratio accordingly to the other samples but using a buffer solution consisting of 150 mM NaCl and 20 mM Tris was used. Here, the refractive index and viscosity of water (1.333 and 0.910 mPas, respectively) was assumed for approximation. About 600 µL or 400 µL of sample was filled into a standard or micro-cuvette, respectively, and mean particle size was measured twice for 120 s. Between measurements, the samples were mixed carefully by pipetting. Samples were measured in duplex with a relative standard deviation ≤15.7%.

4 Results and Discussion

Following, three different processes are presented for purification of clarified, inactivated, concentrated IV harvests. If a specific recovery value is not further specified, it is always referring to the product fraction, i.e. in case of virus recovery to the virus yield.

4.1 Flow-through process (AEC-nuclease-LCC)

The following section describes the development of the flow-through process. It comprises a screening of AEC matrices and conditions, the characterization of a nuclease digestion step, the implementation of the LCC step and a robustness test of the final flow-through process train with three IV strains. Furthermore, the results of the final flow-through process are re-evaluated based on follow-up experiments.

4.1.1 Results: Screening & process steps characterization

Screening of AEC and LCC

In order to select the optimal AEC resin and optimal binding conditions for DNA, the performance of two AEC resins and one LCC resin were investigated with respect to salt concentration and residence time. The influenza strain A/PR was used for all screenings.

In the AEC screening, DEAE and Capto Q were tested with different NaCl concentrations in the loading buffer and residence times. The relevant results for the flow-through fractions are shown in Table 5.

Table 5: Screening for optimal conditions of the AEC resins DEAE and Capto Q. NaCl concentration in the loading buffer and residence time were modified. Shown are relevant results for the flow-through fractions (product fraction). Used influenza strain: A/PR. Virus and DNA recoveries were determined by HA and PicoGreen® assay, respectively.

NaCl concentration	Residence time	Recovery		DNA/Virus
		Virus	DNA	
[mM]	[min]	[%]	[%]	[-]
AEC resin: DEAE				
50	5	0	<0.3 [a]	-
175	5	32 [b]	<0.3 [a,b]	$<9.4 * 10^{-3}$
210	5	73	<0.3 [a]	$<4.1 * 10^{-3}$
250	5	81 [c]	0.7 [c]	$8.6 * 10^{-3}$
350	5	93	1.6	$17.2 * 10^{-3}$
500	5	95	101	106.3
250	0.5	92	0.9	$9.8 * 10^{-3}$
250	1	87	0.8	$9.2 * 10^{-3}$
250	3	86	0.5	$5.8 * 10^{-3}$
250	5	81 [c]	0.7 [c]	$8.6 * 10^{-3}$
AEC resin: Capto Q				
500	0.5	108	1.5	$13.9 * 10^{-3}$
500	1	101	1.1	$10.9 * 10^{-3}$
500	2	101 [b]	1.2 [b]	$11.9 * 10^{-3}$
500	4	98	1.2	$12.2 * 10^{-3}$
500	10	77 [b]	1.6 [b]	$20.8 * 10^{-3}$

[a] out of assay range
[b] mean of technical replicates, n=2
[c] same experiment

Optimal conditions regarding DNA depletion with acceptable virus recoveries (>80%) were found for DEAE at a salt concentration of 250–350 mM NaCl. Here, virus recovery was in the range of 81–93% with residual DNA content of 0.7–1.6%. With increasing residence time (0.5–5 min) virus recovery seemed to drop slightly (92→81%) while DNA levels remained more or less constant (0.5–0.9%) (Table 5).

For Capto Q the optimal salt concentration (500 mM NaCl) for the applied pH range (7.2−7.4) was taken from literature (GE Healthcare, 2010). For a residence time in the range of 1–4 min

HA recoveries between 98–101% were obtained, while also the DNA level was more or less stable in the range of 1.1–1.2% (Table 5).

For LCC virus recoveries (yields) of 93–96% for 150 and 500 mM NaCl were achieved, respectively (Table 6). Furthermore, the DNA and total protein levels were reduced to 71–83% and 31–43%, respectively. Closer examination of recoveries and total protein contamination levels at 150 mM NaCl demonstrated that residence time had no significant influence on results in the range of 0.4–3 min (Table 6).

Table 6: Screening for optimal conditions of the LCC resin Capto Core. NaCl concentration in the loading buffer and residence time were modified. Shown are results for the flow-through fractions (product fraction). Used influenza strain: A/PR. Virus, DNA and total protein recoveries were determined by HA, PicoGreen® and Bradford assay, respectively.

NaCl concentration	Residence time	Recovery		
		Virus	DNA	Total protein
[mM]	[min]	[%]	[%]	[%]
150	3	93	71	43
500	3	96	83	31
150	0.4 [a]	93	ND	39
150	1 [a]	92	ND	37
150	1.5	94	ND	39
150	3 [a]	92	ND	37

[a] nuclease pretreated material loaded
ND: not determined, as focus of this unit operation was on protein depletion.

Dynamic binding capacities

The AEC resin DEAE showed a low $DBC_{2\%}$ of <108 µg DNA/mL resin. For Capto Q no breakthrough for DNA could be observed with the loaded amount of virus material (30 CV), giving a $DBC_{2\%}$ >281 µg DNA/mL resin. With the LCC resin the breakthrough for total protein was also not reached (loaded amount of virus material: 44.6 CV), yielding a DBC >1.57 mg total protein/mL resin (data not shown).

Nuclease endpoint determination

Two nuclease activities (50 and 300 U/mL) and two DNA starting concentrations (6837 ng/mL and 126 ng/mL) were tested with respect to incubation time using dialyzed virus material (Figure 18). Furthermore, the potential impact of ions in the virus material (as used in the later

process train) on the nuclease performance was examined by using undialyzed but conditioned virus material.

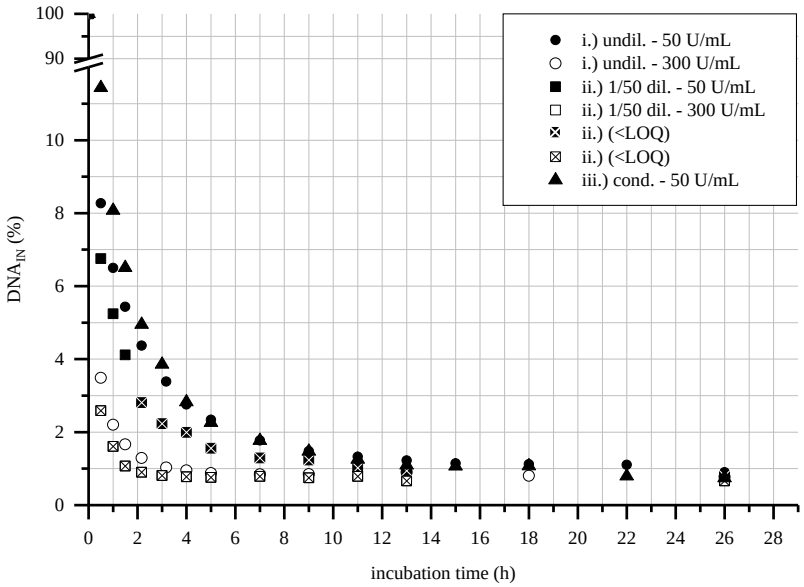

Figure 18: Endpoint determination of digestion of DNA by nuclease with variations in nuclease amount, DNA starting concentration and buffer composition. Values are set in proportion to the starting DNA concentrations (DNA_{IN}). A/PR virus material was used for all experiments. Legend: **i)** "undil. (undiluted) – 50 U/mL", "undil. – 300 U/mL": 50 and 300 U/mL nuclease tested with dialyzed undiluted virus material; starting DNA concentration 6837 ng/mL. **ii)** "1/50 dil. (diluted) – 50 U/mL", "1/50 dil. – 300 U/mL": 50 and 300 U/mL nuclease tested with dialyzed 1/50 diluted virus material; starting DNA concentration: 126 ng/mL. The crossed points (see legend: "(<LOQ)") indicate values below the limit of quantification of the DNA assay (PicoGreen®) in this experimental set. **iii)** "cond. (conditioned) – 50 U/mL": 50 U/mL nuclease tested with undialyzed virus material conditioned as in the process; starting DNA concentration 1650 ng/mL.

For the dialyzed undiluted virus material complete DNA digestion was not achieved (Figure 18; i). With both nuclease activities (50 and 300 U/mL) similar final DNA levels of 0.8% (53 ng/mL) and 0.9% (62 ng/mL) (reduction by about two orders of magnitude) were reached after 26 h. While with 300 U/mL most DNA was digested after 5 h (DNA level: 0.9%; 60 ng/mL), with 50 U/mL a minimum of 13 h was required (DNA level: 1.2%; 84 ng/mL).

For a DNA starting concentration comparable to the level after an AEC purification (about 71–149 ng/mL), a test with a 1/50 dil. dialyzed material (126 ng/mL) was performed (Figure 18; ii), but even early samples were below the limit of quantification (LOQ).

Finally, using conditioned virus material and a nuclease activity of 50 U/mL, the enzymatic digestion process was completed with a residual amount of 1.1% (18.1 ng/mL) after 13 h

(Figure 18; iii), and no significant adverse effect of the medium on the nuclease activity (e.g., by monovalent ions) could be found with respect to the final DNA concentration.

4.1.2 Discussion: Screening & process steps characterization

Screening of AEC and LCC including dynamic binding capacities

A strong and a weak AEC resin (Capto Q and DEAE) were compared. Both showed a strong and comparable reduction of DNA in the virus material. Although showing a slightly lower DNA depletion performance than DEAE (at virus recoveries >80%: DEAE: 0.7% versus Capto Q: 1.1%; Table 5), Capto Q was chosen over the DEAE for the final flow-through process due to the higher DBC (>>2.6 fold). Moreover, weak AEC resins, such as DEAE, have general drawbacks: High charge variability with respect to pH can affect capacity or selectivity. Also, weak AEC resins can act as solid phase buffers which might lead to significant increase in pH during chromatography (Gagnon, 2013). Overall, the selected strong AEC seems to be a good compromise regarding DNA reduction, virus yield, DBC and process robustness.

With respect to virus recovery, both AEC resins showed a residence time dependency. With decreasing flow rates, the amount of bound virus particles increased (reduced virus particle content in the flow-through fraction; Table 5). Virus particles are mostly excluded from pores due to their size, which renders pore diffusion effects unlikely to be the source. Possibly, a lower shear force might be the reason for an increase in bound virus particles at reduced flow rates. Regarding the DNA depletion, no clear trend could be observed with respect to the tested flow rates.

The high virus recoveries seen for LCC (Table 6; >93%) are in accordance with its special resin features (unfunctionalized outer layer and spatial exclusion of the virus particle by the resin pores). Furthermore, the resin showed a wide salt tolerance with high virus recoveries. The substantial removal of proteins (Table 6; ≤69% of total protein) in the tested range of salt concentrations is in accordance with the ligand type of this resin (octylamine), which has not only strong anionic but also strong hydrophobic binding characteristics. The poor depletion of DNA observed in both first cases (Table 6) was probably due to high DNA fragment length exceeding the pore size of the beads (700 kDa molecular weight cut-off). Within the tested protein concentration range the flow rate had no impact on the protein removal efficiency. The small variation in total protein levels are in the typically range of variation observed in scouting experiments (data not shown). Nevertheless, at higher protein concentrations a dependency of purification performance and flow rate could become apparent due to pore diffusion effects.

Since a $DBC_{2\%}$ of the LLC resin for total proteins could not be reached (>1.57 mg total protein/mL resin), the DBC is more than sufficient for intended protein removal.

Nuclease endpoint determination

Various concentration and digestion times have been reported for virus particle purification in vaccine or viral vector manufacturing processes ranging from 1 U/mL to 1000 U/mL, and from 15 min to 24 h (2–37°C) (Hagen et al., 1996a; Sastry et al., 2004; Kistner et al., 2007; Transfiguracion et al., 2007; Allay et al., 2011; Bandeira et al., 2012; Vyas et al., 2012). Therefore, optimal parameters had to be tested specifically for the presented process.

Experiments with various starting materials using 50 U/mL and 300 U/mL nuclease showed that complete digestion of DNA could apparently not be reached under the used conditions even at extended incubation times (residual DNA concentration: 53–62 ng/mL; digestion time: 26 h; Figure 18; i). However, the trend observed in the case of 1/50 dil. dialyzed virus material (Figure 18; ii); DNA starting concentration: 126 ng/mL), which mimic a similar DNA level as after the AEC step (71–149 ng/mL), demonstrated high potential for the three-step process (remark: relevant values were below LOQ of the intermediate range DNA assay (PicoGreen® assay)).

In the literature, few processes had been described where the Benzonase® has shown to achieve a complete digestion of DNA (Sastry et al., 2004). In other downstream processes dealing with viral material, a small DNA level usually seemed to remain (Hagen et al., 1996b) especially if Benzonase® was used on unpurified material (Merten et al., 2011; Bandeira et al., 2012; GE Healthcare, 2012b). In the presented work an unspecific Benzonase® degradation (for instance by protease activity of the virus harvest) seems unlikely as spiking of Benzonase®-treated samples with fresh virus material showed high residual Benzonase® activity (data not shown). This suggests that residual DNA might not be accessible for the nuclease. A possible explanation might be the binding of DNA to proteins or virus particles, which might in addition trigger virus particle aggregation. For a more detailed discussion, please refer to section 4.4.

With respect to costs and process time a nuclease activity of 50 U/mL for 13 h was selected for the final process. An extension of the nuclease step beyond 13 h could be shown to have little effect on final DNA contamination levels. Previous dialysis/diafiltration was not necessary (refer to 3.2) which minimizes the number of process steps.

4.1.3 Results: Flow-through process

Process performance and robustness

In Figure 19, the performance for each step of the flow-through process (AEC (Capto Q), nuclease treatment, LCC) as well as the final recoveries of the proposed three-step process are shown for A/PR, A/Wis and B/Mal IV strains. Furthermore, Table 7 shows the corresponding concentrations and volumes of the process steps. For the corresponding chromatograms refer to the annex section 9.1.1.

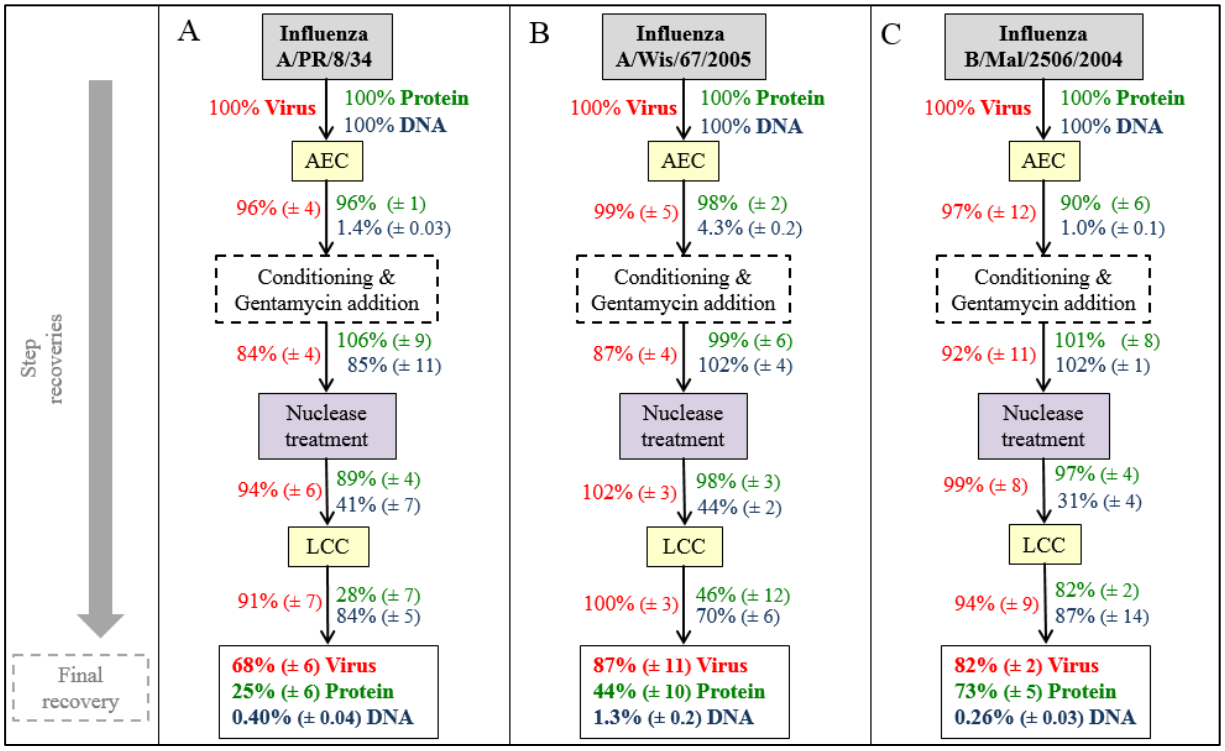

Figure 19: Flow-through process performed with three influenza strains. Shown are the step and the final recoveries (in %) in the product fractions measured by HA (→ Virus), PicoGreen® (→ DNA) and Bradford assay (→ Protein). **A)** influenza strain A/PR; **B)** influenza strain A/Wis; **C)** influenza strain B/Mal. The virus material for the AEC step was pre-processed and conditioned as described in section 3.1. Mean and standard deviation of technical replicates, n=3.

In the first process step, the AEC resulted in a reduction of DNA to a level of 1.0–4.3% with less than 4% loss in virus recovery. The total protein level remained almost unchanged with a minimum of 90% for B/Mal. The following conditioning step was required to adjust buffer conditions for optimal nuclease activity in the next step. In addition, gentamycin was added to suppress bacterial growth in process material potentially contaminated due to unsterile process conditions under laboratory conditions. This conditioning and addition of gentamycin, however, led to a significant loss of HA activity in the process of 8–16%. In the following

nuclease digestion step, more than 94% of virus particles were recovered while the DNA could be further depleted by 56–69%. Finally, during the third process step (LCC), less than 9% of the virus particles were lost, while total protein could be depleted to 28–82%. In addition, the level of DNA was further reduced by up to 30%.

Overall, the final virus recoveries were 68% (A/PR), 87% (A/Wis), and 82% (B/Mal), respectively. Final total protein levels could be reduced to 25%, 44% and 73% (including the viral proteins), and the levels of residual DNA decreased to 0.4%, 1.3% and 0.26%, respectively. For all IV strains the residual amount of the nuclease added after the AEC step was below the limit of detection in the final harvest (data not shown; refer to supervised master thesis (Peuker, 2013)).

Table 7: Flow-through process performed with three influenza strains. Corresponding process data to Figure 19. Shown are the volumes and concentrations (HA-activity) of virus particles (a_{HA}), DNA and total protein for each process step product fraction (entering (IN) and exiting (OUT)). Mean and standard deviation of technical replicates, n=3.

Steps	Volume [mL]				a_{HA} [kHAU/mL]				DNA [ng/mL]				Total protein [µg/mL]			
	IN		OUT		IN		OUT		IN		OUT		IN		OUT	
A/PR																
AEC	25.0	(±0.0)	29.8	(±0.0)	31.5	(±2.7)	25.3	(±2.0)	6138	(±233)	70.5	(±1.2)	42.8	(±2.5)	34.7	(±2.4)
Conditioning & gentamicin addition	23.3	(±0.6)	78.5	(±1.9)	25.3	(±2.0)	6.3	(±0.2)	70.5	(±1.2)	17.8	(±2.6)	34.7	(±2.4)	10.9	(±0.3)
Nuclease treatment	60.4	(±0.7)	60.4	(±0.7)	6.3	(±0.2)	5.9	(±0.6)	17.8	(±2.6)	7.3	(±0.2)	10.9	(±0.3)	9.7	(±0.4)
LCC	35.0	(±0.0)	39.4	(±0.0)	5.9	(±0.6)	4.8	(±0.2)	7.3	(±0.2)	5.4	(±0.4)	9.7	(±0.4)	2.4	(±0.6)
A/Wis																
AEC	25.0	(±0.0)	29.8	(±0.0)	25.9	(±1.6)	21.4	(±0.3)	2007	(±46)	72.0	(±4.3)	36.2	(±1.0)	29.8	(±1.1)
Conditioning & gentamicin addition	23.0	(±0.0)	77.4	(±0.0)	21.4	(±0.3)	5.5	(±0.2)	72.0	(±4.3)	21.9	(±1.7)	29.8	(±1.1)	8.8	(±0.6)
Nuclease treatment	61.9	(±0.2)	61.9	(±0.2)	5.5	(±0.2)	5.6	(±0.4)	21.9	(±1.7)	9.5	(±0.9)	8.8	(±0.6)	8.7	(±0.9)
LCC	35.0	(±0.0)	39.3	(±0.0)	5.6	(±0.4)	5.0	(±0.4)	9.5	(±0.9)	6.0	(±0.8)	8.7	(±0.9)	3.6	(±0.9)
B/Mal																
AEC	25.0	(±0.0)	30.5	(±0.6)	70.0	(±7.8)	55.3	(±1.7)	19132	(±722)	149.1	(±5.4)	74.5	(±3.5)	55.1	(±3.2)
Conditioning & gentamicin addition	22.9	(±0.1)	77.1	(±0.5)	55.3	(±1.7)	15.2	(±1.9)	149.1	(±5.4)	45.2	(±1.5)	55.1	(±3.2)	16.5	(±0.4)
Nuclease treatment	61.7	(±0.2)	61.7	(±0.2)	15.2	(±1.9)	15.0	(±0.7)	45.2	(±1.5)	13.9	(±1.4)	16.5	(±0.4)	16.1	(±0.4)
LCC	35.0	(±0.0)	39.4	(±0.0)	15.0	(±0.7)	12.6	(±1.8)	13.9	(±1.4)	10.6	(±1.1)	16.1	(±0.4)	11.7	(±0.2)

Impurity level estimation

In Table 8, the total amount of HA determined by SRID assay, the DNA contamination level determined by the Threshold® assay and the total protein levels of the final product together with estimations for dose contaminant levels are shown.

Table 8: Final product fraction of the flow-through purification process for IV A/PR, A/Wis and B/Mal. Shown are the HA protein concentrations, relevant impurity levels, and estimated impurity levels for a dose input of 15 µg HA protein (monovalent dose for cell culture-derived vaccines for human use). HA protein concentration was determined by SRID assay as required for blending of human influenza vaccines. For the DNA level determination in the final product, the Threshold® assay was applied. Total protein concentration is based on Bradford assay. Mean and standard deviation of technical replicates, n=3.

	IV strain A/PR	IV strain A/Wis	IV strain B/Mal
Measured concentrations			
HA [µg/mL]	2.0 (±0.6)	3.1 (±0.3)	4.2 (±0.3)
DNA [ng/mL] (Threshold® assay)	1.0 (±0.1)	1.5 (±0.9)	1.2 (±0.1)
Total Protein [µg/mL]	2.4 (±0.6)	3.6 (±0.9)	11.7 (±0.2)
Estimated impurities			
ng DNA/15 µg HA [a]	7.3 (±1.4)	7.8 (±5.0)	4.2 (±0.8)
µg Total Protein/15 µg HA	18.7 (±7.9)	17.3 (±3.3)	41.9 (±3.5)

[a] calculations based on Threshold® assay data

The different strains had a final HA content between 2.0 and 4.2 µg/mL (unconcentrated harvest from LCC step). For A/PR 7.3 ng DNA and 18.7 µg total protein, for A/Wis 7.8 ng DNA and 17.3 µg total protein, and for B/Mal 4.2 ng DNA and 41.9 µg total protein were calculated per dose of vaccine (Table 8). Accordingly, the total protein amounts per dose were below the required limits for all strains despite the previously mentioned variations in depletion efficiency. Regarding the DNA, the limit was exceeded 1.3–2.4 fold for the three virus strains (based on a limit of 3.33 ng DNA per strain for a trivalent dose).

4.1.4 Discussion: Flow-through process

Process performance and robustness

The starting material of three different influenza strains for the establishment of the purification process showed a relatively high variation in viral HA, DNA and protein starting concentrations (Table 7). Therefore, starting conditions mimic closely potential variations in the virus harvest of industrial manufacturing processes.

Overall, the combination of AEC, nuclease treatment and LCC resulted in high virus recoveries for all IV strains, as shown in Figure 19 (≥96% for AEC step and ≥91% for LCC step). A 13 h nuclease treatment after the AEC step had no significant impact on the virus recovery (e.g., by virus particle disruption caused by stirring). Recoveries were in the typical range of variation (Figure 19; 94–102%). Significant losses of HA activity, however, were encountered during conditioning and gentamycin addition after the AEC step (Figure 19; 8–16%). Although screening experiments performed did not indicate any problems (data not shown), HA activity of AEC purified material dropped significantly. Subsequent experiments confirmed an adverse effect of gentamycin on purified virus particles (about -17% (±5%); at extended incubation times of the flow-through process only; Peuker (2013)). However, as the addition of antibiotics is not relevant for GMP in vaccine production (due to sterile process conditions any addition of antibiotics for industrial downstream processing would be avoided in general) that problem would only exist in laboratory scale purifications.

Final contamination levels of DNA were in the narrow range of 0.26–1.3% of the virus material for all three influenza strains (PicoGreen® assay data). However, after previous depletion of DNA by the AEC step in the process, the use of nuclease for DNA depletion was not as efficient (Figure 19; step recovery: 31–44%) as compared to the nuclease endpoint determination experiments with unpurified virus material (Figure 18; recovery: 1.1%). A potential DNA starting level effect on the Benzonase® digestion efficiency can been ruled out to a certain degree (see previous data: Figure 18, ii)), here. However, after Benzonase® digestion in the process the achieved final DNA concentration (Table 7; A/PR; 5.9 ng/mL) was in a similar range compared to the last verified DNA concentration (>LOD) from the nuclease endpoint determination experiments (Figure 18; ii) “1/50 dil.– 50 U/mL”; 4.1% = 5.2 ng/mL). So, there might be a limit to the achievable minimum final DNA concentration for a Benzonase® digestion with the given samples. In addition, adverse effects for the Benzonase® digestion by medium components or salt concentrations from the preceding AEC step can be ruled out to some extent based on the previous data (4.1.2; Figure 18; iii) “cond. – 50 U/mL”). For a more detailed discussion, please refer to section 4.4.

The variations in final protein level (25–73% (Figure 19); 2.4–11.7 µg/mL (Table 7)) might reflect strain-dependency caused by cell death and cell lysis during virus propagation in the bioreactors. However, such differences could also originate from batch to batch variations or from protein remnants after removal of spent growth medium containing serum before infection, which cannot be excluded completely. Overall, before purification, the protein concentration in the virus material of the three tested virus strain batches varied between 36.2–74.5 µg/mL (Table 7). Furthermore, pre-processing of inactivated harvests may play a role. With a cut-off of 750 kDa used for ultrafiltration (concentration) and the freeze-thaw step applied before loading to AEC column, variations in aggregation behavior of virus particles and precipitation of larger proteins can also not be ruled out completely.

Impurity level estimation

The variations in DNA dose levels between the different strains can be considered to be acceptable, while based on the data the absolute DNA level should be further reduced in order to comply with regulatory requirements.

Apart from that, a discrepancy between the PicoGreen® and the Threshold DNA values after the final step could be observed (Table 7 and Table 8). The Threshold value was 4–9 times lower than the PicoGreen® value. Such an assay discrepancy (up to 2.6–fold) has been already reported by Ikeda et al. (2009) for Chinese hamster ovary (CHO) cell culture-derived products as well as by P. Marichal-Gallardo et al. (2017) (5–7-fold; also with nuclease treatment as process step). Here, nuclease digestion might have played a role, too. Most likely, differences in DNA fragment size can be regarded as the main cause for the variation in measurements. Benzonase® is an unspecific endonuclease, which is able to cut nucleic acids to pieces as small as 3–5 bps (base pairs) (Martin, 1991). The Threshold® assay gives reliable data above a minimum fragment size of 600–800 bps (King et al., 1991), although lower fragment size limits of 100–600 bps have also been reported (Wolf et al., 2007; Ikeda et al., 2009). On the other side, the PicoGreen® assay detects fragments down to a size of 20–100 bps (Invitrogen, 2005; Wolf et al., 2007), but quantification might again depend on fragment size (Sedlackova et al., 2013). For further discussion of the residual DNA concentrations please refer to section 4.4.

Since the Threshold® assay showed a higher sensitivity and the risk for neoplastic transformation with tumor genes from the production cell line can be considered to be low for fragments smaller than 1,000 bps (Petricciani et al., 1987; Sheng et al., 2008; Sheng-Fowler et al., 2009), the data of the Threshold® assay should be given here priority over the PicoGreen® data for estimation of contamination levels.

4.1.5 Process performance re-evaluation based on gentamycin and SRID assay impact

As discussed in section 4.1.4, the gentamycin addition apparently affected the virus recovery. Assuming a process performed under sterile conditions without the need for addition of an antibiotic, the final virus recovery would improve to 81% (instead of 68%) for A/PR, 101% (instead of 87%) for A/Wis, and 90% (instead of 82%) for B/Mal, respectively.

Furthermore, SRID analysis of additional process samples (loaded virus material and a product fraction sample taken between both chromatographic steps) showed that HA protein recovery based on the SRID assay results was estimated to be significantly lower than the virus recovery based on the HA assay, especially for A/PR (Table 9).

Table 9: Comparison of final (total) process virus and HA protein recoveries (product fraction) based on the HA and SRID assays, respectively. In parts, the data for the three tested IV strains used for Table 7 and Figure 19 is shown.

IV strain	Final process recoveries [%]	
	Virus recovery (based on HA assay)	HA protein recovery (based on SRID assay (estimated))
A/PR	68 (±6)	28 (±4)
A/Wis	87 (±11)	60 (±3)
B/Mal	82 (±2)	67[a] (±4)

[a] B/Mal only showed recovery losses only at the second step, while the other virus strains showed losses at both chromatography steps.

Since both assays rely on the same HA protein of the IV particles, the reason for the deviation was suspected to lie in the SRID assay or sample preparation for the assay. Follow-up experiments (supervised internship project (Solomaier, 2013a)) showed that the cause was the SRID sample preparation: Although the SRID assay worked correctly for crude virus material, chromatography-purified virus samples required the addition of a lyoprotectant, such as saccharose, in order to avoid losses in the SRID sample preparation using lyophilization. Probably, the losses occurred due to the high degree of purification reducing also the amount of contaminating, but stabilizing proteins (such as BSA). Similar effects have been observed by Amorij et al. (2007), too. De Jonge et al. (2007) has successfully used inulin for preserving the structural integrity and biological activity of influenza virosomes during freeze-drying and storage. The utility of sugars in the frozen state is a result of their inability to crystallize (except for mannitol) and the lack of eutectic phase separation (Singh et al., 2010). Furthermore, many of the sugars induce glass formation. Lyoprotectants are preferentially excluded from the

protein surface (Carpenter, 1991). Carpenter (1991) analyzed the effect of freeze-thawing and freeze-drying on proteins, the effects of different cryoprotectants as well as the mechanism of protection. He concluded that the cryoprotectants serve as substitutional hydration shell for the protein preventing the proteins from irreversible inactivation. He tested a wide variety of cryoprotectants, with trehalose being one of the highest protecting agents. According to his findings, e.g., trehalose seems to create temporary hydrogen-bonds to the polar groups of proteins while acting as water substitute, thereby preventing intra- and inter-protein hydrogen bonding, which would otherwise induce unfolding/aggregation of the protein upon rehydration.

Here, trehalose showed no significant benefit over saccharose with the used virus material. Repeating the process for one strain (A/PR) with SRID analysis for all process steps with and without 1% saccharose in the SRID sample preparation (lyophilization), clearly showed that only by using a lyoprotectant the HA protein recoveries (SRID assay) were correlating with the virus recoveries (HA assay) (supervised bachelor thesis of Solomaier (2013b)).

Therefore, it can be estimated that the HA protein recoveries of the previous presented flow-through process would have been significantly higher, also changing the estimated vaccine dose contamination levels for this process. For estimating the process performance without the deviating effects of gentamycin and SRID assay sample preparation (using the correction factor from Solomaier (2013b)), the process data have been re-evaluated giving the expected dose impurity levels of 2.5 ng DNA/15 µg HA, 4.6 ng DNA/15 µg HA and 3.2 ng DNA/15 µg HA for A/PR, A/Wis and B/Mal, respectively. These results would render the flow-through process suitable for influenza vaccine production according to European Pharmacopeia (refer to section 2.4) for at least two of the three IV strains tested here. Nevertheless, repeating the final process runs with all IV strains would be required for a final confirmation.

4.2 Membrane-based process (SCMA-STMA)

The following section describes the development of the complete membrane-based process. It comprises screenings of STMA conditions using a 96-well filter plate and a STMA module. No screening or optimization was performed for the SCMA since optimal single-step conditions were known (section 3.4.2), but the STMA step was optimized with respect to the SCMA parameters. Besides demonstrating the performance of the final membrane-based process train (SCMA-STMA) for the model strain A/PR, the process robustness was tested with two further IV strains.

4.2.1 Results: STMA screening and characterization

STMA screening – Filter plates

In order to test STMA membranes for their ability to separate contaminants (in particular DNA) from virus particles, membrane filter plates were tested at different combinations of concentrations of NaCl and Na_2HPO_4/NaH_2PO_4 (Figure 20). First scouting experiments suggested that separation by step-wise elution had little potential, since virus particles, once bound to the membrane, were difficult to elute with the tested NaCl and Na_2HPO_4/NaH_2PO_4 concentrations (data not shown). Therefore, the process was designed to keep virus particles in the flow-through fraction with contaminants binding to the membrane.

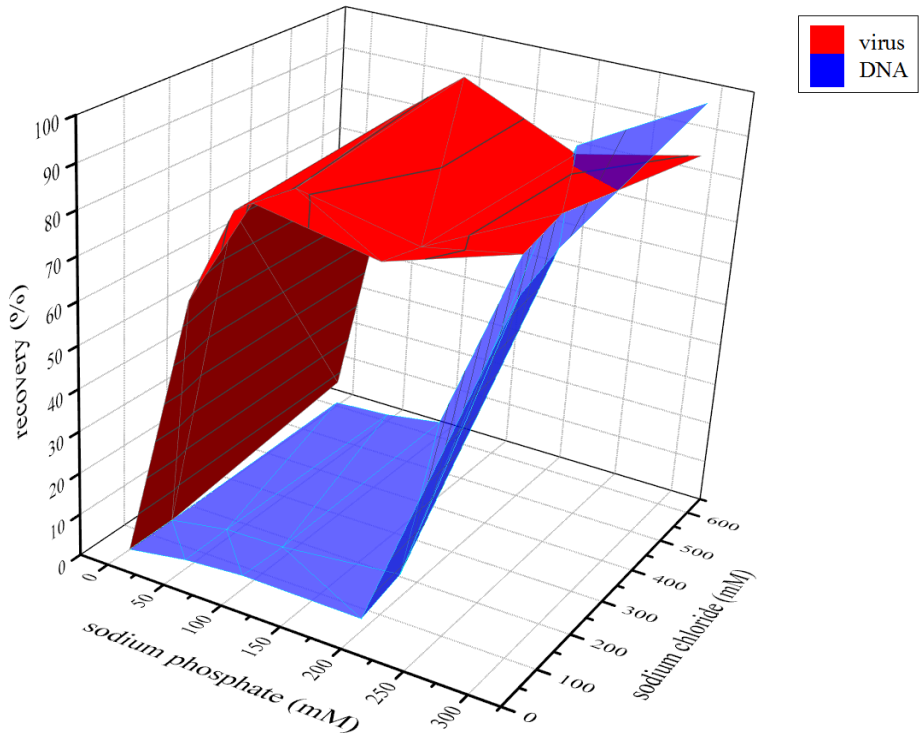

Figure 20: Screening of STMA in a 96-well format. Shown are the virus and DNA recoveries in the flow-through fraction (product fraction) with respect to sodium chloride (NaCl) and sodium phosphate (Na_2HPO_4/NaH_2PO_4) concentrations in the sample/loading buffers. IV strain: A/PR. Virus and DNA recoveries based on HA and PicoGreen® assay, respectively.

HA and DNA profiles shown in Figure 20 clearly demonstrate that separation of virus particles and DNA is possible over a wide range of concentrations (50–600 mM NaCl and 50–200 mM Na_2HPO_4/NaH_2PO_4). Best results were achieved using 100 mM Na_2HPO_4/NaH_2PO_4 in combination with 50–600 mM NaCl with a virus recovery between 86–92% (208–225

HAU/100 µL; 5.82–6.29 kHAU) and a residual DNA content of ≤4% (≤22.7 ng/mL; total amount of removed DNA: >1.3 µg).

STMA screening and characterization – Single module

In a next step, the results obtained by the filter-plate-screening were transferred to chromatographic laboratory scale and process conditions. Due to the intended use after a SCMA purification step involving 600 mM NaCl in the product fraction, this NaCl concentration was fixed accordingly and the Na_2HPO_4/NaH_2PO_4 concentration was altered in small intervals.

Table 10: Optimization of Na_2HPO_4/NaH_2PO_4 concentrations for separation of virus particles and DNA using a STMA chromatography module. NaCl concentration in the loading buffer was set to 600 mM, while the Na_2HPO_4/NaH_2PO_4 concentration was modified. Shown are relevant results for the flow-through fractions (product). Flow rate: 0.5 mL/min. IV strain: A/PR. Virus and DNA recoveries based on HA and PicoGreen® assay, respectively.

Na_2HPO_4/NaH_2PO_4 concentration	Recovery		DNA/Virus
	Virus	DNA	
[mM]	[%]	[%]	[-]
0	0	0.14 [a]	-
50	78.7	<LOQ	-
67	76.7	0.73[a]	9.5×10^{-3}
83	84.8 (±6.9) [b]	0.72 (±0.03) [a,b]	8.6×10^{-3}
100	97.0 (±4.1) [c]	0.81 (±0.02) [a,b]	8.5×10^{-3}
150	89.3	6.4	7.2×10^{-2}
300	102.4	100.3	1.0

[a] sample concentrated by lyophilization
[b] mean and standard deviation of technical replicates, n=2
[c] mean and standard deviation of technical replicates, n=3

The data in Table 10 indicated an optimal setting in the range of 50–100 mM Na_2HPO_4/NaH_2PO_4. While the virus recoveries were in the range of the screening experiments, with the highest virus recovery of 97% (225 HAU/100 µL) at 100 mM Na_2HPO_4/NaH_2PO_4, the DNA content showed a reduction to at least 0.81% (3.7 ng/mL; total amount of removed DNA: >6.15 µg) in that buffer range, which corresponds to a LRV ≥2.1. Above 100 mM Na_2HPO_4/NaH_2PO_4, separation of virus particles and DNA was not satisfactory.

Also the flow rate was altered between 0.25–1.7 mL/min (Table 11). Taking into account the variability of both assays, flow rates between 0.5–1.7 mL/min (linear velocity 0.04–0.14 cm/h)

had no significant impact on STMA performance. In contrast, at flow rates below 0.5 mL/min virus recovery was reduced.

Table 11: Optimization of flow rate for separation of virus particles and DNA using a STMA module at selected process conditions. Loading buffer was set to 600 mM NaCl and 100 mM Na_2HPO_4/NaH_2PO_4. Shown are relevant results for the flow-through fractions (product). IV strain: A/PR. Virus and DNA recoveries based on HA and PicoGreen® assay, respectively.

Flow rate	Recovery		DNA/Virus
	Virus	DNA	
[mL/min]	[%]	[%]	[-]
0.25	81.7	0.79 [a]	9.7×10^{-3}
0.5	97.0 (±4.1) [c]	0.81 (±0.02) [a,b]	8.5×10^{-3}
1.0	94.9	0.77 [a]	8.1×10^{-3}
1.7	93.6	0.78 [a]	8.3×10^{-3}

[a] sample concentrated by lyophilization
[b] mean and standard deviation of technical replicates, n=2; experimental data from Table 10
[c] mean and standard deviation of technical replicates, n=3; experimental data from Table 10

In an additional experiment, a $DBC_{10\%}$ was determined with 633 µg DNA/mL of packed membrane material (17.5 µg DNA/cm^2 membrane area; data not shown).

STMA strain-dependent single-process step robustness

Recovery of virus particles and DNA was tested with three IV strains (A/PR, A/Wis and B/Mal) at STMA process step conditions as used in the 2-step process (Table 12). For A/Wis as well as for B/Mal the recovery of virus particles was about 14% lower than for the A/PR virus (all experiments performed at 100 mM Na_2HPO_4/NaH_2PO_4), while the residual DNA contents increased from 0.9% (3.7 ng/mL; LRV: 2.1) to 4.9% (5.6 ng/mL; LRV: 1.3) and 4.0% (65.8 ng/mL; LRV: 1.4), respectively.

Table 12: Impact of batches with different IV strains on recovery of HA and DNA using STMA at process conditions (single-unit). Shown are relevant results for the flow-through fractions (product). Loading buffer was set to 600 mM NaCl and 100 mM Na_2HPO_4/NaH_2PO_4. IV strains: A/PR, A/Wis and B/Mal. Virus and DNA recoveries based on HA and PicoGreen® assay, respectively. Mean and standard deviation of technical replicates, n=3 (if not stated otherwise).

IV strain	Recovery		DNA/Virus [-]
	Virus [%]	DNA [%]	
A/PR	100.9 (±5.8)	0.9 (±0.0) [a]	8.9×10^{-3}
A/Wis	86.9 (±2.0)	4.9 (±1.6) [b]	5.6×10^{-2}
B/Mal	87.5 (±2.6)	4.0 (±2.5) [c]	4.6×10^{-2}

[a] mean and standard deviation of technical replicates, n=2; samples concentrated by lyophilization
[b] mean and standard deviation of technical replicates, n=2; samples not lyophilized
[c] samples not lyophilized.

4.2.2 Discussion: STMA screening and characterization

STMA screening – Filter plates

The demonstrated relatively wide salt concentration operation range of STMA with good overall performance at varying salt concentrations indicates high process robustness. Furthermore, by modulating the NaCl and Na_2HPO_4/NaH_2PO_4 concentrations in relation to each other, a wide applicability for different virus particle-based processes is to be expected operating in a simple flow-through (negative) mode. Using the STMA membrane adsorber for binding and eluting virus particles (capture mode) was not possible, probably due to a strong interaction of virus particles with the membrane ligands, which did not allow for virus particle release and elution at the tested conditions (data not shown). Unfortunately, the mechanism behind the observed effect of polyvalent ions on salt-tolerant ion-exchange membrane adsorbers or virus particles is widely unknown (Iyer et al., 2012). Since an increase of the concentration of monovalent ions (such as chloride ions) does not enable the separation of virus particles from DNA, a more complex interaction mechanism than for monovalent ions can be assumed. One may speculate that polyvalent ions interact with the virus particle surface, possibly the surface proteins, shielding virus particles from interactions with the membrane adsorber ligands. In that case, the concentration of phosphate in solution required for efficient separation should depend on the virus particle concentration. In addition, separation performance might also depend on the total protein composition. In contrast, assuming that the mechanism depends on interaction of polyvalent ions with the membrane adsorber – e.g., a polyvalent ion bond between virus particle and membrane required for binding and at the same

time a phosphate interaction with the membrane ligands reducing the charge-density, and resulting in only suitable conditions for binding of DNA – the virus particle or the total protein concentration should have no or little impact on the process performance.

STMA screening and characterization – Single module

Overall, the use of STMA resulted in very high yields (about 100%) combined with very good DNA depletion (about 122-fold) at laboratory scale. The observed improvement in DNA depletion in comparison to the data obtained by the screening (refer to section 4.2.1 and previous discussion) can be most likely attributed to a change in the ratio of loaded sample amount/membrane volume after the scale up. Moreover, an additional variation in experimental data would be expected due to the low number of sheets (three) in the 96-well-plate of the screening and the more or less uncontrolled flow conditions (centrifugation). Although it is known that membrane adsorbers behave flow rate independent over a wide range (Orr et al., 2013) further experiments under process conditions should be performed to better characterize process performance. In particular, it is possible that a yield decrease could be observed at very low flow rates (such as 0.25 mL/min) due to increased interaction time with the membrane matrix. However, since high flow rates are of interest to achieve maximum productivity, yield and purity, this aspect was not further pursued in this study. Finally, higher flow rates as recommended by the manufacturer (up 2.4 mL/min) could not be achieved due to build-up of a module and/or system-specific backpressure.

The measured $DBC_{10\%}$ of STMA for DNA (17.5 µg/cm^2) was not in accordance with the manufacturer's data (0.3 mg/cm^2) (Sartorius Stedim Biotech, 2011). However, since defined salmon DNA was used as a model system (most likely also having a different DNA molecule size compared to the samples here), and experiments were performed with a different buffer (150 mM NaCl, 20 mM Tris; here: 100 mM Na_2HPO_4/NaH_2PO_4, 600 mM NaCl, 20 mM Tris) and at an unknown flow rate, differences are to be expected.

STMA strain-dependent single-process step robustness

While differences in virus yield are close to the observed experimental variations (see for instance Table 10: 100–300 mM Na_2HPO_4/NaH_2PO_4), the differences in DNA levels between virus strains after STMA can be regarded as significant, in particular for the IV strain B/Mal. Slightly different applied flow rates would be considered as the first cause for variation, but it has been shown before, that flow rate changes in the given range should not affect the virus yield and the DNA depletion (for A/PR, refer to 3.2). Another option could be that the higher DNA levels of the second and third technical replicates for A/Wis and B/Mal were caused by

aging effects as STMA modules were used repeatedly before replacement to avoid impact of STMA lot variation on experimental results. However, no or little aging effect could be observed with manifold more reused modules for the virus strain A/PR. It also has to be taken into account that a decrease in DNA removal in general might be explained by the differences in contaminant levels and concentrations of the various virus harvests (before loading), which originate from differences in time of cell death and cell lysis during virus propagation, harvest or pre-processing of inactivated harvest. Finally, the different DNA sample preparation methods (required lyophilization of A/PR samples prior to PicoGreen® analysis) add to the complexity.

4.2.3 Results: Membrane-based process

Process performance (two-step chromatography purification process)

First trial runs at laboratory scale suggested that a slight adaptation in the Na_2HPO_4/NaH_2PO_4 concentration used for the STMA was required to achieve results similar to those obtained by the screening experiments (data not shown; see annex: 9.1.2/Table 22 for experimental confirmation). Eventually, a slight increase in the Na_2HPO_4/NaH_2PO_4 concentration from 100 mM (section 4.2.1) to 150 mM resulted in the expected process performance. In Figure 21, the performance of the two-step membrane purification strategy (SCMA-STMA) is shown, including the buffer addition step (conditioning) between both unit operations (refer to section 3.4.3). Furthermore, Table 13 shows the corresponding concentrations and volumes of the process steps. For the corresponding chromatograms refer to the annex section 9.1.1.

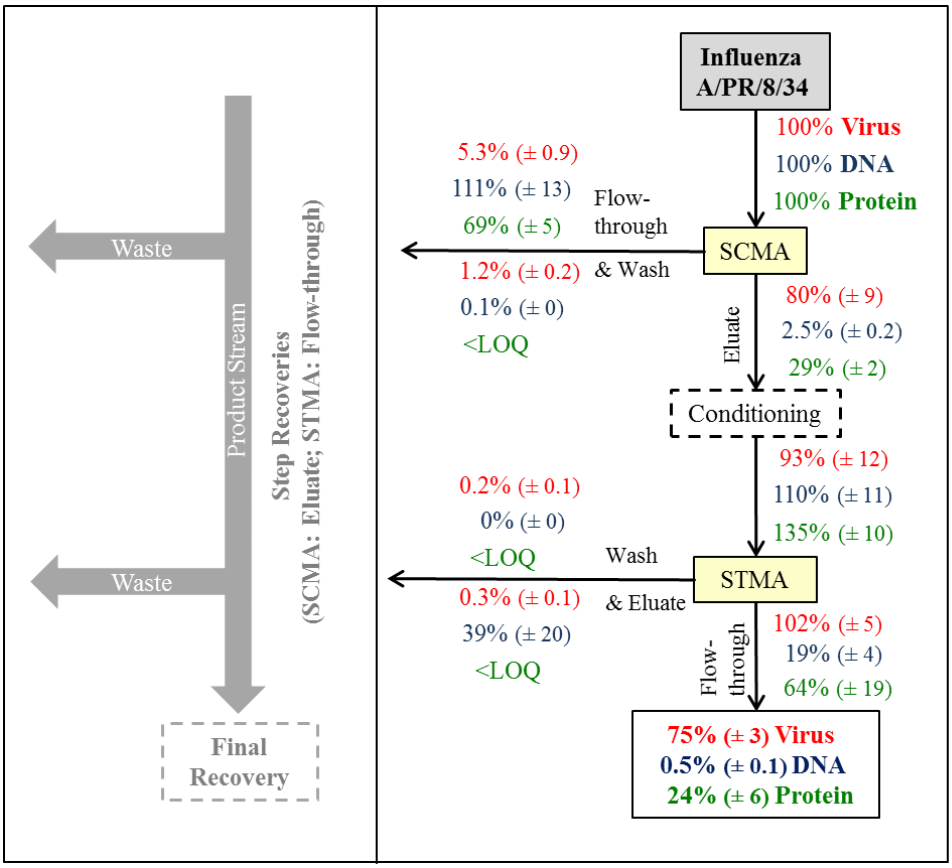

Figure 21: Two-step membrane purification process using a SCMA capture step and a STMA flow-through step. Shown are the step and the final recoveries (%) for the product stream and the wastes based on HA assay (→ Virus), PicoGreen® assay (→ DNA) and Bradford assay (→ Protein). The virus material entering the SCMA step was pre-processed and conditioned as described in section 3.2 and 3.4.3. The conditioning step represents the addition of buffer to adjust the Na_2HPO_4/NaH_2PO_4 concentration. IV strain: A/PR. Mean and standard deviation of technical replicates, n=4. For a corresponding data set refer to Table 13.

Significant virus particle losses (179 kHAU; 20%) could only be found during the SCMA step. Besides that, both steps showed significant reduction of DNA (step depletion: SCMA: 97.5%, 160.3 µg, LRV: 1.6; STMA: 81%, 1.53 µg, LRV: 0.7). With respect to reduction of residual proteins, the SCMA step removed 71% (1.07 mg), while the 36% removal of proteins by STMA needs to be discussed (refer to section 4.3.4).

Overall, 75% (±3%) (9.1 kHAU/mL) of the virus particles could be recovered, while reducing the residual DNA level to 0.5% (±0.1%) (LRV: 2.3; 11 ng/mL) (according to the PicoGreen® assay) and the residual protein level to about 24% (±6%) (LRV: 0.7; 4.9 µg/mL).

Table 13: Two-step membrane chromatography purification process. Experimental values of Figure 21 in absolute values including volumes, concentrations/HA-activities and step recoveries of the product fractions. Mean and standard deviation of technical replicates, n=4.

Steps	Volume		**a_{HA}**		**Virus**
	IN [mL]	OUT [mL]	IN [kHAU/mL]	OUT [kHAU/mL]	Step recovery [%]
SCMA	68.0 (±0.0)	18.3 (±0.1)	13.3 (±0.6)	39.4 (±6.0)	79.9 (±8.9)
Conditioning	11.5 (±0.6)	34.5 (±1.7)	39.4 (±6.0)	12.1 (±0.7)	93.2 (±12.3)
STMA	23.0 (±0.0)	31.1 (±0.3)	12.1 (±0.7)	9.1 (±0.8)	101.7 (±4.7)

Steps	Volume		**DNA**		**DNA**
	IN [mL]	OUT [mL]	IN [ng/mL]	OUT [ng/mL]	Step recovery [%]
SCMA	68.0 (±0.0)	18.3 (±0.1)	2418 (±219)	224 (±23.6)	2.5 (±0.2)
Conditioning	11.5 (±0.6)	34.5 (±1.7)	224 (±23.6)	81.6 (±9.4)	109.6 (±10.8)
STMA	23.0 (±0.0)	31.1 (±0.3)	81.6 (±9.4)	11.0 (±1.6)	18.5 (±3.9)

Steps	Volume		**Total Protein**		**Total Protein**
	IN [mL]	OUT [mL]	IN [µg/mL]	OUT [µg/mL]	Step recovery [%]
SCMA	68.0 (±0.0)	18.3 (±0.1)	22 (±1)	23.3 (±1.9)	28.6 (±2.5)
Conditioning	11.5 (±0.6)	34.5 (±1.7)	23.3 (±1.9)	10.5 (±0.8)	135.2 (±9.5)
STMA	23.0 (±0.0)	31.1 (±0.3)	10.5 (±0.8)	4.9 (±1.3)	64.1 (±19.0)

Impurity level estimation

The estimated impurity levels of the process are shown in Table 14. Based on the impurity levels per monovalent dose the contamination levels of a trivalent dose can be estimated with 3.6 ng DNA and 59.4 µg of total protein, respectively. Even without introduction of an additional nuclease digestion step this clearly fulfills the purity requirements for manufacturing of human influenza vaccines.

Table 14: Final product fraction of the two-step membrane chromatography purification process for IV A/PR. Shown are the HA protein concentration, relevant impurity levels, and estimated impurity levels for a dose input of 15 µg HA protein (monovalent dose for cell culture-derived vaccines for human use). HA protein concentration was determined by SRID assay as required for blending of human influenza vaccines. For the DNA level determination in the final product, the Threshold® assay was applied. Total protein concentration is based on Bradford assay. Mean and standard deviation of technical replicates, n=4.

	IV strain A/PR
Measured concentrations	
HA [µg/mL]	3.8 (±0.2)
DNA [ng/mL] (Threshold® assay)	0.3 (±0.1)
Total Protein [µg/mL]	4.9 (±1.3)
Estimated impurities	
ng DNA/15 µg HA [a]	1.2 (±0.4)
µg total protein/15 µg HA	19.8 (±5.8)

[a] calculations based on Threshold® assay data

4.2.4 Discussion: Membrane-based process

Membrane-based process

A small increase in the Na_2HPO_4/NaH_2PO_4 concentration was necessary in order to achieve the expected process performance similar to that seen in the screening experiments (data not shown; see annex section: Table 22 for experimental confirmation). Whether this might have been due to the SCMA step-elution profile resulting in a change in the expected salt-concentration of the product fraction or differences in the composition of the SCMA product itself (e.g., DNA, protein and virus particle concentration) is unclear.

Overall, the combination of SCMA and STMA resulted in high virus recoveries (Figure 21, Table 13; final recovery: 75%) without using any buffer exchange between these two steps. Significant virus particle losses were only observed after the SCMA step, which is in accordance to Opitz et al. (2009b) while the STMA step allowed for full virus recovery.

With a final DNA contamination level of 0.5% (±0.1%) (11 ng/mL) (based on PicoGreen® assay values) the process was able to remove most of the host cell DNA (161.9 µg). While the majority of DNA was removed by the SCMA step (97.5%; 160.3 µg), an additional 2% (1.53 µg) of total DNA depletion can be ascribed to the following STMA step. In comparison to the STMA optimization (refer to section 3.2: ≥99.2% (6.15 µg) depletion) this suggests a significantly reduced efficiency in the later unit operation.

However, DNA removal depends on the starting concentration, which might explain this large observed difference. Interestingly, the introduction of a nuclease digestion step (Benzonase®; conditions: 50 U/mL sample, 37°C, gentle stirring, 13 h) at various intermediate process steps (before loading onto SCMA or after STMA (including a dialysis before nuclease step to meet optimal nuclease conditions)) did not result in a significantly reduced final DNA content of the A/PR IV strain tested in the final process scheme (data not shown). For further discussion of the residual DNA concentrations please refer to section 4.4.

With respect to the protein contamination level, the two-step purification process (Figure 21) was able to reduce the protein content to 24% (±6%) (4.9 µg/mL). Again, most of the protein was removed by the SCMA step (71%; 1.07 mg), which is in agreement with Opitz et al. (2009b), who has also shown that the use of a SCMA allows to achieve a protein contamination level accepted for blending of cell culture-derived human influenza vaccine. Differences in the applied flow rates and a different SCMA membrane batch as used by Opitz et al. (2009a) might account for the small difference in final protein levels. In the two-step purification process, the introduction of the conditioning step seems to increase the protein content of the SCMA eluates. However, as only concentrated fresh buffer solution has been added, this is likely caused by aggregation/disaggregation effects and/or due to a relatively high error in the Bradford assay at this low protein concentration. Whatsoever, measured values of the following STMA step could be affected as well and should be interpreted with caution. In addition, it has to be taken into account that the STMA step has not been optimized for protein depletion here due to the high efficiency of the SCMA step.

Impurity level estimation

Overall, by combining SCMA with STMA all contamination levels could be reduced below the required limits without using a nuclease step. Comparing the Threshold value (Table 14) with the PicoGreen® value (Table 13), the Threshold value was 37-fold lower (recalculation of process yields based on Threshold value: 0.014% final DNA content; 0.50% STMA step recovery; 2.3 LRV for STMA). Furthermore, this Threshold value is now in agreement with the values obtained in the DBC experiment and the results obtained by single-step STMA optimization (Table 10), section 4.2.1). Discrepancies between PicoGreen® and Threshold values have also been seen in section 4.1.4 and have been reported before (Ikeda et al., 2009; P. Marichal-Gallardo et al., 2017). As discussed in section 4.1.4, the fragment size specificity of both DNA assays could be the reason for the discrepancy. Refer section 4.4 for a detailed discussion of the residual DNA in the product fraction.

4.3 Orthogonal process (AEC-HIC)

The following section describes the development of the orthogonal process. It comprises a screening of a wide selection of different HIC resins, salts and salt concentrations. Selected parameters were further optimized and characterized on a larger chromatography scale. Finally, the optimized HIC was transferred to a two-step chromatographic downstream process including an AEC.

4.3.1 Results: Screening & process steps characterization

Determination of critical salt concentration for virus particle aggregation

In order to assess selected salts for their salting-out abilities and to find the CACs, various salts were tested at different concentrations (where required close to their solubility limit) for their impact on RMPS (Figure 22). An increase of the RMPS (up to 4.5-fold) was used for detecting aggregation of IV particles.

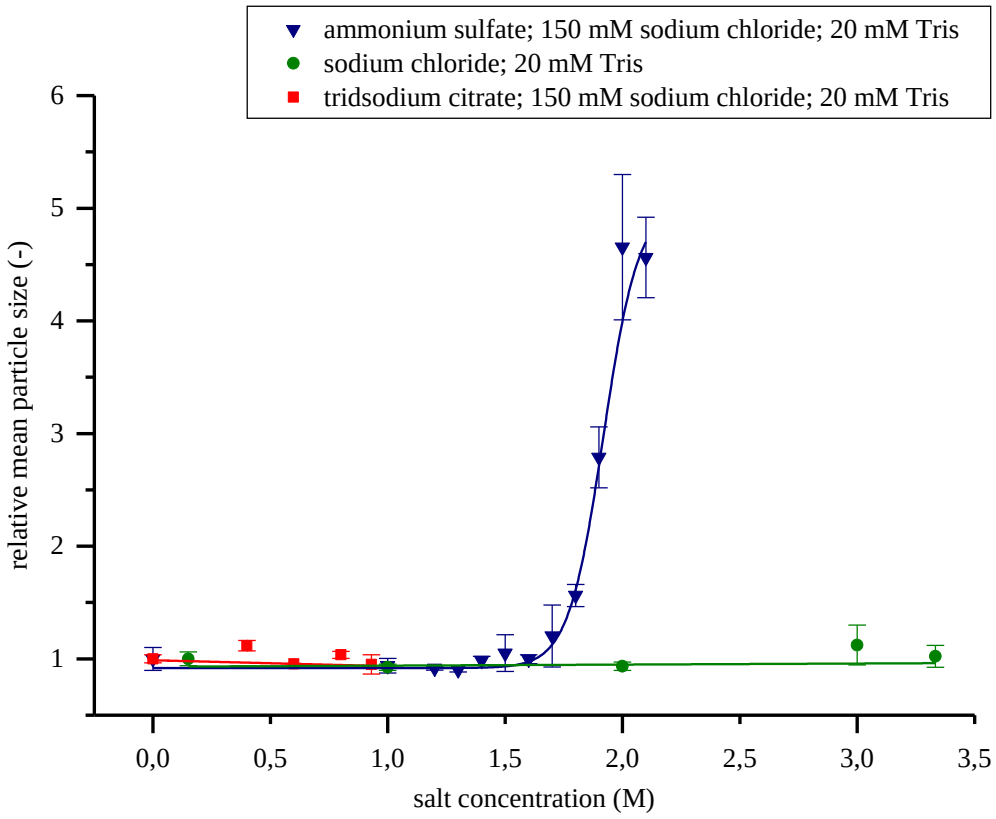

Figure 22: Determination of critical virus particle aggregation concentration – effect of selected salts on virus particles. Particle diameter distributions were measured at different salt concentrations of ammonium sulfate ($(NH_4)_2SO_4$), sodium chloride (NaCl) and trisodium citrate ($Na_3C_6H_5O_7$) by dynamic light scattering particle size distribution analyzer. Values show the relative mean particle size (RMPS). Mean and standard deviation of technical replicates, n=2.

With $(NH_4)_2SO_4$ a significant shift in RMPS could be observed starting at a concentration of about 1.7 M. Therefore, a concentration range of 0.48–1.6 M was selected for the following screening experiments. For $Na_3C_6H_5O_7$ and NaCl no increase in RMPS could be observed for the tested concentration range. Other salts, such as $MgCl_2$, were tested additionally with no significant effect on virus particle aggregation (data not shown).

HIC – 96-well-plate screening for conditions

A variety of resins and salts were tested in a 96-well format in order to identify suitable combinations for separation of virus particles (Figure 23, Figure 24) and DNA (Figure 25, Figure 26). Salt concentrations were tested in a wide range in order to investigate binding for both weak and strong HIC resins.

In general, a trend was observed that a closed virus recovery balance (based on the HA assay) could not be obtained in the screening format once virus particles showed (partial) binding to the HIC resins (Figure 23, Figure 24), while DNA (Figure 25, Figure 26) could be fully accounted for at most conditions. This finding will be further discussed in section 4.3.2.

$(NH_4)_2SO_4$ showed the best separation of virus particles and DNA at concentrations of 1.04 M and 1.6 M for Methyl, PPG and Phenyl resins (Figure 23, Figure 25); with PPG and Phenyl showing only a small fraction of the loaded virus particles in the flow-through. Additionally, at 1.6 M, a good separation could be observed for SEC and the Ether resin.

$Na_3C_6H_5O_7$ showed similar results as $(NH_4)_2SO_4$ (Figure 23, Figure 25), with the difference that at higher concentrations significant amounts of DNA were bound and eluted from strong as well as from medium strength HIC resins (PPG/Hexyl resin; Figure 25).

For NaCl only a partial separation of virus particles and DNA could be observed with PPG and the Phenyl resin at the highest salt concentrations (Figure 24, Figure 26). $MgCl_2$ showed no separation of virus particles and DNA (Figure 24, Figure 26).

In summary, $(NH_4)_2SO_4$ together with the resins Ether, PPG and Phenyl were selected for subsequent experiments due to the separation performance of $(NH_4)_2SO_4$ at moderate concentrations. $Na_3C_6H_5O_7$ was not chosen due its general tendency to facilitate binding and elution of DNA, in particular at high salt concentrations.

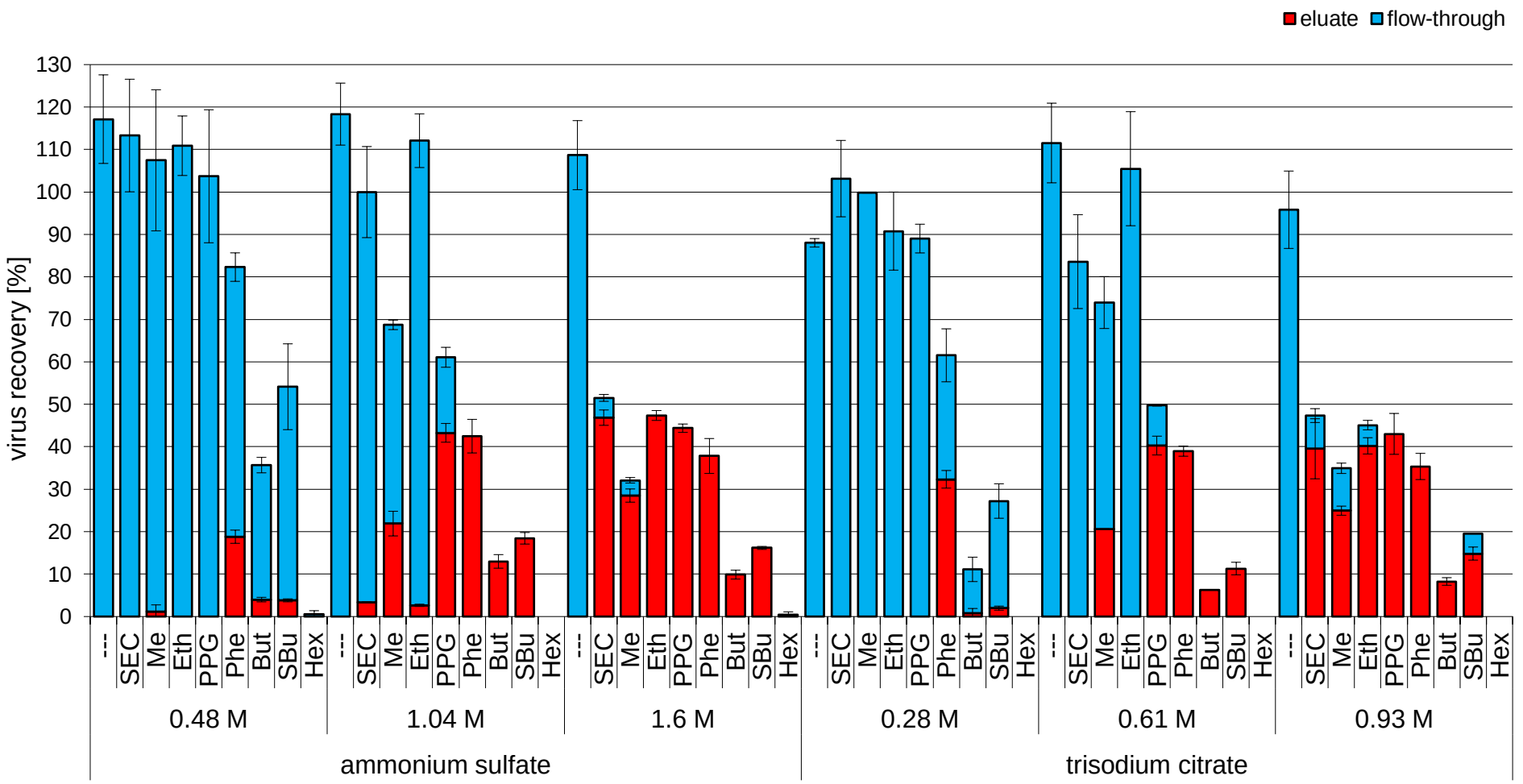

Figure 23: Semi-high-throughput screening in 96-well format – virus recoveries using loading buffers with two different salts (ammonium sulfate ($(NH_4)_2SO_4$) or trisodium citrate ($Na_3C_6H_5O_7$)) at different concentrations with an assortment of HIC resins in 96-well filter plates. Resins are sorted based on their expected hydrophobicity: ---: no resin (control), SEC: size-exclusion chromatography resin (i.e. no functional group (control), Tosoh), Me: methyl group (Bio-Rad), Eth: ether group (Tosoh), PPG: polypropylene glycol group (Tosoh), Phe: phenyl group (Tosoh), But: butyl group (Tosoh), SBu: butyl group (remark: smaller pore size, Tosoh), Hex: hexyl group (Tosoh). Elutions were performed with an identical low-salt buffer for all experiments. Shown are the virus recoveries in the flow-through and eluate fraction. Mean and standard deviation of technical replicates, n=2.

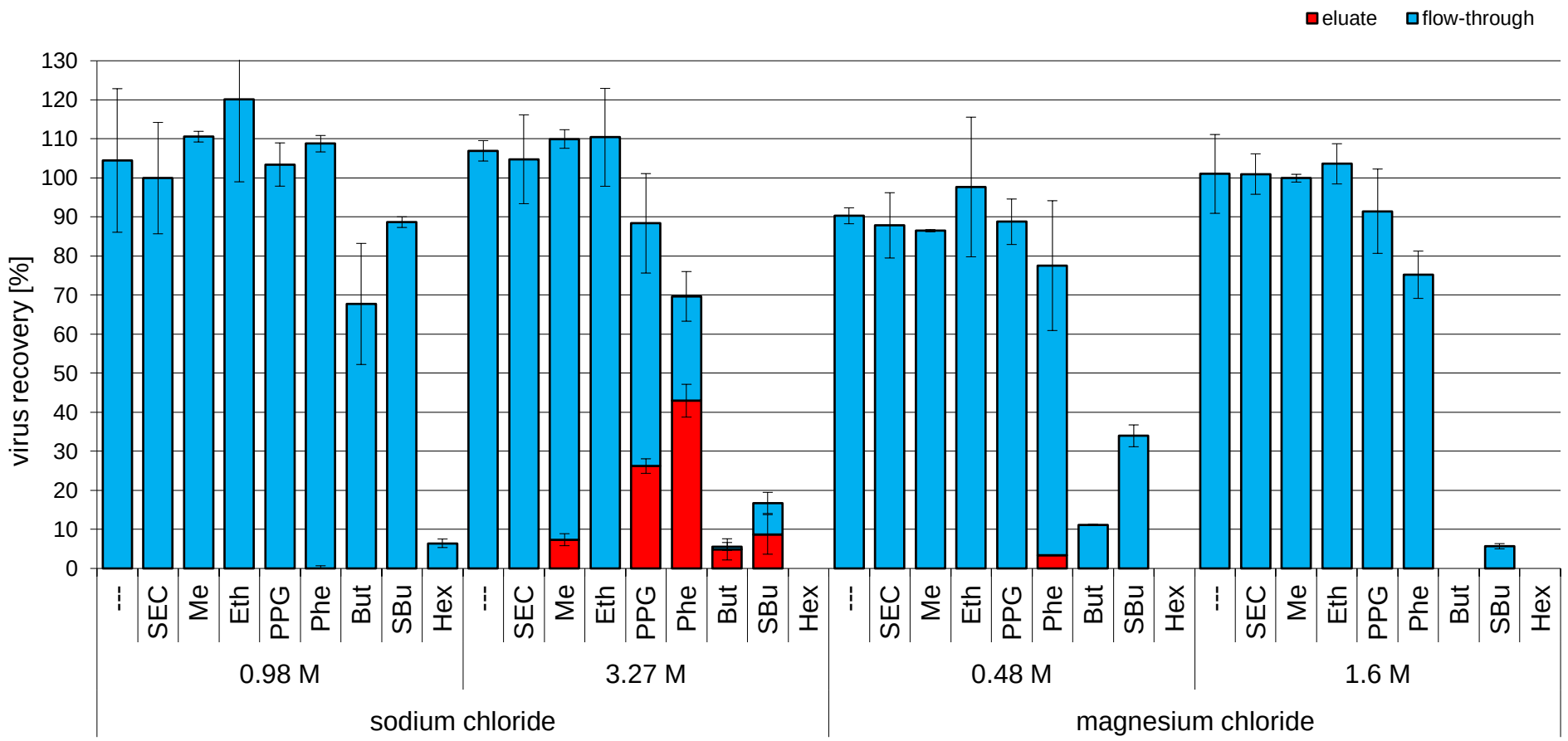

Figure 24: Semi-high-throughput screening in 96-well format – virus recoveries using loading buffers with two different salts (sodium chloride (NaCl) or magnesium chloride ($MgCl_2$)) at different concentrations with an assortment of HIC resins in 96-well filter plates. Resins are sorted based on their expected hydrophobicity: ---: no resin (control), SEC: size-exclusion chromatography resin (i.e. no functional group (control), Tosoh), Me: methyl group (Bio-Rad), Eth: ether group (Tosoh), PPG: polypropylene glycol group (Tosoh), Phe: phenyl group (Tosoh), But: butyl group (Tosoh), SBu: butyl group (remark: smaller pore size, Tosoh), Hex: hexyl group (Tosoh). Elutions were performed with an identical low-salt buffer for all experiments. Shown are the virus recoveries in the flow-through and eluate fraction. Mean and standard deviation of technical replicates, n=2.

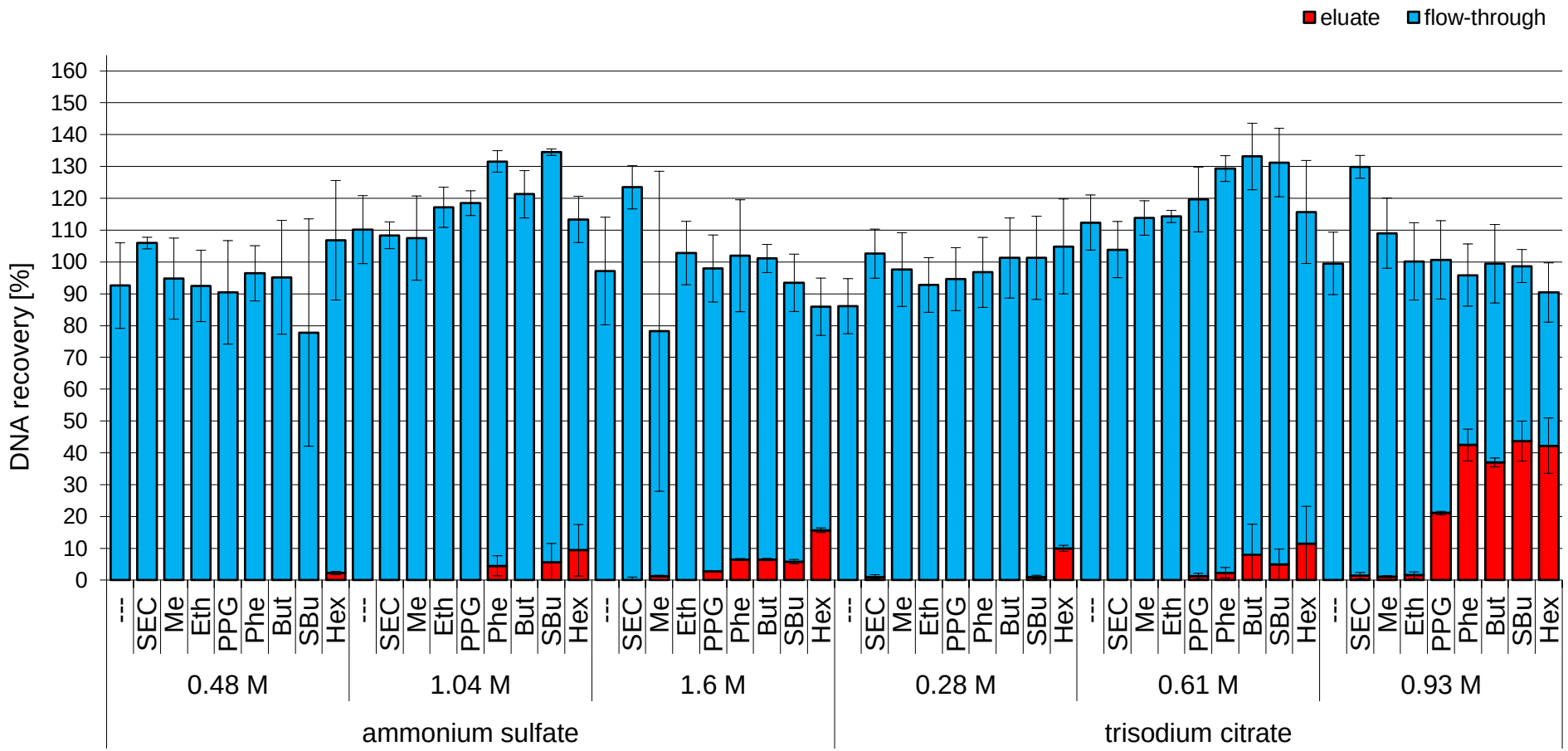

Figure 25: Semi-high-throughput screening in 96-well format – DNA recoveries using loading buffers with two different salts (ammonium sulfate ($(NH_4)_2SO_4$) or trisodium citrate ($Na_3C_6H_5O_7$)) at different concentrations with an assortment of HIC resins in 96-well filter plates. Resins are sorted based on their expected hydrophobicity: ---: no resin (control), SEC: size-exclusion chromatography resin (i.e. no functional group (control), Tosoh), Me: methyl group (Bio-Rad), Eth: ether group (Tosoh), PPG: polypropylene glycol group (Tosoh), Phe: phenyl group (Tosoh), But: butyl group (Tosoh), SBu: butyl group (remark: smaller pore size, Tosoh), Hex: hexyl group (Tosoh). Elutions were performed with an identical low-salt buffer for all experiments. Shown are the DNA recoveries in the flow-through and eluate fraction. Mean and standard deviation of technical replicates, n=2.

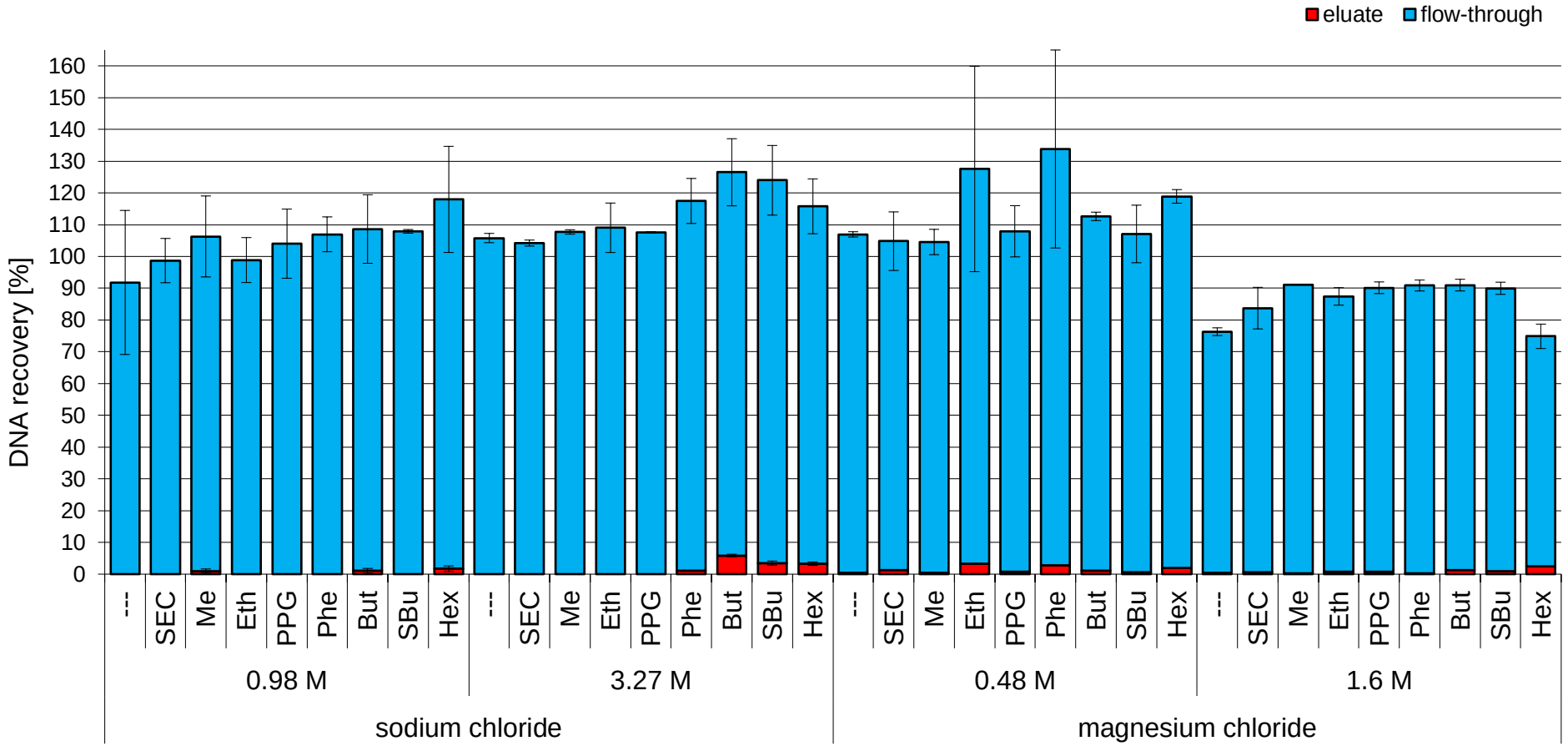

Figure 26: Semi-high-throughput screening in 96-well format – DNA recoveries using loading buffers with two different salts (sodium chloride (NaCl) or magnesium chloride ($MgCl_2$)) at different concentrations with an assortment of HIC resins in 96-well filter plates. Resins are sorted based on their expected hydrophobicity: ---: no resin (control), SEC: size-exclusion chromatography resin (i.e. no functional group (control), Tosoh), Me: methyl group (Bio-Rad), Eth: ether group (Tosoh), PPG: polypropylene glycol group (Tosoh), Phe: phenyl group (Tosoh), But: butyl group (Tosoh), SBu: butyl group (remark: smaller pore size, Tosoh), Hex: hexyl group (Tosoh). Elutions were performed with an identical low-salt buffer for all experiments. Shown are the DNA recoveries in the flow-through and eluate fraction. Mean and standard deviation of technical replicates, n=2.

HIC – Preparative chromatography and optimization (single-step)

In a next step, the three selected HIC resins (Ether, PPG, and Phenyl) from the semi-high-throughput screening (sHTS) were tested at different concentrations of $(NH_4)_2SO_4$ for optimal separation conditions of virus particles, DNA, and total protein (Figure 27a-c). Also, the robustness/operation window for the preparative scale was further narrowed down.

The Ether resin showed the best separation with highest virus recoveries of 90–97% above a $(NH_4)_2SO_4$ concentration of 1.45 M, while DNA and total protein contents were reduced to about 1% and 41–46%, respectively (Figure 27a). The PPG resin showed the best separation with highest virus recoveries of 83–96% in the range 1.04–1.325 M. DNA and total protein contents were reduced to about 0.7–1.3% and 55–65%, respectively (Figure 27b). Above 1.325 M $(NH_4)_2SO_4$, DNA started to bind and to elute with virus particles. The Phenyl resin showed best separation with highest virus recoveries 77–82% in the range 0.75–1.04 M, while DNA and total protein contents were reduced to about 0.6–1.0% and 31–42%, respectively (Figure 27c). Here, above 1.04 M $(NH_4)_2SO_4$ DNA started to bind and to elute with virus particles.

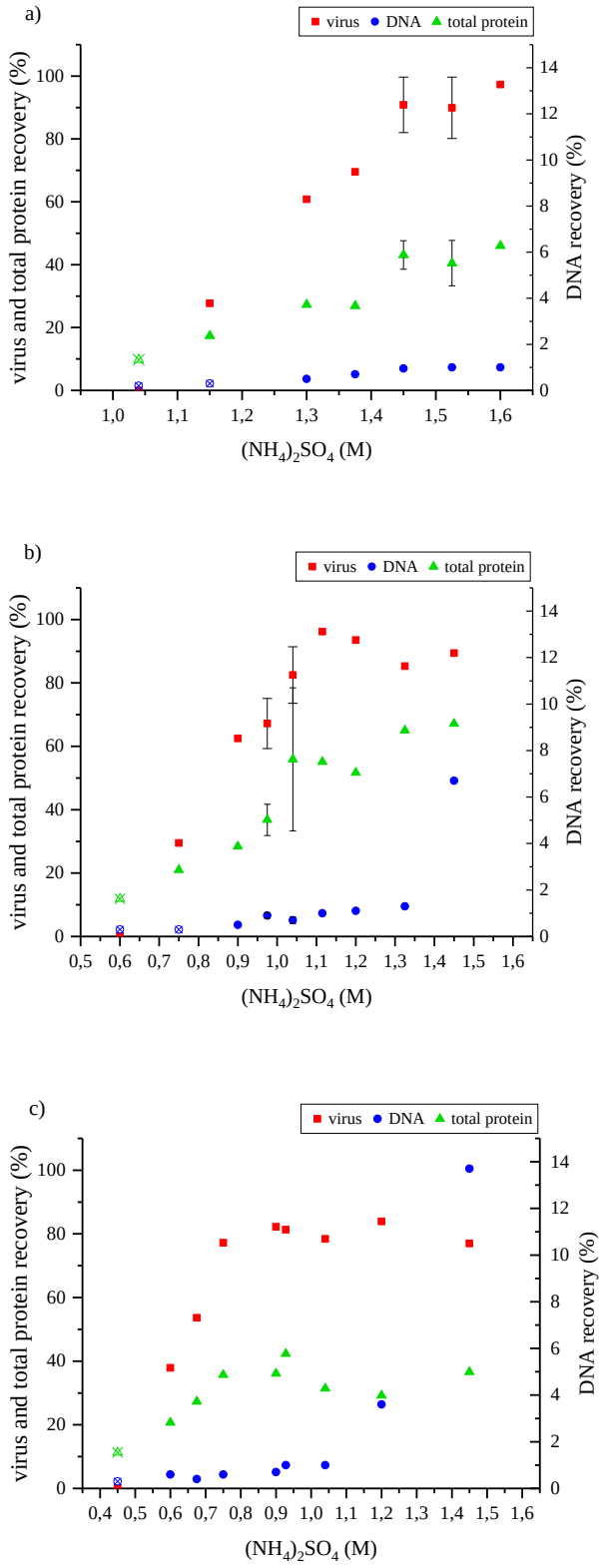

Figure 27: Chromatographic screening of selected parameters for separation of virus particles, DNA and total protein. $(NH_4)_2SO_4$ was tested at different concentrations with three HIC resins: a) Ether, b) PPG, c) Phenyl. Shown are the virus, DNA and total protein recoveries in the product fraction (eluate). Experiments were performed in simplex except for selected experiments in a) and b): mean and standard deviation of technical replicates, n=2 (refer to data points with error bars). Data points containing a cross were below the assays quantification range and are only shown here for displaying a potential trend.

HIC – Flow rate dependencies

In order to verify, that the residence time of the virus particles in the HIC columns is sufficient in terms of binding kinetics, a range of flow rates was tested.

As shown in Figure 28, no significant flow rate impact on the separation performance could be observed (for the Phenyl resin).

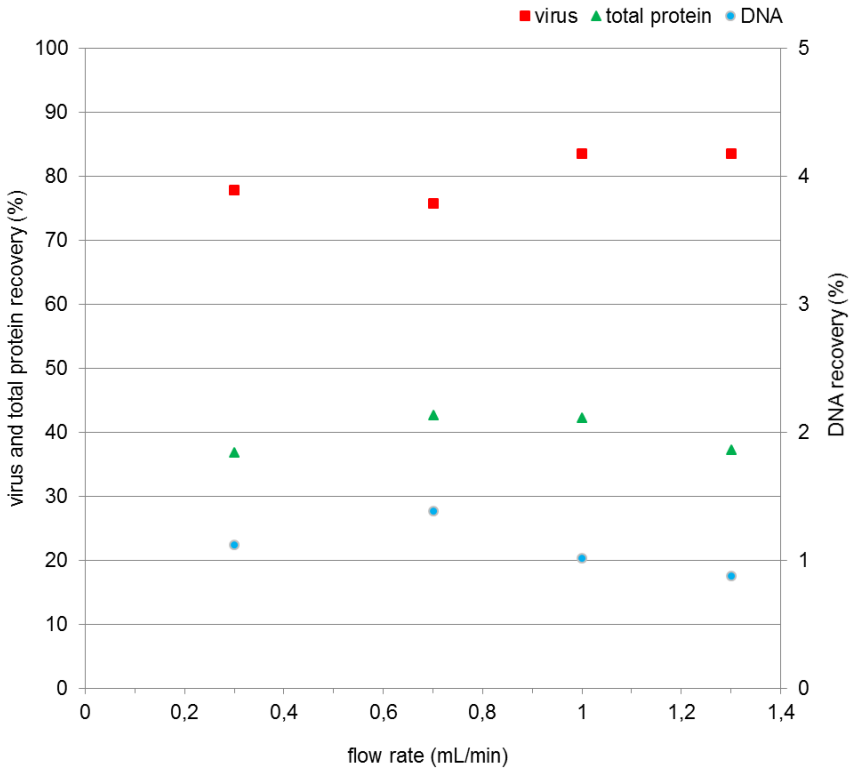

Figure 28: Impact of flow rate on virus, DNA and protein recoveries in the product fractions (eluate) using a Phenyl HIC column.

HIC – Salt performance based on ion strength

In order to evaluate the performance of selected salts and the usability of the parameter ion strength, various salt concentrations were tested with the Phenyl resin at similar ion strengths (Table 15) (with at least 0.15 M NaCl in each solution for preservation of virus particle integrity). Also, different ratios of $(NH_4)_2SO_4$ and NaCl at similar ion strengths were tested here in order to evaluate the option to partially substitute one salt against the other salt based on ion strength. Overall, at the same ion strength the use of $Na_3C_6H_5O_7$ showed comparable virus recovery as $(NH_4)_2SO_4$ (both at a minimum NaCl concentration of 0.15 mM for maintaining

HA assay activity) with 83.5% (±0.7%) and 90.2% (±13.7%), respectively. In contrast, with NaCl alone a strongly reduced virus recovery was obtained at a similar ion strength (55.8%, ±6.7%). Yet, partial substitution, where about half of $(NH_4)_2SO_4$ was substituted by NaCl according to ion strength (0.5 M $(NH_4)_2SO_4$, 1.8 M NaCl) still yielded high virus recoveries (84.0%), while substituting more $(NH_4)_2SO_4$ (0.2 M $(NH_4)_2SO_4$, 2.7 M NaCl) resulted in significantly reduced virus recovery (62.0%, ±5.7%).

Table 15: Salt performance based on ion strength. Phenyl HIC resin was tested at comparable ion strengths while modulating the $(NH_4)_2SO_4$, NaCl, and $Na_3C_6H_5O_7$ concentrations. Shown is the virus recovery in the product fraction (eluate) based on HA assay. Mean and standard deviation of technical replicates, n=2.

$(NH_4)_2SO_4$ [M]	**NaCl [M]**	**$Na_3C_6H_5O_7$ [M]**	**Ion strength [-]**	**Virus recovery [%]**
1.04	0.15	0	3.27	90.2 (±13.7)
0.5	1.8	0	3.3	84.0 (±5.7)
0.2	2.7	0	3.3	62.0 (±5.7)
0	3.27	0	3.27	55.8 (±6.7)
0	0.15	0.61	3.2	83.5 (±0.7)

HIC – Dynamic binding capacities

For the final selection of the HIC resin type, the $DBCs_{10\%}$ for the Phenyl and PPG resin were determined at their optimal separation salt concentration (Table 16). While for the stronger HIC Phenyl resin, a $DBC_{10\%}$ of 95 kHAU/mL resin was determined, the weaker HIC resin PPG showed a 40% higher $DBC_{10\%}$ (133 kHAU/mL resin) with increased salt concentration (by about 0.2 M). Furthermore, a partial substitution of $(NH_4)_2SO_4$ with NaCl resulted in a 39% reduction of the $DBCs_{10\%}$ with the Phenyl resin (95 kHAU/mL resin to 58 kHAU/mL resin) besides having a higher ion strength.

Table 16: Dynamic binding capacities (DBCs) of selected resins and salt concentrations. Shown are the DBCs at 10% breakthrough concentration ($DBC_{10\%}$ for virus particles at a flow rate of 1 mL/min. Experiments were performed in simplex, except for the experiment "Phenyl/0.928 M $(NH_4)_2SO_4$/0.15 M NaCl": Mean and standard deviation of technical replicates, n=2.

HIC resin	$(NH_4)_2SO_4$ [M]	NaCl [M]	$DBC_{10\%}$ [kHAU/mL]
Phenyl	0.5	1.8	58
Phenyl	0.928	0.15	95 (±2)
PPG	1.15	0.15	133

HIC – Salt effects on HA protein recovery

A total of four runs were performed using the optimal selected parameters from the previous experiments (PPG resin, 1.15 M $(NH_4)_2SO_4$). Also, due to potential adverse effects of the elevated salt concentration on virus particle stability, the selected conditions were also tested for the recovery of virus HA protein using the SRID assay (Figure 29).

Overall, 86.7% (±7.4%) of virus particles could be recovered in the product fraction, while DNA and total protein could be depleted to 1.3% (±0.3%) and 46.5% (±6.2%), respectively. Furthermore 81.8% (±6.6%) of virus HA protein was recovered, giving a recovery ratio of 94.5% (HA protein recovery/virus recovery).

Overall, no adverse effects of the selected HIC parameters on the process balance or virus particle stability could be observed.

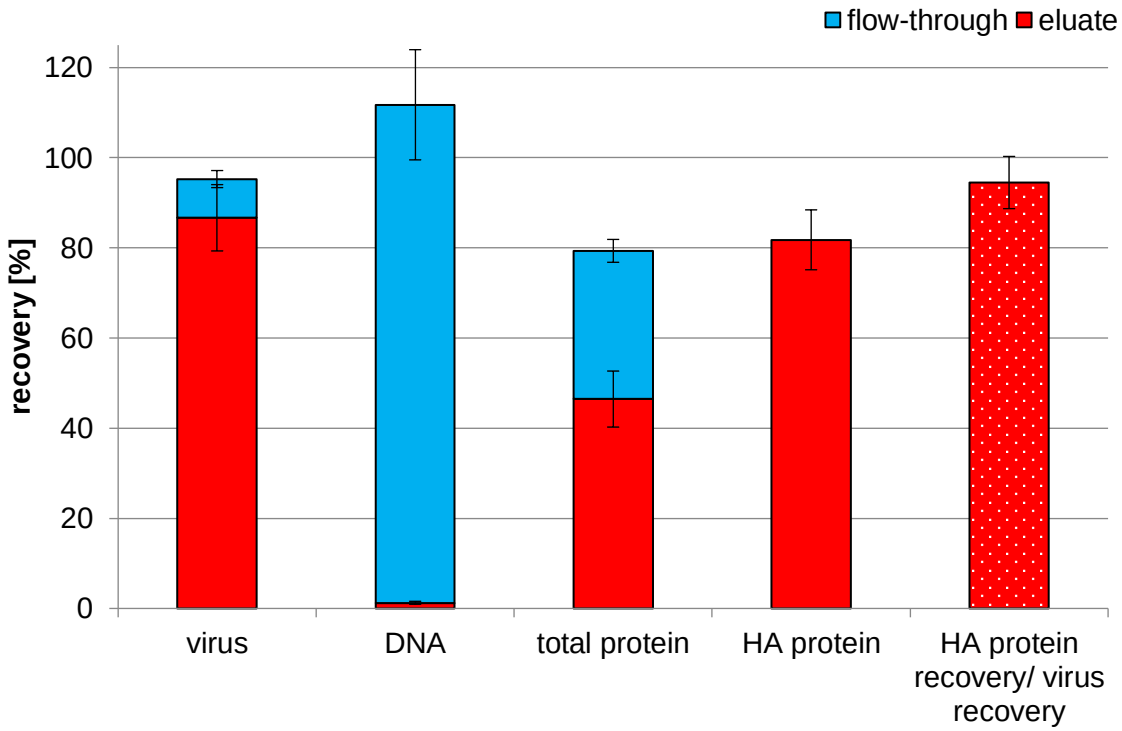

Figure 29: Salt effects on HA protein recovery at optimized HIC condition. Chromatography was performed using PPG HIC resin and 1.15 M $(NH_4)_2SO_4$, 0.15 M NaCl, 50 mM Tris, pH 7.4 for equilibration and loading. Shown are the virus recovery measured by the HA assay, the DNA recovery, the total protein recovery and the virus HA protein recovery measured by the SRID assay in the flow-through and eluate fractions (product fractions) (remark: HA protein recovery only measured in eluate fraction). Furthermore, the virus HA protein recovery is set in proportion with the virus recovery to give the recovery ratio "HA protein recovery/virus recovery". Mean and standard deviation of technical replicates, n=4.

HIC – Effects of process conditions adaptation

In order to implement the optimized HIC (single-step) in a process scheme with a preceding AEC step, HIC was tested with adjusted salt concentrations similar to concentrations of an AEC product fraction (section 4.3.3). In particular, the potential impact of a required partial salting-out salt exchange ($(NH_4)_2SO_4$ and NaCl) on the HIC separation performance was evaluated (Figure 30). A NaCl concentration of 0.41 M was assumed in the AEC product fraction and $(NH_4)_2SO_4$ concentration was corrected based on ion strength giving a concentration of 1.063 M. With a virus recovery of 91.4% and a DNA and total protein depletion to 0.8% and 53%, respectively, the separation performance of the here adapted HIC was very similar to the previously optimized HIC (section 4.3.1; section "HIC – Salt effects on HA protein recovery").

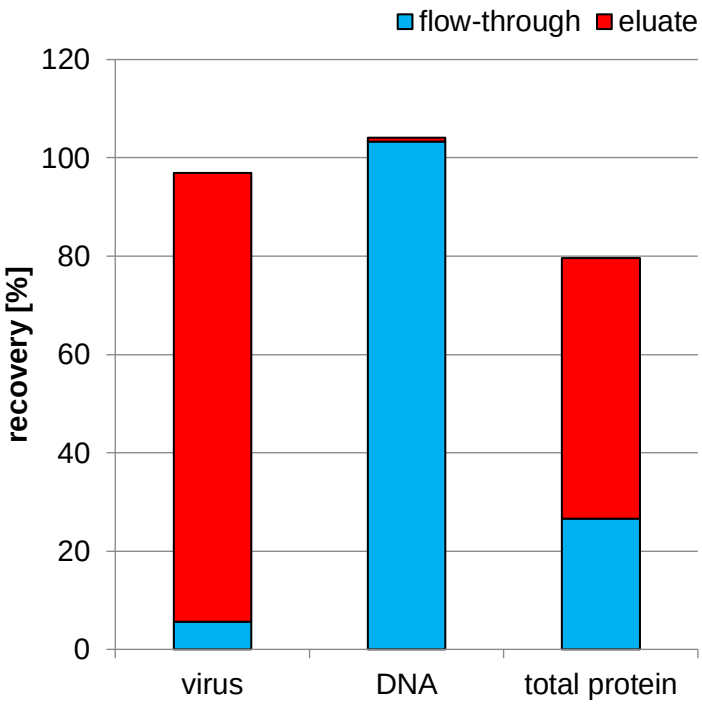

Figure 30: Effects of process conditions adaptations with adjustments made for $(NH_4)_2SO_4$ and NaCl concentrations. Chromatography was performed using PPG HIC resin and 1.063 M $(NH_4)_2SO_4$, 0.41 M NaCl, 50 mM Tris, pH 7.4 for equilibration and loading. Shown are virus recovery, DNA recovery and total protein recovery in flow-through and eluate (product) fractions.

HIC – Influenza virus strain dependency/single-process step robustness

Finally, the recovery of virus particles and DNA was tested with two other IV strains (A/Wis and B/Mal) for the optimized HIC (single-step) (Figure 31). For A/Wis as well as for B/Mal the virus recovery was about 62% and 66%, respectively. This corresponded to a reduction of about 25% (A/Wis) and 20% (B/Mal) compared to the A/PR virus. The residual DNA contents changed from 1.3% (LRV: 1.8, A/PR) to 3.3% (LRV: 1.5, A/Wis) and 0.7% (LRV: 2.2, B/Mal), respectively. Total protein depletion was similar for all three influenza strains and in the range of 45.6–50.8% (LRV: 0.3).

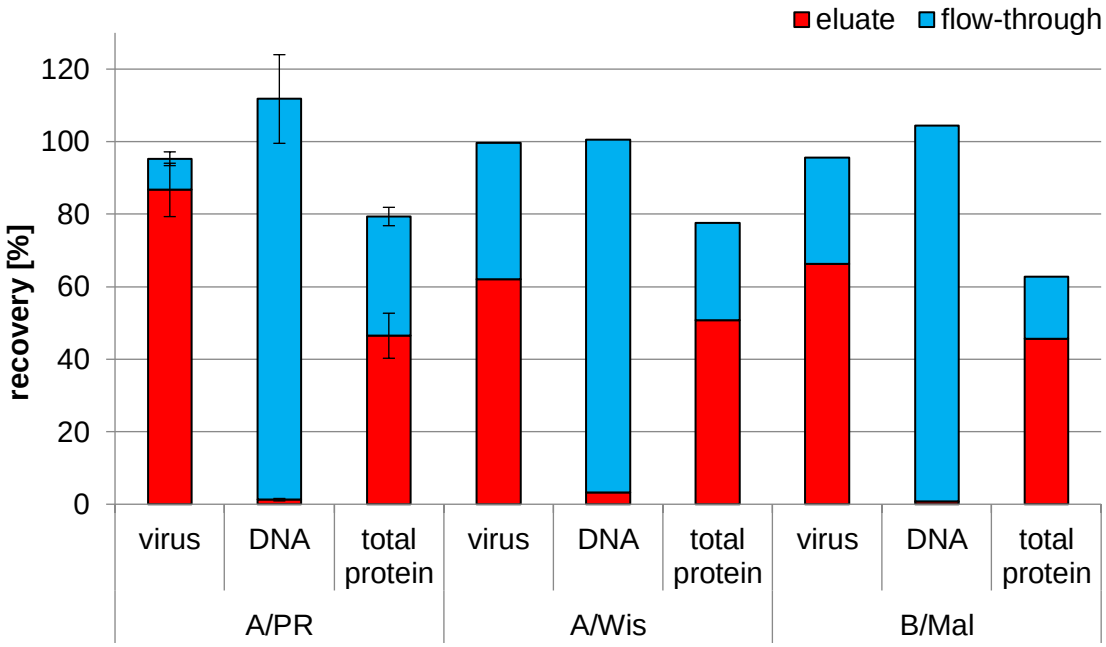

Figure 31: IV strain dependency of yield and purity in HIC. Chromatography was performed using a PPG HIC resin and 1.15 M $(NH_4)_2SO_4$ with 150 mM NaCl, 50 mM Tris, pH 7.4. Shown are virus recovery, DNA recovery and total protein recovery in flow-through and eluate (product) fractions of three different IV strains (A/PR, A/Wis, B/Mal). A/PR: Mean and standard deviation of technical replicates, n=4, data from Figure 29; A/Wis, B/Mal: Experiments were performed in simplex.

4.3.2 Discussion: Screening & process steps characterization

The aim of this study was the assessment of HIC for the purification process of IV for producing cell culture-derived human influenza vaccines. The effectiveness of HIC mostly depends on the resin hydrophobicity, the salt type, and the concentration in order to control binding and elution (Porath et al., 1973; Melander et al., 1977; Narhi et al., 1989; Mahn et al., 2007b). A number of theories have been proposed to explain the salting phenomenon, which can be grouped into hydration, water dipole, electrostatic, internal pressure and van der Waals forces based theories (Grover et al., 2005). Unfortunately, the mechanisms behind salting effects or HIC is still not fully understood (Baldwin, 1996; Grover et al., 2005; Zhang et al., 2006). This is mainly due to the vast spectrum of acting intermolecular forces. Furthermore, the applicability of mathematical models is usually limited to the investigated or ideal targets (Helling et al., 2012), and predictions about the hydrophobicity of complex proteins are mostly only semi-quantitative (McCue, 2009). In particular, few data is available regarding virus particle purification by HIC. A rational step-wise selection process for the identification of HIC parameters was therefore chosen in this study. It has been shown by Szepesy et al. (1992) that it is crucial in process

development for HIC to investigate different combinations of salts and stationary phases. Salts modulate not only the affinity of proteins for particular resins and non-specific protein–protein or protein–surface interactions but also affect the binding capacity (Tsumoto et al., 2007). The screening therefore comprised a reasonable number of HIC resins with increasing hydrophobicity, two strong salting-out salts ($(NH_4)_2SO_4$ and $Na_3C_6H_5O_7$), a weak salting-out salt (NaCl), and a salting-in-salt ($MgCl_2$). $(NH_4)_2SO_4$ is the standard choice for HIC due to its high solubility, high molal surface tension increment, resistance to microbial growth and high UV transparency (Wu et al., 1996) as well as its low costs. $Na_3C_6H_5O_7$ was selected as a second strong salting-out salt because it has characteristics different from those of $(NH_4)_2SO_4$ (el Rassi et al., 1990). NaCl was chosen because it is already present at a certain concentration in most process steps. $MgCl_2$ was chosen for its known potential specific interaction with proteins and protein-specific effects on retention in HIC (Szepesy et al., 1988).

After HIC optimization, a two-step purification process was established with AEC as flow-through step (based on section 4.1) followed by HIC as a capture step that focusses on the separation of virus particles and DNA – the latter representing a significant challenge in downstream processing of cell culture-derived IVs so far.

Determination of critical salt concentration for virus particle aggregation

The CAC was determined by measuring RMPS in solution to screen for adequate salts and salt concentrations for use in HIC in order to exclude precipitation and aggregation at the selected salt conditions. For $(NH_4)_2SO_4$, RMPS measurements provided a suitable and fast method for determination of the CAC, while for $Na_3C_6H_5O_7$ and NaCl no CAC could be found. Since, in general, the adsorption of virus particles to HIC resins could be observed at concentrations much lower than the CAC, it is possible that the CAC lies beyond the tested concentration ranges of both salts.

HIC – 96-well-plate screening for conditions

In general, whenever significant binding of virus particles occurred, a loss of virus particles in the overall balance was found in the 96-well format (Figure 23). However, no significant amounts of virus particles were found in the washing fractions (data not shown). In further experiments with chromatography columns using identical salt concentration and resins (refer to chromatographic experiments in section "HIC – Preparative chromatography and optimization (single-step)" and annex section 9.1.4), it could be verified that most of the here observed depletion of eluate recoveries for weak (Methyl, Ether) and medium strength (PPG, Phenyl) HIC resins was due to the 96-well format or protocol. Only the reduced virus recovery

for strong HIC resins (such as Butyl) was confirmed on preparative scale. The reasons for these differences between both chromatographic formats (96-well filter plates and preparative scale) are not known at the moment but should be further investigated in case additional screens for matrices, salts, and salt concentrations need to be performed in future process optimization efforts. Reducing the centrifugation time or speed might lead to improved recoveries.

Using HIC for binding DNA while keeping virus particles in flow-through could be ruled out as a process option, as the hydrophilic nature of DNA usually will not allow for interaction with the hydrophobic resin ligands. Nevertheless, adsorption of DNA could be observed with strong HIC resins and high concentrations of $Na_3C_6H_5O_7$. This can be probably attributed to an interaction between hydrophobic resin ligands and the nitrogen bases in the nucleotides (Bonturi et al., 2013). Moreover, specific binding effects of the organic salt $Na_3C_6H_5O_7$, such as potential ion-pairing with proteins, might play a role (el Rassi et al., 1990). The final choice for $(NH_4)_2SO_4$ based on experimental results was also supported by aspects of process design. It has been reported, that sulfate ions stabilize the native protein structure, while, e.g., chloride ions have a destabilizing effect (Arakawa et al., 1982).

HIC – Preparative chromatography and optimization (single-step)

Overall, three resins (Ether, PPG, Phenyl) showed comparable separation performance with high virus recoveries (77–97%) and good DNA depletion (about 77–167-fold) at preparative scale. All "salt concentration – virus particle binding curves" showed an almost linear increase up to certain concentrations, which is in agreement with the results from Kennedy (2001), who reported a similar binding behavior for proteins. Furthermore, the operating range for PPG and Phenyl was similar with about 300 mM of $(NH_4)_2SO_4$.

HIC – Flow rate dependencies

Within the tested virus particle and contaminants concentration ranges the flow rate had no impact on the protein removal efficiency (the small variation are in the typically range of variation observed in scouting experiments). Although, at higher contaminant concentrations a dependency of purification performance and flow rate could become apparent due to pore diffusion effects. However, since HIC is usually applied as a follow-up step, high contaminant concentrations are usually not be expected.

HIC – Salt performance based on ion strength

Since HIC is suitable for dealing with high salt concentrations, it qualifies as a consecutive step for chromatographic separations involving high salt concentrations in the product fraction, i.e. AEC. However, in order to achieve a comparable performance with a consecutive HIC

operation as with an independently optimized HIC (single-step, section 4.3.1), it is necessary to adapt and optimize the salt types and concentrations to the preceding product fraction. Hence, in order to achieve similar salting-out capabilities as in the independently optimized HIC (single-step), means have to be found to (partially) quantitatively substitute different salts with each other in the required concentration, while keeping the salting-out strength of the applied buffer similar. This experiment was used to evaluate ion strength as a (semi-) quantitative measure for salt substitutions. The results suggested that ion strength might be a suitable indicator for (partially) substituting equally strong salting-out salts. In addition, substituting a strong salting-out salt by a weaker salting-out salt was shown to be possible to some extent. But, there seems to be a limiting concentration paired with a non-linear relationship between substitution extent and virus recovery, which might also be influenced by the operation window/robustness of the process regarding the salting-out salt concentration. Possibly, taking into account the molal surface tension increment as suggested by Melander et al. (1977) and Mahn et al. (2007a) could give an even better indicator for the effects of a salt substitution.

HIC – Dynamic binding capacities

The results confirmed that affinity and binding capacity both increase with the salting-out strength of the salt and the salt concentration (Melander et al., 1977; Sikorski, 1988; Oscarsson, 1995; To et al., 2007). The highest determined $DBC_{10\%}$ (133 kHAU/mL resin) in this study was comparable to the $DBC_{10\%}$ of lectin-affinity chromatography (DBC: 89–233 kHAU/mL resin) (Opitz et al., 2008). The binding capacity could be likely further improved by further increasing the salt concentration (at least up to the point, where DNA starts to bind) or by switching to a weaker HIC resin (such as Ether), if required. A beneficial effect of a dual-salt strategy with regard to the dynamic binding capacity could not be observed. On the contrary, the partial replacement of $(NH_4)_2SO_4$ with NaCl reduced the dynamic binding capacity. That is in accordance with the salt strength as described by the Hofmeister series (Melander et al., 1977). Possibly, using a strong salting-out salt, such as $Na_3C_6H_5O_7$, as an additional salting-out salt might further increase the binding capacity (Senczuk et al., 2009), but would lead to a ternary salt system in most multi-step processes, where the rather weak salting-out salt NaCl is often used as a standard salt for elution in preceding steps (Gagnon et al., 1996a).

HIC – Salt effects on HA protein recovery

HA protein concentration is the basis for the determination of the total protein and DNA contamination level according to the European Pharmacopeia (refer to section 2.4). Especially, due to the well-known risk of protein denaturation at the high salt concentrations used in HIC, a confirmation of an unaffected HA protein recovery (as determined by the SRID assay, section

3.6.5), i.e. comparable to the virus recovery, is crucial in process development. The observed slightly reduced ratio of HA protein recovery/virus recovery of 94.5% lies within the error range of both assays. This suggests that the HA protein is not affected by the purification process (remark: both HA and SRID assay rely on intact HA protein, while the SRID assay is known to be the more sensitive one in terms of an affected HA protein).

HIC – Effects of process conditions adaptation

The ratio of $(NH_4)_2SO_4$/NaCl in the sample applied to HIC was adapted successfully to the expected multi-step conditions based on the ion strength. Although the salts had different salting-out capabilities, no process performance reduction was observed, which might be explained by the rather small change of the salt ratio.

HIC – Influenza virus strain dependency/single-process step robustness

For usage as a platform technology for purification of IV, a strain independency of the HIC step is of high relevance. At first, the differences in virus recoveries suggest a certain virus strain or batch dependency. However, based on the results from section "HIC – Preparative chromatography and optimization (single-step)", a straight forward adaption of the $(NH_4)_2SO_4$ concentration should be able to compensate for such dependencies. Also, for evaluating minor variations in DNA contaminant levels after HIC, different DNA starting concentrations of the various virus harvests (before loading) need to be taken into account. These different DNA starting concentrations are due to differences in virus-induced apoptosis, cell death, and cell lysis, harvest time points, and pre-processing of inactivated harvest. For A/Wis, the DNA starting concentration was about half of A/PR, while for B/Mal, the DNA concentration was almost twice as high (data not shown), which correlates with differences in DNA recoveries (%) of the HIC product fraction for the different IV strains. However, with a DNA concentration in the product fraction of 28 ng/mL (±7 ng/mL), 21 ng/mL, and 19 ng/mL for A/PR, A/Wis and B/Mal (PicoGreen® assay), respectively, the final concentrations and therefore the separation performances can be considered to be in a comparable range.

4.3.3 Results: Orthogonal process

Process performance (two-step chromatography purification process)

Next, the adapted HIC process step (refer to section "HIC – Effects of process conditions adaptation") was coupled to an AEC step. Figure 32 and Table 17 show the performance of this two-step chromatographic purification strategy (AEC-HIC), including the buffer addition step (conditioning) between both chromatography steps (refer to section 3.5.2). For the corresponding chromatograms refer to the annex section 9.1.1.

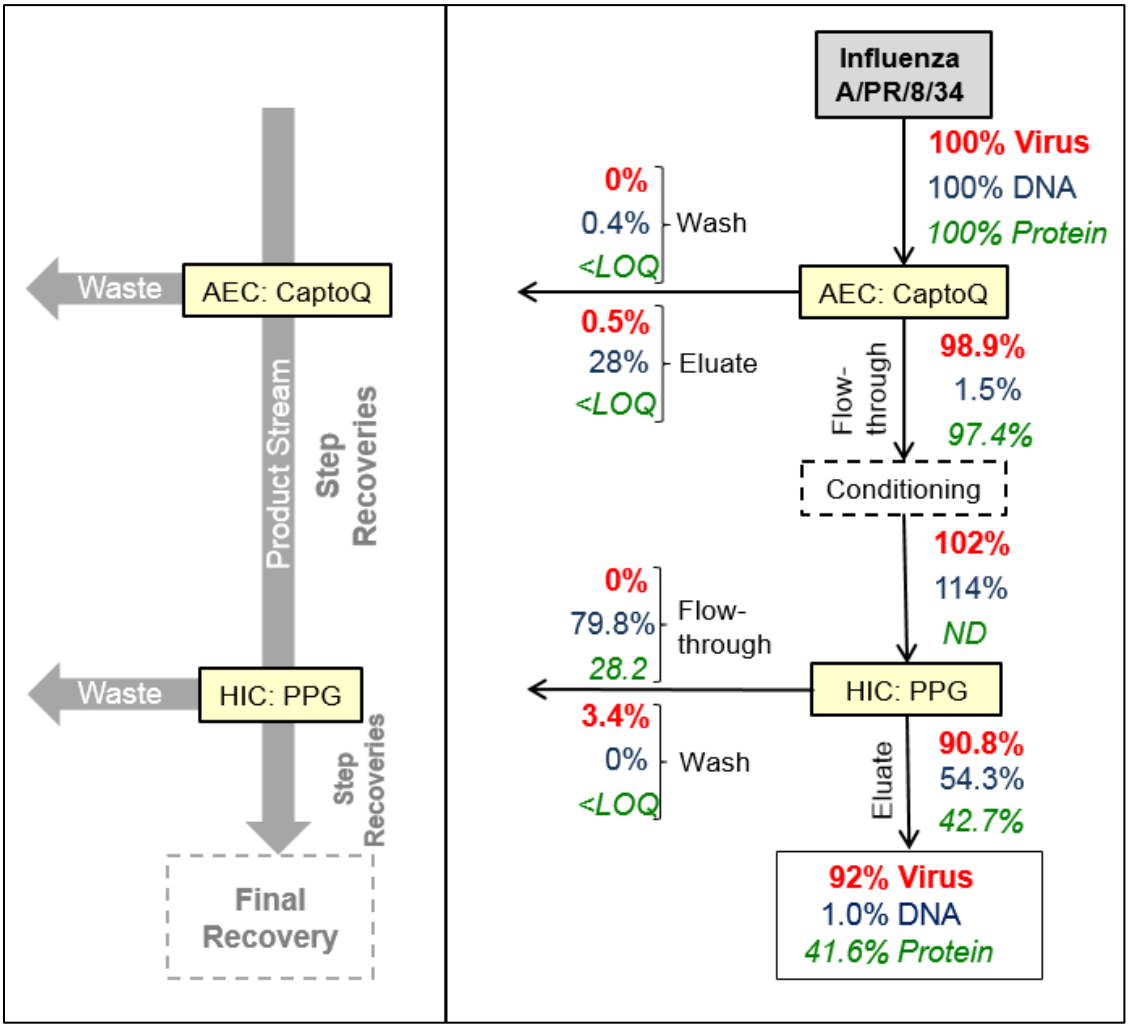

Figure 32: Two-step chromatography purification process using an AEC flow-through step and a HIC capture step. Shown are the step and the final recoveries (in %) for virus particles (→ virus), DNA and total protein (→ protein) for the product stream and the wastes based on HA assay, PicoGreen® assay and Bradford assay, respectively. The virus material entering the AEC step was pre-processed and conditioned as described in section 3.5.2. The conditioning step represents the addition of buffer to adjust the $(NH_4)_2SO_4$ concentration. For corresponding data set refer to Table 17.

Minor virus particle losses could only be found during the HIC step (9.2%; within the error range of the assay). Both steps also showed a significant reduction of DNA (step depletion: AEC: 98.5%/LRV: 1.8; HIC: 45.7%/LRV: 0.3). With respect to reduction of residual proteins, only the HIC step removed a significant amount (57.3%/LRV: 0.4).

Overall, 92.2% (9.2 kHAU/mL) of the virus particles could be recovered while reducing the residual DNA level to 1.0% (LRV: 2; 18 ng/mL) (according to the PicoGreen® assay) and the residual protein level to about 42% (LRV: 0.4; 6 µg/mL).

Table 17: Two-step chromatography purification process. Shown are the experimental values of Figure 32 including concentrations/HA-activities and volumes of each process step and final (overall) process recoveries in the product fraction.

Steps	Volume		a_{HA}		Virus
	IN [mL]	OUT [mL]	IN [kHAU/mL]	OUT [kHAU/mL]	Step recovery [%]
Capto Q	80.0	86.7	24	22	98.9
Conditioning	55.0	123.8	22	10	102.6
HIC	90.0	87.8	10	9	90.8
Final recovery [%]					92.2

Steps	Volume		DNA		DNA
	IN [mL]	OUT [mL]	IN [ng/mL]	OUT [ng/mL]	Step recovery [%]
Capto Q	80.0	86.7	4394	63	1.5
Conditioning	55.0	123.8	63	32	114.3
HIC	90.0	87.8	32	18	54.3
Final recovery [%]					1.0

Steps	Volume		Total Protein		Total Protein
	IN [mL]	OUT [mL]	IN [µg/mL]	OUT [µg/mL]	Step recovery [%]
Capto Q	80.0	86.7	32	29	97.4
Conditioning	55.0	123.8	29	ND	ND
HIC	90.0	87.8	13*	6	42.7
Final recovery [%]					41.6

*calculated based on dilution by conditioning.
ND: not determined

Impurity level estimation

The estimated impurity levels per monovalent dose achieved by the process are shown in Table 18. The contamination levels of a trivalent dose can be estimated with 6.0 ng DNA and 51.6 µg total protein, respectively. Even without using a nuclease step this clearly fulfills the purity requirements for manufacturing of human influenza vaccines.

Table 18: Final product fraction of the two-step chromatography purification process for IV A/PR. Shown are the HA protein concentration, relevant impurity levels, and estimated impurity levels for a dose input of 15 µg HA protein (monovalent dose for cell culture-derived vaccines for human use). HA protein, total protein, and DNA concentration are based on SRID, Bradford, and Threshold® assay, respectively.

Measured concentrations	**IV strain A/PR**
HA protein [µg/mL]	5.0
DNA [ng/mL] (Threshold® assay)	0.7
Total protein [µg/mL]	5.7
Estimated impurities	
ng DNA/15 µg HA [a]	2.0
µg total protein/15 µg HA	17.2

[a] calculations based on Threshold® assay data.

4.3.4 Discussion: Orthogonal process

Process performance and robustness (two-step chromatography purification process)

Overall, the combination of AEC and HIC resulted in high virus recoveries (Figure 32; final recovery: 92%) without requiring any buffer exchange after the first chromatography step. The essentially loss-free AEC step is in agreement with previous observations (refer to section 4.1.3). Small virus particle losses were only observed after the HIC step, which was in agreement with the HIC optimization experiments (sections "HIC – Salt effects on HA protein recovery" and "HIC – Effects of process conditions adaptation").

With a final DNA contamination level of 1.0% (based on PicoGreen® assay values), the process was able to remove most of the host cell DNA. While the majority of DNA was depleted using AEC (98.5%), an additional 0.5% of total DNA was removed using the subsequent HIC step. In comparison to the single-step HIC results (sections "HIC – Salt effects on HA protein recovery" and "HIC – Effects of process conditions adaptation", ≥98.7% depletion) this

suggests a significantly reduced efficiency in the later process step. However, it is well known that DNA removal often depends on the starting DNA concentration as well as sample composition and might be attributed to a possibly different nature of the remaining DNA (e.g., fragment length; for a detailed discussion of DNA concentrations determined by PicoGreen® assay and the residual DNA levels also refer to section 4.4) (Opitz et al., 2007; GE Healthcare, 2012b).

The two-step purification process (Figure 32) was able to reduce the total protein content to 41.6%. In accordance with section 4.1.3, AEC had only a limited impact on total protein depletion. Most of the protein was removed by the HIC step (57.3%), which is in good agreement with the HIC optimization experiments (sections "HIC – Salt effects on HA protein recovery" and "HIC – Effects of process conditions adaptation").

Impurity level estimation

Comparing the Threshold value (Table 18) for the DNA depletion with the PicoGreen® value (Table 17), the Threshold value was significantly lower (recalculation of process yields based on Threshold value: 0.04% final DNA content; 2.1% HIC step recovery; 1.7 LRV for HIC). Furthermore, this Threshold value is now in good agreement with the PicoGreen® results obtained by single-step HIC optimization (Figure 29 and Figure 30). However, the final Threshold value was about 26-fold lower than the final PicoGreen® value. Comparable discrepancies between PicoGreen® and Threshold values have been seen for the membrane-based process (section 4.2.3). As discussed in section 4.1.4, the fragment size specificity of both DNA assays could be the reason for the discrepancy. For a detailed discussion, please refer to section 4.4.

Overall, the orthogonal process was able to reach the required contamination limits, while achieving high virus recoveries. While a nuclease digestion step was not required to reach the required contamination level for DNA, the addition of such a step might help to increase process robustness in case of larger batch-to-batch variations in the DNA content of virus harvests (i.e. strain dependence of cell lysis, see below). In addition, it serves as an additional safety measure to reduce the risk of residual host-cell and unwanted viral nucleic acids, especially by cutting down long DNA fragments.

4.4 Discussion of sources for residual DNA in the product fraction

Although it could be shown that the developed processes are able to reduce the product contamination content to the required levels, stricter limits requested by the national health departments, such as in China (100 pg DNA/dose), for instance, might require further reduction of the DNA and protein contamination levels in the future. But, despite using different purification approaches such as nuclease digestion, polar and nonpolar chromatographic resins, DNA contamination level of the product fraction seems to remain at a concentration range between 1 to 10 ng DNA regardless of the used numbers of steps. Therefore, other potential sources for the residual DNA in the product fraction should be discussed.

First, a false positive signal of the DNA assays needs to be excluded. As demonstrated in section 4.1.3, 4.2.3 and 4.3.4 the results of the PicoGreen® and Threshold® assay results do not match. As discussed before, both assays have different fragment size specificities as well as different DNA type specificities (PicoGreen®: only dsDNA, Threshold: dsDNA and single stranded deoxyribonucleic acid (ssDNA)) (Wolf et al., 2007; Invitrogen, 2008; Ikeda et al., 2009; Sedlackova et al., 2013). In particular, processes that make use of nuclease digestion steps (refer to section 4.1 and P. Marichal-Gallardo et al. (2017)) show lower discrepancies between both assays indicating that fragment size specificity of the assay plays a role in the diverging assay results.

It is also known that PicoGreen® measurements can be influenced by various proteins (e.g., BSA) (Invitrogen, 2008) while proteins are digested prior to measurement in the Threshold® assay. The fact that the composition of proteins is altered during purification, adds to the complexity of this problem. Furthermore, the impact of RNA on the PicoGreen® quantification assay appears to be minor according to the manufacturer, but might still be present (remark: an average amount of 13.5 kb RNA per virus particle can be assumed (N. Lee et al., 2017)). Information about the Threshold® assay is less abundant, although it is well established in pharmaceutical industry. As shown in case of the SRID assay (refer to section 4.1.5), the sample composition changes significantly throughout the purification process making it difficult to rely on assay validations which were based on samples containing only one type of model DNA, artificially composed samples or unpurified starting material. Considering the sensitivity of the DNA assays, especially the LOQ should be determined with a wide selection of different samples (also samples purified by different methods) and compared. Also, it would be advisable to use a third orthogonal DNA quantification method for confirming the assay results, such as a qPCR (Nissom, 2007). The qPCR is a valuable method for detecting contaminations or quantification of the vaccine dose content (Wolf et al., 2007).

Moreover, it can be used for specifically quantifying host-cell DNA and has a low LOD. However, qPCR suffers from fragment length specificity as well being an indirect measurement method (often requiring other methods such as PicoGreen® for calibration). Furthermore, proteins in the sample can affect the results making a DNA extraction or protein digestion by proteases necessary. The selection of targets, the design of primers and probes and the selection of the fluorescence dye have a critical impact on the results making a comparison between different published processes difficult. In general, comparison of qPCR data between different labs poses a problem (Bustin et al., 2009). In addition, the sensitive multi-step qPCR protocol often results in non-congruent results between different laboratories despite using identical equipment and kits. Most importantly, the application of most IV inactivation substances, such as β-propiolactone, would forbid the use of a PCR technique as the nucleic acid as well as polymerase efficiency is altered as shown by Perrin et al. (1995).

Another aspect is the sample preparation for DNA analysis. Due to the limited quantification range of the PicoGreen® assay, samples after the final purification step have to be concentrated by lyophilization. Although the method had been successfully used in our research group before, changes in sample structure, DNA loss by adsorption effects or minor variations in the lyophilization procedure might also contribute to variations in concentrations.

Once, a false-positive signal of both assays is excluded, residual DNA can be assumed to be present. In literature, similar residual DNA levels have been observed in IV particle purification processes (Opitz et al., 2007; GE Healthcare, 2012b).

The fact that the nuclease Benzonase®, known to be rather unspecific, was not able to decrease the DNA content in the product fraction in this study any further (see flow-through and membrane-based process) adds to the complexity of the problem. Moreover, keeping in mind that flow-through as well as capture chromatography steps have been used, the DNA might be absorbed or attached to the virus particles. A binding of residual cellular nucleic acids, treated with β-propiolactone, to rabies virus particles has been reported by Perrin et al. (1995). Due to the claimed ability of Benzonase® to digest also bound DNA (to proteins or virus particles) and its non-specificity (Martin, 1991), DNA adsorbed to virus particles or a specific DNA fragment sequence seems less likely to be the reason for the residual DNA. Also, a co-localization of DNA with virus particles could not be observed by P. Marichal-Gallardo et al. (2017) (data not shown in the publication). On the other hand, similar residual DNA limitations, despite using a wide variety of DSP methods, have been reported previously, confirming aggregation of DNA and virus particles (Konz et al., 2005). There, aggregates were eliminated by using non-ionic

detergents (to attenuate hydrophobic interactions) and NaCl (to attenuate electrostatic interactions).

Also, the presence of inaccessible DNA containing entities such as extracellular vesicles (EV) or chromatin should be considered as a source. EVs released from cells during virus production (Meckes et al., 2011; Choi et al., 2015) could contain proteins in its lipid bilayer and DNA inside (Lamichhane et al., 2015; Qian et al., 2015), rendering them potentially indiscernible for most chromatographic methods, while the enclosed DNA being also inaccessible to nucleases. Chromatin, on the other hand, is a complex of DNA, histones and non-histone-proteins (such as actin, HMG-proteins und polymerases) and is regarded as (partially) nuclease-resistant (Svetlikova et al., 1979; Tsanev et al., 1992). Especially its aggregation with the process product can lead to difficulties in purification processes (Gan et al., 2013; Gagnon et al., 2014; Gagnon et al., 2015). The presence of histone proteins and/or DNA in purified virus particle preparations and the presence of EVs was already confirmed by P. Marichal-Gallardo et al. (2017; 2019) using stimulated emission depletion microscopy and transmission electron microscopy, respectively. Moreover, formation of aggregates of DNA with virus particle membrane fragments (including the HA protein) could lead to highly stable and inaccessible (but soluble) aggregates or compact DNA conformations, which might show similar purification behavior as the virus particles.

Furthermore, a chemical alteration of the DNA structure might be the reason for the observed DNA clearance limitation. β-propiolactone was used for inactivation of the IV particles for all tested batches here as well as in other research projects of the research group. It consists of an highly reactive ring structure (intramolecular ester), which forms with amines, thiols and other nucleophiles the corresponding amides, thiol carboxylic acids and other carbonic acid derivates of the 3-hydroxy-propionic acid. However, the exact nature of the reactions of β-propiolactone with viral components is still largely unknown. According to literature, it modifies DNA or RNA (Roberts et al., 1963; Colburn et al., 1965; Mate et al., 1977; Budowsky et al., 1991; Perrin et al., 1995). Besides, modification on the protein level have also been reported (Goldstein et al., 1970; Herrera-Rodriguez et al., 2019). Uittenbogaard et al. (2011) showed that modification can occur in deoxyguanosine, deoxyadenosine and/or cytidine. Therefore, the DNA might become inaccessible to nucleases in DSP, especially considering a zwitterionic polymerization. Also, they have furthermore shown, that β-propiolactone also modifies proteins to a large extend. Nevertheless, experiments in the context of this PhD thesis, where virus samples were treated with different concentrations of β-propiolactone and other inactivation substances and afterwards treated with Benzonase® could not show any adverse effects on the

DNA level after nuclease digestion (data not available). However, confirmation with a low-range DNA assay would still be required.

Moreover, the contamination of the sample with minor amounts of bacterial particles should be considered in this study, since harvest and purification was conducted under non-sterile conditions (in contrast to processes that are established following GMP guidelines in industry).

The following discussion of the results in the context of the state-of-the-art (section 4.5) also sheds more light on the origin of the residual DNA content in the present results identifying the serum-containing medium and the freeze-thaw cycle after concentration as a possible source for the residual DNA content.

4.5 Comparison of the three purification processes

In order to compare the three proposed processes, most relevant aspects of each process are summarized here (Table 19).

Table 19: Comparison of the three purification processes: flow-through, membrane-based and orthogonal. Data summarized from the specific sections.

	Flow-through process (bead-based)	Membrane-based process	Orthogonal process (bead-based)
Final virus recovery [%]	68–87	75	92
Final DNA contamination level [ng DNA/15 µg HA]	2.5/ 3.2/ 4.6*	1.2	2.0
Final total protein contamination level [µg total protein/15 µg HA]	18.7/ 17.3/ 41.9	19.8	17.2
Pros	least strain-/ batch-/upstream process-dependency (in principle)	high flow-rates (low pressure drop) and low mass transfer resistance → high productivity	high adaptability (by change of salts and salt concentrations)
	nuclease safety step and removal included	easy to scale-up	access to separation of a wider range of contaminants possible
		disposable/single-use membranes/ reduced cleaning-in-place (CIP)	
		only two purification steps	only two purification steps
Cons	no concentration of sample (additional concentration step required)	potential strain dependency → specific condition adaptation potentially necessary	potential strain dependency → specific condition adaptation potentially necessary
	limited flow rate/ reduced productivity		limited flow rate/ reduced productivity
	nuclease step required; 3rd step; additional costs		

*data from section 4.1.5

Overall, it could be shown that all processes are able to reduce both total protein and DNA contamination levels below the required limits requested by the EMA (European Medicines Agency) (European Pharmacopoeia, 2018) (except for DNA of the A/Wis sample in the flow-through process). All processes have shown comparable and high purification performances. Also, each process has been set-up so rebuffering between the steps (e.g., by diafiltration) is not required. Furthermore, all processes use off-the-shelf materials with existing GMP-certified corresponding products (except for SCMA, which is not yet available as GMP-certified product), are reduced to a minimum amount of steps and can be expected to be easily and quickly implemented in an industrial influenza vaccine manufacturing process. Therefore, the decision will mostly depend on the aspects shown in Table 19.

The proposed flow-through process represents a potential solution for establishment of a simple and robust platform technology for production of cell culture-derived influenza vaccines. Although showing a certain batch or strain dependency, it can be expected to be the most robust process because of the absence of a virus particle capture step. Due to a three step purification strategy as well as the need for an additional concentration step (no concentration of the harvest in the process), the costs can be expected to be slightly higher in comparison to the other processes (that is, if the other processes are operated without a nuclease digestion step and without an additional concentration). Moreover, if the applied sample has a high level of contamination, an increased amount of resin might be required in the two chromatography steps. Nevertheless, the flow-through process inspired already other research groups to further optimize this process (Tseng et al., 2018). Besides, the detailed data on the nuclease digestion gives valuable data for future downstream process designs utilizing a nuclease step. The consequent use of chromatographic flow-through process units would also avoid some typical problems found with chromatographic capture steps. As elution steps with, e.g., high amounts of salts can be omitted, the risk for reduction of immunogenicity and aggregation of the virus particles is reduced, too. In particular, for virus harvest with moderate DNA and protein contamination levels, non-capture processes should be highly suitable for efficient virus particle purification. Finally, the expiration of patents for Benzonase® and the availability of new nucleases makes an enzymatic digestion step in the process chain an affordable and additional safety step. Also, the added nuclease could be successfully removed in the following purification step.

Relying completely on membranes after clarification and concentration (both also using filters and membranes), the proposed membrane-based purification process should be the most economic, simplest and fastest approach compared to the other two processes of this work.

Membranes are usually operated in single-use, omitting cost-intensive CIPs. Furthermore, no labor-intensive packing and characterization of columns is required. The membrane modules are easy to operate and can be scaled up without problems (such as bed integrity, feed distribution, column pressure or dimension ratio limits). A certain batch or strain dependency ((Opitz et al., 2009a; Opitz et al., 2009b) and section "STMA strain-dependent single-process step robustness") could be encountered by process condition adaptions or an additional nuclease step.

The proposed orthogonal process approach efficiently combines a charge-based (flow-through) with a hydrophobicity-based chromatography (capture) step. It achieved the highest virus yield and the second best DNA depletion result of the three processes. So far, HIC has been mostly neglected for virus particle purification, mostly due to its cumbersome method protocol establishment involving a certain care with the high salt concentrations. However, applying two complementing purification steps leaves a lot of room for further process improvements and adaptations, making this process rather versatile and adaptable. It could be successfully shown, that the exposure to the high salt concentration had no detrimental effect on the virus recovery. Also, the orthogonal process can be expected to be applicable for a wider range of contaminants and virus strains. The observed batch or strain dependency could be counteracted by straightforward salt concentration adaptations, if required.

Overall, each of the three processes represents an interesting option for the influenza vaccine industry with the final decision depending on the demands towards the production process (e.g., robustness, costs, flexibility) and on the already existing facilities.

4.6 Discussion in the context of the state-of-the-art

In general, most downstream processes require a minimum number of two steps. Since each purification method has its own advantages and disadvantages (e.g. in terms of productivity, specificity, yield, operation or production costs) and the performance will vary based on the product and contaminant composition, for a rational downstream process design it is necessary to have a tested toolbox of methods at hand.

For an overview and easier comparison of available purification processes for cell culture-produced IV, the relevant published data has been divided into single-steps and whole/multi-step processes (Table 20 and Table 21).

Table 20 gives an overview of the single-step purifications of all three processes from this research (either from the whole process (1st step) or from the single-step optimization) as well

as from literature. In particular, the overview allows for evaluation of the purification performance in terms of product (IV) losses. The data regarding DNA and total or host cell protein depletion needs to be evaluated with caution, since (in general) all research groups used different starting materials, in particular different culture media, or used a different pre-processing approach. In addition, some research groups applied assays other than those used here (although the effect should be mitigated to some extent as percentage recoveries are shown). Therefore, the starting concentrations and composition of the contaminants would vary significantly affecting also the recovery "rates". Moreover, a preceding purification step will generally reduce the effectiveness of the following step.

Overall, monoliths appear to show reduced virus recoveries (Banjac et al., 2014; Fischer et al., 2018), if no zwittergents are used. Furthermore, the virus recoveries seem to depend strongly on the cell culture medium selection, which reduces its process robustness. Yet, monoliths are of high interest for virus particle purification due to their high dynamic binding capacity. Also, the DNA and protein removal capabilities are good. Since it is still a material with a rather short product development history, it can be expected to produce improved results in the future. In particular, fouling, respectively pressure increase, seems to require special attention.

Using lectins for affinity chromatography (Opitz et al., 2007; Opitz et al., 2008) has shown very good overall results, but in particular the potential toxicity of leaching ligands and the high price would need to be addressed for an industrial usage.

Although not showing as high virus recoveries as other published processes, Iyer et al. (2012) data clearly shows that applying larger beads (e.g., 200 µm) will improve the virus recovery in flow-through processes. Also, using membranes in a flow-through mode, applying a dual-salt approach in combination with the ChromaSorb™ membrane appeared to be highly efficient (Iyer et al., 2012). Unfortunately, the production of this membrane material was discontinued.

The usage of SEC in the influenza process appears to be an obvious choice due to the prominent attribute of IV particle size versus the contaminants. It is the only truly size-based chromatography and therefore of high interest for virus particle separation, since, in principle, it can also be considered as rather batch, medium, host-cell and IV strain independent. Unfortunately, applying SEC in the IV purification process does not yield much benefit due to its incapability to significantly deplete the critical contaminant DNA. Furthermore, the typical low productivity in a classical DSP chain is disadvantageous.

Steric exclusion chromatography (SXC) (P. Marichal-Gallardo et al., 2017) is a rather new approach for downstream processing of vaccines, which has also been successfully applied for

other viral vaccines and viral vectors (K. Lothert et al., 2020; Keven Lothert et al., 2020; P. Marichal-Gallardo et al., 2021). It requires the presence of polyethylene glycol (PEG). Although the mechanism behind it is still not fully understood, it is assumed that it separates based on size and charge (zeta-potential). The interaction with the chosen hydrophilic material (e.g., a membrane such as regenerated cellulose) does not seem to be based on a direct chemical interaction but on a thermodynamical effect related to precipitation. The process performance can be mainly adjusted by varying the PEG chain length, the PEG concentration and the salt concentration. The published process seems to give excellent product recoveries (112%), while depleting DNA and total protein levels very efficiently. Moreover, PEG is considered non-toxic and is widely accepted due to its use in medicine/pharmacology and cosmetics. Also, the GRAS-Status (i.e. generally regarded as safe) has been assigned to it. The only known disadvantage of PEG is the increase in viscosity of the solution, which can cause back pressure problems in the process.

Regarding the purification steps established for the three processes (HIC, AEC, LCC, STMA), in short all of them showed the ability to reach a virus recovery of at least 90% (Weigel et al., 2014; Weigel et al., 2016; Weigel et al., 2019). Also, the used SCMA step, thoroughly established by Opitz et al. (2009b) and in-detail characterized by Fortuna et al. (2014; 2019), showed an acceptable virus recovery (80%). Furthermore, with the exception of LCC, which was therefore used in combination with a nuclease step, all used purification steps were able to achieve a high DNA depletion (>95%; most even ≥99%). In summary, all used/established purification steps of this work showed a combined virus recovery and DNA depletion performance belonging to the best performing purification steps published so far. Also, the recoveries of all processes were conclusive (i.e. no recoveries beyond 100%) and most of the here established steps were tested for robustness using multiple IV strains.

With the LCC, the STMA and the HIC, three new tools with unique characteristics are now available for the design of downstream processes in viral vaccine production. Overall, with the addition of recent works, a sufficient toolbox seems to be available in order to design adequate industrial IV purification processes. Although the comparison of published process performances is not straightforward due to missing data or different process parameters (e.g., IV strains, cell culture medium and IV producing cells) candidates can be identified for different process options. As seen in the present work, it would be favorable, if at least the IV strain dependency would be incorporated in all research works to get a first estimate of the process step robustness.

Table 20: Overview of published data of established chromatographic single purification steps for cell culture-produced IV particles (alphabetical order). Only references with a considerable amount of accompanying data and overall conclusive data (by and large closing mass balances) are listed. If multiple batches or IV strains were tested, a range is given. Values ≥10% were expressed in round numbers; ---: no data (in %) available.

author, year	chromatography type	material type	operation mode	virus recovery [%]	DNA recovery [%]	protein recovery [%]
Banjac et al. 2014	AEC (CIM-QA)	monolith	capture	54	0.4	7.1
Carvalho et al. 2018	Pseudo-affinity C. (SCMA)	membrane	capture	64	---	---
Fischer et al. 2017	AEC (CIM-QA)	monolith	capture	18–70	1	---
Fortuna et al. 2019	Pseudo-affinity C. (SCMA)	membranes	capture	75–81	0.3–2.6	12–22
Iyer et al. 2012	AEC (200 µm beads)	beads	flow-through	80	---	28
Iyer et al. 2012	Mix: AEX-HIC (200 µm beads)	beads	flow-through/capture	72	---	16
Iyer et al. 2012	Mix: AEX-HIC-CEX (200 µm beads)	beads	flow-through/capture	71	---	14
Iyer et al. 2012	AEC (ChromaSorb™)	membrane	flow-through	~100	≥0	---
Kalbfuss et al. 2007	AEC (Sartobind Q)	membrane	capture	72	105	23
Kalbfuss et al. 2007	SEC (Sepharose 4 FF)	beads	size-exclusion	85	34	35
Kalbfuss et al. 2007	AEC (Sepharose Q)	beads	flow-through	82	1.6	68
Kalbfuss et al. 2008	SEC (Sepharose 4 FF)	beads	size-exclusion	96	---	50
M.-Gallardo et al. 2017	SCX (regenerated cellulose + PEG)	membrane	capture (steric exclusion [a])	112	0.3	7.6
Opitz et al. 2006, 2008	Affinity C. (Lectin)	beads	capture	77–87	0.5–2.6	16–36
Opitz et al. 2009	Pseudo-affinity C. (SCMA) [b]	membrane	capture	62–94	1.0–32	15–43
Weigel et al. 2014	AEC (Capto Q)	beads	flow-through	96–99	1.0–4.3	90–98
Weigel et al. 2014	AEC (DEAE)	beads	flow-through	81–87	0.5–0.8	---
Weigel et al. 2014	LCC (Capto Core)	beads	flow-through/size-exclusion	93–96	71–83	31–43
Weigel et al. 2016	Pseudo-affinity C. (SCMA) [b]	membrane	capture	80	2.5	29
Weigel et al. 2016	AEX (STMA)	membrane	flow-through	97	0.81	---
Weigel et al. 2019	HIC (PPG)	beads	capture	83–96	0.7–1.3	53–65
Weigel et al. 2019	HIC (Phe)	beads	capture	62–90	0.6–3.3	31–53

[a] steric exclusion with precipitant PEG; [b] process conditions, membrane material, cell culture medium and IV strain to the authors knowledge similar.

In Table 21 the most relevant data of the published influenza purification processes (multi-step) is shown, including the three published processes of this work. The overview allows for evaluation of the different purification performances in terms of overall product (IV) losses as well as the expected dose contaminations.

At least some of the published data require careful interpretation. In particular, overall virus recoveries way above 100% show the need for a parallel mass balance based on a second assay (such as the SRID) for cross checking. Here, multiple runs with the same batch in order to avoid batch variability would be also required for data evaluation. Furthermore, the process robustness proofed to be an issue for all processes, where it was tested.

Of the shown processes, (1) the continuous centrifugation process (Kistner et al., 1998), (2) the four-step process (He et al., 2011), (3) the flow-through processes (Weigel et al., 2014; Tseng et al., 2018), (4) the membrane-based process (Weigel et al., 2016), (5) the SMB-CIM-QA (simulated moving bed-convective interaction media® (monolith) quaternary amine) process (Fischer et al., 2018) and (6) the orthogonal process (Weigel et al., 2019) were (apparently) able to meet the required contamination limits.

Although P. Marichal-Gallardo et al. (2017) have utilized a nuclease, they were not yet able to achieve the required DNA contamination levels. Considering the already achieved low DNA content, a combination with a second membrane step using the STMA or SCMA established in this work or by Opitz et al. (2009b), respectively, should be sufficient to achieve the required DNA level. By using membranes only, the productivity of the process would still be high. As first experimental results suggested little benefit from the combination of the SCX step with the SCMA step (P. A. Marichal-Gallardo, 2019), adding a STMA step would be the next option. Alternatively, a combination with a hydrophobicity-based method, such as HIC, should result in the required purity.

Kalbfuss et al. (2007b) used a SEC step in combination with an AEC step (flow-through), but was also not able to reach the required DNA content levels. However, even if a satisfying purity would have been achieved, the low productivity of the SEC step as an early purification step would probably still remain the bottleneck of the process.

Using a simulated-moving-bed approach does strongly increase the productivity of the SEC addressing one of its biggest disadvantages. Therefore, the suboptimal yields (70%) achieved by Kroeber et al. (2013) could be accepted. While using the SMB did not solve the DNA issue, the latter was addressed by using a nuclease in advance. Unfortunately, the enzymatic digestion of DNA was not sufficient to decrease the DNA concentrations to the required levels.

Furthermore, the protein concentration was already below the contamination limit before the SMB-SEC to begin with. So, currently, this approach (nuclease + SMB-SEC), requiring at least one further purification step, appears to be a rather complex and expensive work-around with little benefit.

Table 21: Overview of published process data of influenza purification processes (multi-step) for cell culture-produced IV particles (sorted by publication date). Only references with considerable accompanying data are listed. If multiple batches or IV strains were tested, a range is given. Values do not include data from harvesting and pre-processing (e.g. crossflow filtration) steps. Values ≥10% were expressed in rounded values; ---: no data available.

Author, year	No. of steps	Process steps	Purification step types	Process mode	Virus recovery [%]	DNA dose levels [ng/15µg]	Protein dose levels [µg/15µg]
Kistner et al. 1998	3–4	1. Nuclease (Benzonase®) 2. UF 3. Protamin-Sulfate-Precipitation 4. Continuous-Centrifugation	precipitation + gradient centrifugation	enzymatic + salting-out + density/size-separation	---	≤0.033 [b]	≤83 [b]
Kalbfuss et al. 2007	2	1. SEC (Sepharose 4 FF) 2. AEC (Sepharose Q XL)	beads	mixed (orthogonal)	53	455–620	88
He et al. 2011	4	1. SEC (Sephadex G-50) 2. AEC (DEAE) 3. PseudoAffinity (Cellufine Sulfate) 4. SEC (Sepharose 6 FF)	beads	mixed (orthogonal)	121	0.033	87
Kröber et al. 2012	1 (SMB)	1. SMB (SEC; 3 columns)	beads	size-exclusion	70	---	73–124
Weigel et al. 2014	3	1. AEC (Capto Q) 2. Nuclease (Benzonase®) 3. LCC (Capto™ Core 700)	beads	flow-through + enzymatic	68–87	4.2–7.8 (2.5–4.6) [a]	17–42
Weigel et al. 2016	2	1. STMA 2. SCMA	membranes	mixed (charge-based)	75	1.2	20
Fischer et al. 2017	2 (SMB)	1. SMB (CIM-QA; 3 columns) 2. Nuclease (Benzonase®)	monolith	capture + enzymatic	89–100	0.08–0.3	34–36
M.-Gallardo et al. 2017	2	1. Nuclease 2. SCX	membranes (+ precipitant)	enzymatic + capture (steric exclusion with PEG)	99–117	4.3–24	38–64
Tseng et al. 2018	2–3	1. AEC (Capto Q) 2. LCC (Capto™ Core 700) (3. UF/DF)	beads	flow-through	78	0.03–0.13	22–72
Fortuna et al. 2019	2	1. SCMA 2. Nuclease	membranes	capture + enzymatic	75–81	4.2–11	38–80
Weigel et al. 2019	2	1. AEC (Capto Q) 2. HIC (Phe)	beads	mixed (orthogonal)	92	2	17

re-evaluated data from section 4.1.5; [b] extrapolated from data of final product

In another SMB process (Fischer et al., 2018), using a monolith with quaternary amine ligands and a following nuclease digestion step, high virus recoveries and contaminant (DNA and Protein) removal below the requested limits could be achieved. To increase virus recoveries, a zwittergent had to be added to the feed and the buffers. Data regarding the IV strain dependency of this capture process was not shown. Also, the nuclease had to be added after the chromatographic purification step in order to achieve a DNA concentration below the contamination limit. Therefore, another purification step (including the additional product losses) would be required for the nuclease removal despite the costly and complex SMB process. Furthermore, the SMB benefit is questionable here: The main purpose for applying a SMB is to increase the separation zone width of the chromatographic process and thereby increasing the productivity. It is therefore particular useful for SEC due to its non-binding separation characteristics. Moreover, it can be beneficially applied for operating a standard binding chromatography process, such as an AEC, HIC, etc., if the column loads in the separation zone are high enough (i.e. significantly above the typical column loads, which are often close to $DBC_{10\%}$, depending on the product value and process costs). As shown, the productivity is below the batch productivity (due to the loading amounts at $DBC_{10\%}$). More importantly, in general, an industrial SMB process would require an accurate and reliable online product quantification method in order to control the process reliably, which is not yet available and challenging for implementation. Variations in product retention might cause deviation from optimal cyclic (quasi-) steady-state operation, which could lead to high product and/or separation losses. Due to the excellent properties of and the results on the CIM-QA (DBC and separation performance), applying and optimizing the CIM-QA in a discontinuous three-step-process with an LCC as the third step might yield a more cost-effective and applicable process.

Kistner et al. (1998) published a data set for a downstream process utilizing the still commonly used continuous centrifugation with a sucrose gradient. Besides a precipitation step, also a nuclease step was applied. So far, it could be the best performing downstream process regarding the purity (DNA and total protein). However, it might be more difficult to maintain sterility with such equipment. Unfortunately, there is no data on process virus recovery. Furthermore, information on the applied DNA assays is missing. Therefore, an evaluation of the process remains incomplete.

He et al. (2011) reported a final virus recovery of 102% from the harvest to the purified product fraction (8 steps). The chromatographic purification train comprised four steps: SEC (Sepharose G50), AEC (DEAE; flow-through mode)), Pseudo-Affinity (Cellufine Sulfate), and SEC (Sepharose 6FF), and achieved a virus recovery of 121%, while the AEC (DEAE) step

achieved even 150% virus recovery. The virus particles were produced with Vero cells grown in serum-free medium. The DNA and total protein contamination levels were reduced to 0.33 ng/15 µg HA protein and 87 µg/15 µg HA protein, respectively. Interestingly, the starting hcDNA level was very low (estimated hcDNA concentration: 0.02–0.05 µg/mL (after centrifugation of harvest) in comparison to other published processes. Unfortunately, process performance had only been demonstrated for one influenza strain, no errors were reported (indicating a single run) and no data on the development of single purification steps were provided. Besides using a high number of purification steps, this process was also performed at 4°C, making the industrial application costly. Moreover, in the here presented work, it could be shown that the DBC of DEAE is relatively low; together with two SEC steps (one of them used as a prefiltration step) with the typical bottlenecks such as loading capacity and column packing quality, the productivity of this process might have to be questioned. Finally, even taking into account the large errors involved in virus particle quantification, the mass balances of several steps were not conclusive (recoveries of up to 150% in the product fractions).

Tseng et al. (2018) have used the flow-through process established by Weigel et al. (2014), but without a nuclease step, and were able to achieve an improved DNA purity over the process of Weigel et al. (2014). While the virus recoveries for the AEC step were comparable, the virus recovery for the LCC step was lower (79%). Also, the protein and DNA removal performance was different: With the AEC step they removed less DNA (8.4% residual DNA), while the protein content was reduced to 42.3%. The total protein depletion in LCC was in a comparable range (remaining total protein content: 31%), while more DNA was depleted (remaining total DNA content: 68%). The latter can likely be attributed to the missing nuclease step, which reduces the absolute DNA amount in the loaded material significantly but at the same time generally reduces the relative depletion performance (%) of the following purification steps. Surprisingly, although the single steps were showing overall similar performance to the here established flow-through process (refer to section 4.1.3) and the nuclease step was missing, Tseng et al. (2018) still achieved a better DNA contamination level per dose with 0.03–0.13 ng DNA/15µg HA than the originally established flow-through process (Weigel et al., 2014) of this work with 2.5–4.6 ng DNA/15µg HA. The more than 10-fold improvement in DNA reduction without using a nuclease digestion step can also not completely be explained by the following UF-concentration and sterile filtration step performed (Tseng et al. (2018)). As the DNA starting concentration of the bulk was in a comparable range, the use of serum-free media and/or not freezing the harvested/inactivated/concentrated material between harvest and purification might be the reason for the improved result. Moreover, the high discrepancies

between their standard DNA assay and the Threshold® assay in the work of Tseng et al. (2018) needs to be considered for the evaluation. Although not using a nuclease digestion step in their process, which is usually considered to be the main reason for the DNA assay data discrepancies due to high abundance of small DNA fragments, the discrepancies between both assays were extremely high (factor 227–552-fold; to the best knowledge of the author, this is the highest discrepancy published so far in this research field). Next, Tseng et al. (2018) have shown that the HA protein content and purity of the final product is not only strain or batch dependent, but can strongly depend on the overall upstream system in general (e.g., stirred tank, high density bioreactor or host cells) even when using a flow-through process. Due to the shown upstream process dependency the implementation of an extra safety measure regarding the contamination limits, e.g., by using a nuclease step, is of high importance for the flow-through process robustness and cannot be omitted here.

Fortuna et al. (2019) combined a thoroughly optimized SCMA step with a following nuclease step. Although removal of the nuclease was not integrated into the process and the required DNA contamination limits were not reached, the achieved productivities and good strain independency clearly shows the clear advantage of membrane-based processes and SCMA, in particular.

In the context of the published processes for cell culture-derived IV purification, the three processes of this work (Weigel et al., 2014; Weigel et al., 2016; Weigel et al., 2019) represent rather comprehensive approaches with a minimum amount of process steps, which are selected without creating a bottleneck in the process (e.g. by combining a low productivity-step, such as SEC, with a high productivity step, such as a membrane adsorber). Each process make use of a single purification material type (either purely membrane- or purely bead-based) reducing the demand for different specific equipment. All three processes of this work showed the ability to clear the contaminants sufficiently, although still work needs to be invested to achieve the required DNA level for all tested strains, a safety margin as well as generally improved IV strain and/or batch robustness, which would also be true for most of the other published processes. The flow-through process resembled the first consequently non-capture-based designed process for IV particle purification for cell culture-derived IV, where compliance with the European Pharmacopeia requirements could be shown. The membrane-based process is the first purely membrane-based multistep purification process for IV successfully achieving the purity requirements. It can be assumed to belong to the most economic, fastest and simplest published processes so far, where compliance with the European Pharmacopeia requirements could be shown (as far as to the author’s knowledge), since it completely relies on membrane-

based separation after inactivation and clarification. Furthermore, the orthogonal process is the first process utilizing not only the charge but also the hydrophobic properties of the IV and contaminants in a separate chromatography step which should be advantageous, e.g., if contaminants with a comparable charge as the IV particle needs to be separated from the IV particle. Moreover, potentially increasing purity demands for vaccines in the future might increase the need for process units utilizing fundamentally different separation mechanisms. For example, it is well known that the performance in nucleotide reduction can only be considerably increased when orthogonal methods are combined (Gagnon, 2006).

Despite the fundamental different characteristics, not one of the three processes was able to achieve contamination levels at least one order of magnitude below the contamination limit which is surprising considering the performance of each single step individually. In view of all data and parameters of the state-of-the-art in the context to each other, the four best performing processes regarding DNA depletion (<0.3 ng/15 µg HA) were all using serum-free medium in cell culture: He et al. (2011), using the serum-free medium VP-SFM (Invitrogen), started out with a DNA concentration of up to 220-fold lower than Weigel et al. (2019). Besides, Fischer et al. (2018), using the serum-free medium Smif8 (Gibco™), had a DNA starting concentration which was only 31% lower than in Weigel et al. (2019). Tseng et al. (2018) used also VP-SFM (Invitrogen), but had comparable DNA starting concentration levels to Weigel et al. and Fischer et al. Moreover, Kistner et al. (1998) used serum-free cell culture medium (Dulbecco's minimal essential medium (DMEM)) for his centrifugation-based approach.

Contrarily, P. Marichal-Gallardo et al. (2017) and Fortuna et al. (2019) used serum-free medium (Smif8 (Gibco™)), but were unable to achieve sufficient DNA depletion despite the use of a nuclease, while the three processes of Weigel et al. (2014; 2016; 2019) showed the ability to achieve the required contamination levels with serum-containing cell culture medium, two of them even without the use of a nuclease.

Nevertheless, the majority of the data indicates that the achieved very low DNA content levels in the DSP product are assisted by culture media selection in the upstream process – with serum-free media being advantageous. The reason for this remains unclear. It might be due to aggregation facilitating components in the serum (e.g., serum proteins). It is also possible, that the usually not fully disclosed composition of the usually synthetic media with one and more components beneficially contributes to the contamination removal. In particular, serum-free media often contain detergents such as Pluronic F-68 or Tween 80 (non-ionic detergents) as shear protectants (Merten, 2002). On the one hand, detergents/zwittergents can have stabilizing

effects on the HA protein (Kon et al., 2016). Moreover, some detergents can reduce the formation of aggregates and/or prevent losses during freeze-thaw cycles (Kreilgaard et al., 1998). On the other hand, they can interact in the chromatography, both advantageously (Fischer et al., 2018) or disadvantageously (O'Farrell, 1996; Ohlendieck, 1996). To complicate matters, due to their detergent-specific critical micelle concentration, detergents can furthermore be present in different states (e.g., monomers or micelles) resulting in concentration dependent effects. Furthermore, the addition of a second detergent as antifoam during the cell cultivation can complicate matters further. Also, detergents can affect assays (Ohlendieck, 1996) and their removal by standard sample preparation methods (such as dialysis) can be challenging, e.g., with non-ionic detergents such as Triton X-100.

But besides the potentially lower final DNA content, defined synthetic media have also the advantage of reduced lot-lot-variations (Doroshenko et al., 2009). Clearly, a generally substantially lower DNA concentration at the end of the upstream process should be highly beneficial for the final DNA product content.

Also, in at least two of the best performing processes regarding DNA depletion (He et al., 2011; Tseng et al., 2018), the samples were not frozen between harvesting and further processing. Unexpected freezing effects, such as DNA aggregation with the virus particles, could also be the reason for a sub-optimal downstream process result.

In conclusion, the DNA contamination level in this study could have been probably further reduced by using a serum-free medium and by avoiding freezing-thaw cycles after the harvest. Based on the results of Weigel et al. (2014), P. Marichal-Gallardo et al. (2017) and Fischer et al. (2018) it can be concluded that a nuclease step should be ideally incorporated between the chromatographic purification steps. A digestion at the beginning of the chromatographic purification (train) does seem to yield worse overall DNA depletion rates for the process. Finally, the addition of stabilizing zwittergents might be relevant for achieving higher HA protein recoveries, if necessary.

Surprisingly, while process robustness would be expected to be an issue for capture-step containing processes, it was also partially observed for the pure flow-through processes (although to a lesser extent). Therefore, testing not only different batches, but different IV strains as well should be a requested standard (recommendation) for all published processes. Ideally, the WHO should suggest 3–5 IV strains as standard test strains for DSP publications of which some should be known to present challenges in vaccine manufacturing. The usage of different cell types or cell culture operation modes, although of high importance, should be of

second priority in the context of the downstream development (or rather a part of the pre-screening) in order to reduce the complexity of influencing factors on the data and to allow for comparison. In a next step, the best performing and most robust downstream process should then be used for testing the different upstream conditions.

Moreover, if a process requires the addition of a nuclease, the removal of it needs to be addressed by a validated assay. The validation of the quantifying assays is of general interest to compare results. Especially, the addition of surface-active components, such as zwittergents or long-chained polymers, have to be treated with care not to affect the assay results, since all used assays are based on an interaction of assay substances with the analyte. In particular, non-conclusive mass balances (often referred to be covered by the assay error range) do indicate a questionable assay-sample preparation procedure, if not backed up by an additional mass balance based on a different assay. In particular, the often found striking discrepancies between the intermediate DNA assay values (e.g., PicoGreen®) and low range DNA assay values (e.g., Threshold) (refer to, e.g., Tseng et al. (2018)) show the urgent need for further in depth validations of the used DNA assays and the establishment of a reliable “gold standard” (as also discussed in section 4.4).

5 Conclusion

In conclusion, three downstream processes for the purification of IV particles have been successfully established. They belong to the very first chromatographic purification processes showing the ability to achieve the required contamination limits according to European Pharmacopoeia. Furthermore, each process shows unique characteristics that distinguish it from other processes. The entirely flow-through-based process was focused on establishing an unspecific and mostly IV strain-independent process, besides also being able to remove reliably the added nuclease. Second, the membrane-based process is avoiding the use of any bead-based chromatographic materials allowing for high flow-rates and productivities for the entire process. Finally, the use of HIC in addition to AEC in the orthogonal process should allow for a highly adaptable process with very good separation.

With LCC and STMA, rather novel chromatographic materials have been utilized with impressive results, while the successful use of HIC for IV particles purification has been shown here for the first time. This represents a significant extension of available chromatography methods for IV particle purification. Together with each of the seven purification steps used for the three processes, which were individually optimized, they seem to belong to the best purification steps in terms of overall separation performance (virus recovery and contamination removal) described in the literature, so far.

Nevertheless, although all three processes comprise high performing purification steps, an “invisible barrier” for the DNA removal seemed to exist. After comparison with the recent literature it can be assumed that the upstream part (bioreactor system, host cells and culture media) has a high impact on the downstream part of the influenza vaccine production process and the final product contamination levels which cannot be efficiently compensated for by the choice of DSP tools. In particular, the evaluation in the context of the published literature suggests that use of serum-containing media might pose a limitation regarding the achievable minimal DNA content, which might not be present in serum-free media. In addition, detergents present in the culture media might also have an impact on the DSP results. Moreover, omitting the freeze-thaw cycle often used in research approaches could potentially improve the results. Therefore, in future, the upstream and downstream process development should be integrated into each other.

Due to the apparent impact of the different upstream processes and virus strains, a detailed comparison and final performance evaluation of all published downstream processes for IV is difficult. Based on the performance of each single purification step used in the three

presented processes it is possible that, changing the former mentioned aspect in the upstream (i.e. using serum-free cell culture medium and omitting the freeze-thaw cycle) would lead to an even further improved process performance in all three processes. Besides, the use of serum-free media and the avoidance of a freeze-thaw cycle is favorable by industrial standards and serum-containing media as well as the freeze-thaw cycle had been used here for research purposes, only.

The observed discrepancies of the DNA assays (PicoGreen® and Threshold) in the research group and in literature hinder the downstream process development for IV vaccines, since it affects an evaluation and rational decisions in early project states. Recently, qPCR has been widely accepted as the standard method for DNA quantification in viral vaccine manufacturing. Whether qPCR will allow for more robust and predictable data for DSP remains to be seen. Until then, for safety measures a purification process should be designed with at least two (orthogonal) chromatographic purification steps until the source of the residual DNA is finally clarified.

In the context of the recent global virus threats (SARS(-CoV-2), avian flu, etc.), the need for efficient, fast, scalable and robust downstream processes is higher than ever. It is likely, that most downstream processes established (or reviewed here) can be transferred to other virus vaccine manufacturing processes. The rather high variability of the influenza virus strains makes it an ideal model for the establishment of platform technologies.

6 Outlook

Overall, due to the IV particle size as well as the surface proteins a large number of purification options are available. The now available toolbox of chromatographic purification steps, which has increased during recent years, offers a wide variety of approaches. In particular, more suitable virus purification materials have been made available and established (e.g. LCC, membranes and monoliths). Furthermore, PEG-based processes show high potential with PEG being widely accepted as non-toxic and additionally having stabilizing effects on the IV. Now, that there are sufficient processes available capable of achieving sufficient product purity, the variability of the IV and the ever changing assortment of IV strains in the vaccines require a change of scope towards process robustness, in particular with regards to different IV strains. Until then, the IV downstream process in industry might remain mostly centrifugation-based.

Overall, a large scale comparative study applying a selection of the best downstream approaches using identical upstream conditions (i.e. the same cell culture media, freeze-thaw-cycle, antifoam-type and -amount, host-cells and cell culture process strategy, etc.) would be required in order to select the best process. Ideally, several serum-free cell culture media should be tested in advance for selecting an optimum medium, also with respect to the containing detergents/ antifoam/ zwittergents and with respect to the USP demands (integrated process design). Following, after the first selection of upstream parameters the best downstream process candidates (see 4.6) should be tested for robustness regarding IV strains and batches with virus material produced under the same upstream conditions. Then, the best of these could be used for an integrated approach (optimization of USP together with DSP), where the upstream part is not only optimized based on virus yields but also towards high HA protein yields and low DNA (and protein) contamination levels, i.e. the critical parameter in product formulation.

Possibly, the purification steps could be scaled down for comparison studies, if necessary. Then, a design of experiments (DoE) approach using a screening format (96-well filter plates or multiple prepacked miniature columns) could be used for the robustness testing and the integrated approach. Most of the processes are operated with step gradients or could be adapted to one allowing for a simple screening format. The here established 96-well format might be of use for this.

However, in order to make efficient use of a high-throughput screening format the analytics would require severe improvements. In particular, many assays such as the low-range DNA assay (Threshold) are not applicable at large scale, while standard DNA assays (e.g.,

PicoGreen®) often do not show sufficient low quantification limits. Also, the HA assay is suboptimal for high-throughput virus quantification.

In general, the standard DNA assay (e.g., PicoGreen®) results usually do not match the results of other assays (Threshold, qPCR), making a rational evaluation of screening results difficult. Due to the discrepancies, there is the urgent need for an additional, cost-effective and quick low-range DNA quantification assay in order to perform a rational downstream process development for vaccines. In particular, a DNA fragment size independent assay, which is ideally (semi-) high-throughput capable would be favorable. Alternatively, comparative assay validation studies need to be undertaken in order to better characterize and evaluate hypothesis regarding deviations between the existing assays and to improve the LOQ of the PicoGreen® assay. Also, as seen in the case of the SRID assay, it would be advisable to validate assays for the DSP not only with crude but also with highly purified samples in order to avoid adverse effects of an altered matrix.

In the future, the membrane and monolith approaches should be characterized better because these materials seem to be most suitable for particulate products, such as virus particles (in comparison to beads). The product range for membranes or monoliths regarding different ligands is still small in comparison to beads. In particular, a variety of membranes with different hydrophobic ligands would be useful, since the selectivity and recovery of HIC is usually defined by binding rather than elution. Furthermore, PEG-based processes should be investigated in detail and the exclusion of a filtration effect should be confirmed, e.g. by inverted flow experiments with high flow rates.

The effect of freeze-thaw-cycles on the downstream process should also be evaluated. Although not used in industrial vaccine production processes, it is of importance for the downstream process development in research labs. Moreover, the effects of detergents commonly used in upstream on the DSP should be better characterized for an improved understanding of the impact of the culture media on the DSP separation performance. At last, previous DSP studies using a SRID protocol without a lyoprotectant should be repeated and re-evaluated regarding the HA-protein recovery and the dose contaminations.

7 References

Ackermann, W., Niemann, H., Wagner, R., Anspach, B., Pfister, H., Wehland, J., Appel, B., Posten, C., Wehlmann, H., Bornscheuer, U. T., Raeder, U., Weiland, P., Gollmer, K.-U., Riedel, K., Wilke, D., Hampel, J., Krämer, R., Micheel, B., Ruttloff, H., Schütte, H., von Schell, T., Wobus, U., Wohlleben, W., Zeng, A.-P., Fuchs, P. G., Jording, D., May, M., Erck, C., Muth, G. and Tiedt, B. (1999). *RÖMPP Lexikon Biotechnologie und Gentechnik*. Stuttgart: Georg Thieme Verlag, p. 376.

Agarwal, N., Jain, R., Vinayak, V. K., Singh, S., Patra, A. and Jambu, L. (2011), *Improved Influenza Vaccine*, WO2011154976A2.

Allay, J. A., Sleep, S., Long, S., Tillman, D. M., Clark, R., Carney, G., Fagone, P., McIntosh, J. H., Nienhuis, A. W., Davidoff, A. M., Nathwani, A. C. and Gray, J. T. (2011). Good Manufacturing Practice Production of Self-Complementary Serotype 8 Adeno-Associated Viral Vector for a Hemophilia B Clinical Trial. *Human Gene Therapy*, 22(5), 595-604.

Ambrose, C. S. and Levin, M. J. (2012). The rationale for quadrivalent influenza vaccines. *Human Vaccines & Immunotherapeutics*, 8(1), 81-88.

Amorij, J. P., Meulenaar, J., Hinrichs, W. L. J., Stegmann, T., Huckriede, A., Coenen, F. and Frijlink, H. W. (2007). Rational design of an influenza subunit vaccine powder with sugar glass technology: Preventing conformational changes of haemagglutinin during freezing and freeze-drying. *Vaccine*, 25(35), 6447-6457.

Arakawa, T. and Timasheff, S. N. (1982). Preferential interactions of proteins with salts in concentrated solutions. *Biochemistry*, 21(25), 6545-6552.

Arora, N., Bhateja, A., Garg, T. and Bilandi, A. (2012). Advances in protein stability. *Journal of Pharmacy Research*, 5(4), 2072-2077.

Bakaltcheva, I., Ganong, J. P., Holtz, B. L., Peat, R. A. and Reid, T. (2000). Effects of high-molecular-weight cryoprotectants on platelets and the coagulation system. *Cryobiology*, 40(4), 283-293.

Baldwin, R. L. (1996). How Hofmeister ion interactions affect protein stability. *Biophysical Journal*, 71(4), 2056-2063.

Bandeira, V., Peixoto, C., Rodrigues, A. F., Cruz, P. E., Alves, P. M., Coroadinha, A. S. and Carrondo, M. J. T. (2012). Downstream Processing of Lentiviral Vectors: Releasing Bottlenecks. *Human Gene Therapy Methods*, 23(4), 255-263.

Banjac, M., Roethl, E., Gelhart, F., Kramberger, P., Jarc, B. L., Jarc, M., Strancar, A., Muster, T. and Peterka, M. (2014). Purification of Vero cell derived live replication deficient influenza A and B virus by ion exchange monolith chromatography. *Vaccine*, 32(21), 2487-2492.

Banta, S., Megeed, Z., Casali, M., Rege, K. and Yarmush, M. L. (2007). Engineering protein and peptide building blocks for nanotechnology. *Journal of Nanoscience and Nanotechnology*, 7(2), 387-401.

Barberis, I., Myles, P., Ault, S. K., Bragazzi, N. L. and Martini, M. (2016). History and evolution of influenza control through vaccination: from the first monovalent vaccine to universal vaccines. *J Prev Med Hyg*, 57(3), E115-E120.

Beyer, W. E., Palache, A. M. and Osterhaus, A. D. (1998). Comparison of Serology and Reactogenicity between Influenza Subunit Vaccines and Whole Virus or Split Vaccines: A Review and Meta-Analysis of the Literature. *Clin Drug Investig*, 15(1), 1-12.

Bhatnagar, B. S., Bogner, R. H. and Pikal, M. J. (2007). Protein Stability During Freezing: Separation of Stresses and Mechanisms of Protein Stabilization. *Pharmaceutical Development and Technology*, 12(5), 505-523.

Blanco-Lobo, P., Nogales, A., Rodriguez, L. and Martinez-Sobrido, L. (2019). Novel Approaches for The Development of Live Attenuated Influenza Vaccines. *Viruses,* 11(2), 190.

Bonturi, N., Radke, V. S. C. O., Bueno, S. M. A., Freitas, S., Azzoni, A. R. and Miranda, E. A. (2013). Sodium citrate and potassium phosphate as alternative adsorption buffers in hydrophobic and aromatic thiophilic chromatographic purification of plasmid DNA from neutralized lysate. *Journal of Chromatography B,* 919(Supplement C), 67-74.

Brands, R., Visser, J., Medema, J., Palache, A. M. and van Scharrenburg, G. J. (1999). Influvac: a safe Madin Darby Canine Kidney (MDCK) cell culture-based influenza vaccine. *Developments in biological standardization,* 98, 93-111.

Brokstad, K. A., Cox, R. J., Major, D., Wood, J. M. and Haaheim, L. R. (1995). Cross-reaction but no avidity change of the serum antibody response after influenza vaccination. *Vaccine,* 13(16), 1522-1528.

Budowsky, E. I., Friedman, E. A., Zheleznova, N. V. and Noskov, F. S. (1991). Principles of selective inactivation of viral genome. VI. Inactivation of the infectivity of the influenza virus by the action of beta-propiolactone. *Vaccine,* 9(6), 398-402.

Bustin, S. A., Benes, V., Garson, J. A., Hellemans, J., Huggett, J., Kubista, M., Mueller, R., Nolan, T., Pfaffl, M. W., Shipley, G. L., Vandesompele, J. and Wittwer, C. T. (2009). The MIQE guidelines: minimum information for publication of quantitative real-time PCR experiments. *Clin Chem,* 55(4), 611-622.

Carpenter, J. F. (1991). Interactions of Stabilizing Additives with Proteins during Freeze-thawing and Freeze-drying. *Int. Symp. on Biol. Product Freeze drying and Formulation 1990,* 74, 225-239.

Carpenter, J. F. and Crowe, J. H. (1988). The mechanism of cryoprotection of proteins by solutes. *Cryobiology,* 25(3), 244-255.

Carroll, K. C., Hobden, J. A., Miller, S., Morse, S. A., Mietzner, T. A., Detrick, B., Mitchell, T. G., McKerrow, J. H. and Sakanari, J. A. (2016). *Jawetz, Melnick & Adelberg's Medical Microbiology*. New York: Mcgraw-Hill Education, chapter 39.

Carvalho, S., Fortuna, A. R., Wolff, M. W., Peixoto, C., P, M. A., Reichl, U. and Jt Carrondo, M. (2018). Purification of influenza virus-like particles using sulfated cellulose membrane adsorbers. *J Chem Technol Biotechnol,* 93(7), 1988-1996.

CDC. (2021). Disease Burden of Influenza. Retrieved from https://www.cdc.gov/flu/about/burden/index.html. Access Date: 02.04.2021.

Charcosset, C. (2006). Membrane processes in biotechnology: an overview. *Biotechnol Adv,* 24(5), 482-492.

Choi, D.-S. and Gho, Y. S. (2015). *Isolation of Extracellular Vesicles for Proteomic Profiling*. New York: Springer New York, pp. 167-177.

Coffman, J. L., Kramarczyk, J. F. and Kelley, B. D. (2008). High-throughput screening of chromatographic separations: I. Method development and column modeling. *Biotechnology and Bioengineering,* 100(4), 605-618.

Colburn, N. H., Richardson, R. G. and Boutwell, R. K. (1965). Studies of the reaction of beta-propiolactone with deoxyguanosine and related compounds. *Biochem Pharmacol,* 14(7), 1113-1118.

Cox, M. M. and Hashimoto, Y. (2011). A fast track influenza virus vaccine produced in insect cells. *J Invertebr Pathol,* 107 Suppl, S31-41.

Cox, R. J. and Brokstad, K. A. (1999). The postvaccination antibody response to influenza virus proteins. *Apmis,* 107(3), 289-296.

De Jonge, J., Amorij, J.-P., Hinrichs, W. L. J., Wilschut, J., Huckriede, A. and Frijlink, H. W. (2007). Inulin sugar glasses preserve the structural integrity and biological activity of influenza virosomes during freeze-drying and storage. *European Journal of Pharmaceutical Sciences,* 32(1), 33-44.

Deering, R. P., Kommareddy, S., Ulmer, J. B., Brito, L. A. and Geall, A. J. (2014). Nucleic acid vaccines: prospects for non-viral delivery of mRNA vaccines. *Expert Opin Drug Deliv,* 11(6), 885-899.

Dormitzer, P. R. (2011). *Cell Culture-Derived Influenza Vaccines*. Basel: Springer Basel, pp. 293-312.

Doroshenko, A. and Halperin, S. A. (2009). Trivalent MDCK cell culture-derived influenza vaccine Optaflu (R) (Novartis Vaccines). *Expert Review of Vaccines,* 8(6), 679-688.

Dragan, A. I., Casas-Finet, J. R., Bishop, E. S., Strouse, R. J., Schenerman, M. A. and Geddes, C. D. (2010). Characterization of PicoGreen interaction with dsDNA and the origin of its fluorescence enhancement upon binding. *Biophysical Journal,* 99(9), 3010-3019.

ECDC. (2018). Overview of available seasonal influenza vaccines in the EU/EEA (2017/18 season). Retrieved from https://ecdc.europa.eu/en/seasonal-influenza/prevention-and-control/vaccines/types-of-seasonal-influenza-vaccine. Access Date: 23.07.2019.

el Rassi, Z., De Ocampo, L. F. and Bacolod, M. D. (1990). Binary and ternary salt gradients in hydrophobic-interaction chromatography of proteins. *Journal of Chromatography,* 499, 141-152.

Ellebedy, A. H. and Ahmed, R. (2016). *The Vaccine Book (Second Edition)*. New York: Academic Press, pp. 283-310.

European Pharmacopoeia. (2018). Influenza vaccine (whole virion, inactivated, prepared in cell cultures). 9.5, 870-872.

Faber, R., Yang, Y. and Gottschalk, U. (2009). Salt Tolerant Interaction Chromatography for Large-Scale Polishing with Convective Media. *Biopharm International*, 11-14.

FDA. (2012). *Cell Lines Derived from Human Tumors for Vaccine Manufacture*. Briefing Document. Vaccines and Related Biological Products Advisory Committee Meeting: Cell Lines Derived from Human Tumors for Vaccine Manufacture.

FDA. (2013). Press release. FDA approves new seasonal influenza vaccine made using novel technology. 16.01.2013. Retrieved from https://wayback.archive-it.org/7993/20170111225529/http://www.fda.gov/NewsEvents/Newsroom/PressAnnouncements/ucm335891.htm. Access Date: 03.06.2017.

FDA. (2018). Influenza Virus Vaccine Safety and Availability. Retrieved from https://www.fda.gov/vaccines-blood-biologics/safety-availability-biologics/influenza-virus-vaccine-safety-availability. Access Date: 29.05.2019.

Fields, B. N., Knipe, D. M. and Howley, P. M. (2007). *Fields Virology*. Philadelphia: Wolters Kluwer Health/Lippincott Williams & Wilkins, pp. 1691-1740.

Fischer-Frühholz, S. (2012). Sartobind Membrane Chromatography. *Sartorius Stedim Biotech*, 1-74.

Fischer-Frühholz, S., Zhou, D. and Hirai, M. (2010). Sartobind STIC salt-tolerant membrane chromatography. *Nat Meth,* 7, 12-13.

Fischer, L. M., Wolff, M. W. and Reichl, U. (2018). Purification of cell culture-derived influenza A virus via continuous anion exchange chromatography on monoliths. *Vaccine,* 36(22), 3153-3160.

Forrest, B. D., Pride, M. W., Dunning, A. J., Capeding, M. R. Z., Chotpitayasunondh, T., Tam, J. S., Rappaport, R., Eldridge, J. H. and Gruber, W. C. (2008). Correlation of Cellular Immune Responses with Protection against Culture-Confirmed Influenza Virus in Young Children. *Clinical and Vaccine Immunology,* 15(7), 1042-1053.

Fortuna, A. R., Pieler, M., Villain, L., Reichl, U. and Wolff, M. (2014). Upcoming Membrane Supports for Influenza Virus Purification. *Chemie Ingenieur Technik,* 86(9), 1501-1501.

Fortuna, A. R., Taft, F., Villain, L., Wolff, M. W. and Reichl, U. (2018). Optimization of cell culture-derived influenza A virus particles purification using sulfated cellulose membrane adsorbers. *Engineering in Life Sciences,* 18(1), 29-39.

Fortuna, A. R., van Teeffelen, S., Ley, A., Fischer, L. M., Taft, F., Genzel, Y., Villain, L., Wolff, M. W. and Reichl, U. (2019). Use of sulfated cellulose membrane adsorbers for chromatographic purification of cell cultured-derived influenza A and B viruses. *Separation and Purification Technology,* 226, 350-358.

Gagnon, P. (2006). The Secrets of Orthogonal Process Design. *Validated Biosystems Resource Guide for Downstream Processing*, 1-4.

Gagnon, P. (2009). *Chromatographic Purification of Virus Particles*, pp. 1-21.

Gagnon, P. (2013). *Downstream Industrial Biotechnology: Recovery and Purification*. Hoboken, NJ: Wiley, pp. 1-872.

Gagnon, P. and Grund, E. (1996a). Large-scale process development for hydrophobic interaction chromatography, Part 3: Factors affecting capacity determination. *Biopharm-the Technology & Business of Biopharmaceuticals,* 9(3), 34-39.

Gagnon, P. and Grund, E. (1996b). Large-scale process development for hydrophobic interaction chromatography, Part 4: Controlling selectivity. *Biopharm-the Technology & Business of Biopharmaceuticals,* 9(5), 54-64.

Gagnon, P., Grund, E. and Lindback, T. (1995a). Large-scale process development for hydrophobic interaction chromatography, Part 2: Controlling process variation. *Biopharm-the Technology & Business of Biopharmaceuticals,* 8(4), 36-41.

Gagnon, P., Grund, E. and Lindback, T. (1995b). Large scale process development for hydrophobic interaction chromatography, Part 1: Gel selection and development of binding conditions. *Biopharm-the Technology & Business of Biopharmaceuticals,* 8(3), 21-27.

Gagnon, P., Nian, R., Lee, J., Tan, L., Latiff, S. M. A., Lim, C. L., Chuah, C., Bi, X., Yang, Y., Zhang, W. and Gan, H. T. (2014). Nonspecific interactions of chromatin with immunoglobulin G and protein A, and their impact on purification performance. *Journal of Chromatography A,* 1340, 68-78.

Gagnon, P., Nian, R., Yang, Y., Yang, Q. and Lim, C. L. (2015). Non-immunospecific association of immunoglobulin G with chromatin during elution from protein A inflates host contamination, aggregate content, and antibody loss. *Journal of Chromatography A,* 1408, 151-160.

Gan, H. T., Lee, J., Latiff, S. M. A., Chuah, C., Toh, P., Lee, W. Y. and Gagnon, P. (2013). Characterization and removal of aggregates formed by nonspecific interaction of IgM monoclonal antibodies with chromatin catabolites during cell culture production. *Journal of Chromatography A,* 1291, 33-40.

GE Healthcare. (2010). Use of Capto™ ViralQ for the removal of genomic DNA from influenza virus produced in MDCK cells. *Application note,* 28-9769-69 AA.

GE Healthcare. (2012a). Capto Core 700. *Application note,* 28-9983-07 AA.

GE Healthcare. (2012b). Purification of influenza A/H1N1 using Capto™ Core 700. *Application note,* 29-0003-34 AA.

Genzel, Y., Behrendt, I., Konig, S., Sann, H. and Reichl, U. (2004). Metabolism of MDCK cells during cell growth and influenza virus production in large-scale microcarrier culture. *Vaccine,* 22(17-18), 2202-2208.

Ghosh, R. (2002). Protein separation using membrane chromatography: opportunities and challenges. *Journal of Chromatography A,* 952(1-2), 13-27.

Goldstein, M. A. and Tauraso, N. M. (1970). Effect of formalin, beta-propiolactone, merthiolate, and ultraviolet light upon influenza virus infectivity chicken cell agglutination, hemagglutination, and antigenicity. *Appl Microbiol,* 19(2), 290-294.

Gooding, K. M. and Regnier, F. E. (2002). *HPLC of Biological Macromolecules, Revised and Expanded*. London: Taylor & Francis, pp. 74-243.

Gottschalk, U. (2013). The Future of Downstream Processing. Retrieved from http://www.biopharminternational.com/future-downstream-processing. Access Date: 02.04.2020.

Grohskopf, L. A., Sokolow, L. Z., Broder, K. R., Walter, E. B., Fry, A. M. and Jernigan, D. B. (2018a). Prevention and Control of Seasonal Influenza with Vaccines: Recommendations of the Advisory Committee on Immunization Practices-United States, 2018-19 Influenza Season. *MMWR Recomm Rep,* 67(3), 1-20.

Grohskopf, L. A., Sokolow, L. Z., Fry, A. M., Walter, E. B. and Jernigan, D. B. (2018b). Update: ACIP Recommendations for the Use of Quadrivalent Live Attenuated Influenza Vaccine (LAIV4) - United States, 2018-19 Influenza Season. *MMWR Morb Mortal Wkly Rep,* 67(22), 643-645.

Grover, P. K. and Ryall, R. L. (2005). Critical Appraisal of Salting-Out and Its Implications for Chemical and Biological Sciences. *Chemical Reviews,* 105(1), 1-10.

Hagen, A. J., Aboud, R. A., DePhillips, P. A., Oliver, C. N., Orella, C. J. and Sitrin, R. D. (1996a). Use of a nuclease enzyme in the purification of VAQTA, a hepatitis A vaccine. *Biotechnology and Applied Biochemistry,* 23(3), 209-215.

Hagen, A. J., Oliver, C. N. and Sitrin, R. D. (1996b). Optimization of poly(ethylene glycol) precipitation of hepatitis a virus used to prepare VAQTA, a highly purified inactivated vaccine. *Biotechnology Progress,* 12(3), 406-412.

Harding, A. T. and Heaton, N. S. (2018). Efforts to Improve the Seasonal Influenza Vaccine. *Vaccines (Basel),* 6(2), 19.

Hay, A. J., Gregory, V., Douglas, A. R. and Lin, Y. P. (2001). The evolution of human influenza viruses. *Philos Trans R Soc Lond B Biol Sci,* 356(1416), 1861-1870.

He, C. Y., Yang, Z. Q. and Tong, K. T. (2011). Downstream processing of Vero cell-derived human influenza A virus (H1N1) grown in serum-free medium. *Journal of Chromatography A,* 1218(31), 5279-5285.

Helling, C., Borrmann, C. and Strube, J. (2012). Optimal Integration of Directly Combined Hydrophobic Interaction and Ion Exchange Chromatography Purification Processes. *Chemical Engineering & Technology,* 35(10), 1786-1796.

Herrera-Rodriguez, J., Signorazzi, A., Holtrop, M., de Vries-Idema, J. and Huckriede, A. (2019). Inactivated or damaged? Comparing the effect of inactivation methods on influenza virions to optimize vaccine production. *Vaccine,* 37(12), 1630-1637.

Hinrichs, W. L., Prinsen, M. G. and Frijlink, H. W. (2001). Inulin glasses for the stabilization of therapeutic proteins. *Int J Pharm,* 215(1-2), 163-174.

Hofmeister, F. (1888). Zur Lehre von der Wirkung der Salze. [Title translation: About the science of the effect of salts.]. *Arch Exp Pathol Pharmakol,* 24, 247-260.

Hoft, D. F., Babusis, E., Worku, S., Spencer, C. T., Lottenbach, K., Truscott, S. M., Abate, G., Sakala, I. G., Edwards, K. M., Creech, C. B., Gerber, M. A., Bernstein, D. I., Newman, F., Graham, I., Anderson, E. L. and Belshe, R. B. (2011). Live and inactivated influenza vaccines induce similar humoral responses, but only live vaccines induce diverse T-cell responses in young children. *The Journal of infectious diseases,* 204(6), 845-853.

Hoft, D. F., Lottenbach, K. R., Blazevic, A., Turan, A., Blevins, T. P., Pacatte, T. P., Yu, Y., Mitchell, M. C., Hoft, S. G. and Belshe, R. B. (2017). Comparisons of the Humoral and Cellular Immune Responses Induced by Live Attenuated Influenza Vaccine and Inactivated Influenza Vaccine in Adults. *Clinical and vaccine immunology : CVI,* 24(1), 1-9.

Horiba Instruments. (2017). A guidebook to particle size analysis.

Ikeda, Y., Iwakiri, S. and Yoshimori, T. (2009). Development and characterization of a novel host cell DNA assay using ultra-sensitive fluorescent nucleic acid stain "PicoGreen". *Journal of Pharmaceutical and Biomedical Analysis,* 49(4), 997-1002.

Invitrogen. (2005). Quant-iT™ Pico Green® dsDNA Assay. *Application note,* 997_9314 Rev.1.1.

Invitrogen. (2008). Manufacturer's operation instructions: Quant-iT™ PicoGreen® dsDNA Reagent and Kits. *Application note,* MP07581.

Iyer, G., Ramaswamy, S., Asher, D., Mehta, U., Leahy, A., Chung, F. and Cheng, K. S. (2011). Reduced surface area chromatography for flow-through purification of viruses and virus like particles. *Journal of Chromatography A,* 1218(26), 3973-3981.

Iyer, G., Ramaswamy, S., Cheng, K.-S., Sisowath, N., Mehta, U., Leahy, A., Chung, F. and Asher, D. (2012). Flow-Through Purification of Viruses- A Novel Approach to Vaccine Purification. *Procedia in Vaccinology,* 6(0), 106-112.

Jiang, S. and Nail, S. L. (1998). Effect of process conditions on recovery of protein activity after freezing and freeze-drying. *European Journal of Pharmaceutics and Biopharmaceutics,* 45(3), 249-257.

Jin, H. and Chen, Z. (2014). Production of live attenuated influenza vaccines against seasonal and potential pandemic influenza viruses. *Curr Opin Virol,* 6, 34-39.

Kalbfuss, B. (2009). *Downstream Processing of Influenza Whole-Virions for Vaccine Production.* (PhD), Otto-von-Guericke University Magdeburg, Magdeburg, Germany.

Kalbfuss, B., Genzel, Y., Wolff, M., Zimmermann, A., Morenweiser, R. and Reichl, U. (2007a). Harvesting and concentration of human influenza A virus produced in serum-free mammalian cell culture for the production of vaccines. *Biotechnology and Bioengineering,* 97(1), 73-85.

Kalbfuss, B., Knochlein, A., Krober, T. and Reichl, U. (2008). Monitoring influenza virus content in vaccine production: Precise assays for the quantitation of hemagglutination and neuraminidase activity. *Biologicals,* 36(3), 145-161.

Kalbfuss, B., Wolff, M., Morenweiser, R. and Reichl, U. (2007b). Purification of cell culture-derived human influenza a virus by size-exclusion and anion-exchange chromatography. *Biotechnology and Bioengineering,* 96(5), 932-944.

Kang, Y., Ng, S., Lee, J., Adaelu, J., Qi, B., Persaud, K., Ludwig, D. and Balderes, P. (2013). Development of an Alternative Monoclonal Antibody Polishing Step. *Biopharm International,* S23-S33.

Kennedy, R. M. (2001). *Current Protocols in Protein Science - Hydrophobic-Interaction Chromatography*. Hoboken, NJ: John Wiley & Sons, chapter 8.4.1-8.4.21.

Keshavarz, M., Mirzaei, H., Salemi, M., Momeni, F., Mousavi, M. J., Sadeghalvad, M., Arjeini, Y., Solaymani-Mohammadi, F., Sadri Nahand, J., Namdari, H., Mokhtari-Azad, T. and Rezaei, F. (2019). Influenza vaccine: Where are we and where do we go? *Rev Med Virol,* 29(1), e2014.

King, R. S. and Panfili, P. R. (1991). Influence of fragment size on DNA quantification using DNA-binding proteins and a sensor-based analytical system - Application in the testing of biological products. *Journal of Biochemical and Biophysical Methods,* 23(1), 83-93.

Kistner, O., Barrett, N., Bruehmann, A., Reiter, M., Mundt, W., Savidis-Dacho, H., Schober-Bendixen, S., Dorner, F. and Aaskov, J. (2007). The preclinical testing of a formaldehyde inactivated Ross River virus vaccine designed for use in humans. *Vaccine,* 25(25), 4845-4852.

Kistner, O., Barrett, P. N., Mundt, W., Reiter, M., Schober-Bendixen, S. and Dorner, F. (1998). Development of a mammalian cell (Vero) derived candidate influenza virus vaccine. *Vaccine,* 16(9-10), 960-968.

Kistner, O., Barrett, P. N., Mundt, W., Reiter, M., Schober-Bendixen, S., Eder, G. and Dorner, F. (1999). A novel mammalian cell (Vero) derived influenza virus vaccine: Development, characterization and industrial scale production. *Wiener Klinische Wochenschrift,* 111(5), 207-214.

Kon, T. C., Onu, A., Berbecila, L., Lupulescu, E., Ghiorgisor, A., Kersten, G. F., Cui, Y. Q., Amorij, J. P. and Van der Pol, L. (2016). Influenza Vaccine Manufacturing: Effect of Inactivation, Splitting and Site of Manufacturing. Comparison of Influenza Vaccine Production Processes. *PloS one,* 11(3), 19.

Konz, J. O., Lee, A. L., Lewis, J. A. and Sagar, S. L. (2005). Development of a purification process for adenovirus: controlling virus aggregation to improve the clearance of host cell DNA. *Biotechnol Prog,* 21(2), 466-472.

Kreilgaard, L., Jones, L. S., Randolph, T. W., Frokjaer, S., Flink, J. M., Manning, M. C. and Carpenter, J. F. (1998). Effect of Tween 20 on freeze-thawing- and agitation-induced aggregation of recombinant human factor XIII. *Journal of pharmaceutical sciences,* 87(12), 1597-1603.

Kroeber, T., Wolff, M. W., Hundt, B., Seidel-Morgenstern, A. and Reichl, U. (2013). Continuous purification of influenza virus using simulated moving bed chromatography. *Journal of Chromatography A,* 1307, 99-110.

Kumar, A., Meldgaard, T. S. and Bertholet, S. (2018). Novel Platforms for the Development of a Universal Influenza Vaccine. *Front Immunol,* 9, 600.

Lamichhane, T. N., Raiker, R. S. and Jay, S. M. (2015). Exogenous DNA Loading into Extracellular Vesicles via Electroporation is Size-Dependent and Enables Limited Gene Delivery. *Molecular Pharmaceutics,* 12(10), 3650-3657.

Lange, W., Vogel, G., E. and Upholff, H. (1999). *Influenza: Virologie, Epidemiologie, Klinik, Therapie und Prophylaxe*. Berlin, Germany: Blackwell-Wissenschafts-Verlag, pp. 1-197.

Laver, W. G. and Webster, R. G. (1976). Preparation and immunogenicity of a purified influenza virus haemagglutinin and neuraminidase subunit vaccine. *Postgraduate medical journal,* 52(608), 373-378.

Lee, N., Le Sage, V., Nanni, A. V., Snyder, D. J., Cooper, V. S. and Lakdawala, S. S. (2017). Genome-wide analysis of influenza viral RNA and nucleoprotein association. *Nucleic Acids Res,* 45(15), 8968-8977.

Lee, P. S. and Wilson, I. A. (2015). Structural characterization of viral epitopes recognized by broadly cross-reactive antibodies. *Curr Top Microbiol Immunol,* 386, 323-341.

Lewith, S. (1887). Zur Lehre von der Wirkung der Salze. *Archiv für experimentelle Pathologie und Pharmakologie,* 24(1), 1-16.

Li, H., Yang, Y., Zhang, Y., Zhang, S., Zhao, Q., Zhu, Y., Zou, X., Yu, M., Ma, G. and Su, Z. (2015). A hydrophobic interaction chromatography strategy for purification of inactivated foot-and-mouth disease virus. *Protein Expression and Purification,* 113(0), 23-29.

Lide, D. R. and Haynes, W. M. (2009). CRC handbook of chemistry and physics : a ready-reference book of chemical and physical data. In. Boca Raton: CRC Press.

Lothert, K., Offersgaard, A. F., Pihl, A. F., Mathiesen, C. K., Jensen, T. B., Alzua, G. P., Fahnøe, U., Bukh, J., Gottwein, J. M. and Wolff, M. W. (2020). Development of a downstream process for the production of an inactivated whole hepatitis C virus vaccine. *Sci Rep,* 10(1), 16261.

Lothert, K., Pagallies, F., Feger, T., Amann, R. and Wolff, M. W. (2020). Selection of chromatographic methods for the purification of cell culture-derived Orf virus for its application as a vaccine or viral vector. *Journal of Biotechnology,* 323, 62-72.

Lottspeich, F. and Engels, J. W. (2018). *Bioanalytics: Analytical Methods and Concepts in Biochemistry and Molecular Biology*. Weinheim, Germany: VCH, pp. 1-1070.

Lu, Y. F., Williamson, B. and Gillespie, R. (2009). Recent Advancement in Application of Hydrophobic Interaction Chromatography for Aggregate Removal in Industrial Purification. *Current Pharmaceutical Biotechnology,* 10(4), 427-433.

Mahn, A., Lienqueo, M. E. and Asenjo, J. A. (2007a). Optimal operation conditions for protein separation in hydrophobic interaction chromatography. *J. Chromatogr., B: Anal. Technol. Biomed. Life Sci.*, 849(1-2), 236-242.

Mahn, A., Lienqueo, M. E. and Asenjo, J. A. (2007b). A simple method for the estimation of protein retention in hydrophobic interaction chromatography under different operation conditions. *Open Biotechnol. J.*, 1, 9-13.

Mahy, B. and Kangro, H. (1996). *Virology Methods Manual (1st ed.)*. Amsterdam, the Netherlands: Academic Press, pp. 41-306.

Malvern Instruments. (2017). Dynamic Light Scattering: An Introduction in 30 Minutes. Retrieved from

Manini, I., Trombetta, C. M., Lazzeri, G., Pozzi, T., Rossi, S. and Montomoli, E. (2017). Egg-Independent Influenza Vaccines and Vaccine Candidates. *Vaccines (Basel),* 5(3).

Margolin, E., Chapman, R., Williamson, A.-L., Rybicki, E. P. and Meyers, A. E. (2018). Production of complex viral glycoproteins in plants as vaccine immunogens. *Plant biotechnology journal,* 16(9), 1531-1545.

Marichal-Gallardo, P., Börner, K., Pieler, M. M., Sonntag-Buck, V., Obr, M., Bejarano, D., Wolff, M. W., Kräusslich, H. G., Reichl, U. and Grimm, D. (2021). Single-use capture purification of adeno-associated viral gene transfer vectors by membrane-based steric exclusion chromatography. *Hum Gene Ther*.

Marichal-Gallardo, P., Pieler, M. M., Wolff, M. W. and Reichl, U. (2017). Steric exclusion chromatography for purification of cell culture-derived influenza A virus using regenerated cellulose membranes and polyethylene glycol. *Journal of Chromatography A,* 1483, 110-119.

Marichal-Gallardo, P. A. (2019). *Chromatographic purification of biological macromolecules by their capture on hydrophilic surfaces with the aid of non-ionic polymers*,

Martin, K. (1991). Benzon-nuclease-characteristics and application of the new type of endonuclease for the elimination of disturbing nucleic acids. *Schweizerische Laboratoriums-Zeitschrift,* 48(6-7), 199-201.

Mate, U., Solomon, J. J. and Segal, A. (1977). In vitro binding of beta-propiolactone to calf thymus DNA and mouse liver DNA to form 1-(2-carboxyethyl) adenine. *Chem Biol Interact,* 18(3), 327-336.

Matrosovich, M. N., Matrosovich, T. Y., Gray, T., Roberts, N. A. and Klenk, H.-D. (2004). Neuraminidase Is Important for the Initiation of Influenza Virus Infection in Human Airway Epithelium. *Journal of virology,* 78(22), 12665-12667.

Matthews, J. T. (2006). Egg-Based Production of Influenza Vaccine: 30 Years of Commercial Experience. *The Bridge.* Retrieved from https://www.nae.edu/7636/Egg-BasedProductionofInfluenzaVaccine30YearsofCommercialExperience. Access Date: 30.04.2019.

McCue, J. T. (2009). *Guide to Protein Purification, Second Edition - Theory and Use of Hydrophobic Interaction Chromatography in Protein Purification and Applications*. Amsterdam, the Netherlands: Elsevier Academic Press Inc, pp. 405-414.

McDevit, W. F. and Long, F. A. (1952). The Activity Coefficient of Benzene in Aqueous Salt Solutions. *Journal of the American Chemical Society,* 74(7), 1773-1777.

McLean, K. A., Goldin, S., Nannei, C., Sparrow, E. and Torelli, G. (2016). The 2015 global production capacity of seasonal and pandemic influenza vaccine. *Vaccine,* 34(45), 5410-5413.

Meckes, D. G. and Raab-Traub, N. (2011). Microvesicles and Viral Infection. *Journal of virology,* 85(24), 12844-12854.

Medina, R. A. and Garcia-Sastre, A. (2011). Influenza A viruses: new research developments. *Nat Rev Microbiol,* 9(8), 590-603.

Meeusen, E. N., Walker, J., Peters, A., Pastoret, P. P. and Jungersen, G. (2007). Current status of veterinary vaccines. *Clinical microbiology reviews,* 20(3), 489-510.

Melander, W. and Horváth, C. (1977). Salt effects on hydrophobic interactions in precipitation and chromatography of proteins: An interpretation of the lyotropic series. *Archives of Biochemistry and Biophysics,* 183(1), 200-215.

Merten, O. W. (2002). Development of serum-free media for cell growth and production of viruses/viral vaccines--safety issues of animal products used in serum-free media. *Dev Biol (Basel),* 111, 233-257.

Merten, O. W., Charrier, S., Laroudie, N., Fauchille, S., Dugue, C., Jenny, C., Audit, M., Zanta-Boussif, M. A., Chautard, H., Radrizzani, M., Vallanti, G., Naldini, L., Noguiez-Hellin, P. and Galy, A. (2011). Large-Scale Manufacture and Characterization of a Lentiviral Vector Produced for Clinical Ex Vivo Gene Therapy Application. *Human Gene Therapy,* 22(3), 343-356.

Miller, G. L., Lauffer, M. A. and Stanley, W. M. (1944). ELECTROPHORETIC STUDIES ON PR8 INFLUENZA VIRUS. *J Exp Med,* 80(6), 549-559.

Mohammed, A. R., Coombes, A. G. and Perrie, Y. (2007). Amino acids as cryoprotectants for liposomal delivery systems. *Eur J Pharm Sci,* 30(5), 406-413.

Mohn, K. G., Brokstad, K. A., Pathirana, R. D., Bredholt, G., Jul-Larsen, A., Trieu, M. C., Lartey, S. L., Montomoli, E., Tondel, C., Aarstad, H. J. and Cox, R. J. (2016). Live Attenuated Influenza Vaccine in Children Induces B-Cell Responses in Tonsils. *The Journal of infectious diseases,* 214(5), 722-731.

Morenweiser, R. (2005). Downstream processing of viral vectors and vaccines. *Gene Therapy,* 12, S103.

Moscona, A. (2005). Neuraminidase Inhibitors for Influenza. *New England Journal of Medicine,* 353(13), 1363-1373.

Moser, C., Müller, M., Kaeser, M. D., Weydemann, U. and Amacker, M. (2013). Influenza virosomes as vaccine adjuvant and carrier system. *Expert Review of Vaccines,* 12(7), 779-791.

Nair, H., Brooks, W. A., Katz, M., Roca, A., Berkley, J. A., Madhi, S. A., Simmerman, J. M., Gordon, A., Sato, M., Howie, S., Krishnan, A., Ope, M., Lindblade, K. A., Carosone-Link, P., Lucero, M., Ochieng, W., Kamimoto, L., Dueger, E., Bhat, N., Vong, S., Theodoratou, E., Chittaganpitch, M., Chimah, O., Balmaseda, A., Buchy, P., Harris, E., Evans, V., Katayose, M., Gaur, B., O'Callaghan-Gordo, C., Goswami, D., Arvelo, W., Venter, M., Briese, T., Tokarz, R., Widdowson, M. A., Mounts, A. W., Breiman, R. F., Feikin, D. R., Klugman, K. P., Olsen, S. J., Gessner, B. D., Wright, P. F., Rudan, I., Broor, S., Simoes, E. A. and Campbell, H. (2011). Global burden of respiratory infections due to seasonal influenza in young children: a systematic review and meta-analysis. *Lancet,* 378(9807), 1917-1930.

Narhi, L. O., Kita, Y. and Arakawa, T. (1989). Hydrophobic interaction chromatography in alkaline pH. *Analytical Biochemistry,* 182(2), 266-270.

Nestola, P., Peixoto, C., Silva, R., Alves, P. M., Mota, J. P. B. and Carrondo, M. J. T. (2015). Improved Virus Purification Processes for Vaccines and Gene Therapy. *Biotechnology and Bioengineering,* 112(5), 843-857.

Nichol, K. L. (2008). Efficacy and effectiveness of influenza vaccination. *Vaccine,* 26 Suppl 4, D17-22.

Nissom, P. M. (2007). Specific detection of residual CHO host cell DNA by real-time PCR. *Biologicals,* 35(3), 211-215.

O'Farrell, P. (1996). Hydrophobic Interaction Chromatography. In S. Doonan (Ed.), *Protein Purification Protocols* (pp. 151-155). Totowa, NJ: Humana Press.

Ohlendieck, K. (1996). *Protein Purification Protocols - Removal of Detergent from Protein Fractions*. Totowa, NJ, USA: Humana Press, pp. 305-312.

Opitz, L. (2010). *Developement and characterization of affinity and pseudo-affinity based methods for cell culture-derived influenza virus capturing.* (PhD), Otto-von-Guericke University Magdeburg, Magdeburg, Germany.

Opitz, L., Hohlweg, J., Reichl, U. and Wolff, M. W. (2009a). Purification of cell culture-derived influenza virus A/Puerto Rico/8/34 by membrane-based immobilized metal affinity chromatography. *Journal of Virological Methods,* 161(2), 312-316.

Opitz, L., Lehmann, S., Reichl, U. and Wolff, M. W. (2009b). Sulfated membrane adsorbers for economic pseudo-affinity capture of influenza virus particles. *Biotechnology & Bioengineering,* 103(6), 1144-1154.

Opitz, L., Salaklang, J., Buttner, H., Reichl, U. and Wolff, M. W. (2007). Lectin-affinity chromatography for downstream processing of MDCK cell culture derived human influenza A viruses. *Vaccine,* 25(5), 939-947.

Opitz, L., Zimmermann, A., Lehmann, S., Genzel, Y., Lubben, H., Reichl, U. and Wolff, M. W. (2008). Capture of cell culture-derived influenza virus by lectins: Strain independent, but host cell dependent. *Journal of Virological Methods,* 154(1-2), 61-68.

Orr, V., Zhong, L. Y., Moo-Young, M. and Chou, C. P. (2013). Recent advances in bioprocessing application of membrane chromatography. *Biotechnology Advances,* 31(4), 450-465.

Oscarsson, S. (1995). Influence of Salts on Protein Interactions at Interfaces of Amphilic Polymers and Adsorbants. *Journal of Chromatography B-Biomedical Applications,* 666(1), 21-31.

Osterholm, M. T., Kelley, N. S., Sommer, A. and Belongia, E. A. (2012). Efficacy and effectiveness of influenza vaccines: a systematic review and meta-analysis. *Lancet Infect Dis,* 12(1), 36-44.

Palache, A., Abelin, A., Hollingsworth, R., Cracknell, W., Jacobs, C., Tsai, T. and Barbosa, P. (2017). Survey of distribution of seasonal influenza vaccine doses in 201 countries (2004-2015): The 2003 World Health Assembly resolution on seasonal influenza vaccination coverage and the 2009 influenza pandemic have had very little impact on improving influenza control and pandemic preparedness. *Vaccine,* 35(36), 4681-4686.

Palache, A. M., Brands, R. and Van Scharrenburg, G. J. M. (1997). Immunogenicity and reactogenicity of influenza subunit vaccines produced in MDCK cells or fertilized chicken eggs. *Journal of Infectious Diseases,* 176(SUPPL. 1), S20-S23.

PEI. (2018). Präpandemische Influenzaimpfstoffe. Retrieved from https://www.pei.de/DE/arzneimittel/impfstoff-impfstoffe-fuer-den-menschen/influenza-grippe/praepandemische-influenzaimpfstoffe/praepandemische-influenzaimpfstoffe-node.html. Access Date: 23.07.2019.

PEI. (2019). Zugelassene Impfstoffe für die Saison 2019/2020 Retrieved from https://www.pei.de/DE/arzneimittel/impfstoff-impfstoffe-fuer-den-menschen/influenza-grippe/influenza-grippe-node.html. Access Date: 23.07.2019.

Perdue, M. L., Arnold, F., Li, S., Donabedian, A., Cioce, V., Warf, T. and Huebner, R. (2011). The future of cell culture-based influenza vaccine production. *Expert Review of Vaccines,* 10(8), 1183-1194.

Pérez Rubio, A. and Eiros, J. M. (2018). Cell culture-derived flu vaccine: Present and future. *Human Vaccines & Immunotherapeutics,* 14(8), 1874-1882.

Perrin, P. and Morgeaux, S. (1995). Inactivation of DNA by β-propiolactone. *Biologicals,* 23(3), 207-211.

Petricciani, J. C. and Regan, P. J. (1987). Risk of neoplastic transformation from cellular DNA: calculations using the oncogene model. *Developments in biological standardization,* 68, 43-49.

Peuker, A. (2013). *Development of a flow-through downstream process for influenza vaccines.* (Master), Max Planck Institute for Dynamics of Complex Technical Systems, Lausitz University of Applied Sciences, Senftenberg, Germany.

Pillet, S., Aubin, E., Trepanier, S., Bussiere, D., Dargis, M., Poulin, J. F., Yassine-Diab, B., Ward, B. J. and Landry, N. (2016). A plant-derived quadrivalent virus like particle influenza vaccine induces cross-reactive antibody and T cell response in healthy adults. *Clin Immunol,* 168, 72-87.

Porath, J., Sundberg, L., Fornstedt, N. and Olsson, I. (1973). Salting-out in amphiphilic gels as a new approach to hydrophobic adsorption. *Nature,* 245(5426), 465-466.

Präve, P., Faust, U., Sittig, W. and Sukatsch, D. A. (1994). *Handbook of Biotechnolgy*. Munich, Germany: Oldenbourg, pp. 479-928.

Qian, Z., Shen, Q., Yang, X., Qiu, Y. and Zhang, W. (2015). The Role of Extracellular Vesicles: An Epigenetic View of the Cancer Microenvironment. *Biomed Res Int,* 2015, 649161.

Rabenstein, D. L. (2002). Heparin and heparan sulfate: structure and function. *Nat Prod Rep,* 19(3), 312-331.

Rajao, D. S. and Perez, D. R. (2018). Universal Vaccines and Vaccine Platforms to Protect against Influenza Viruses in Humans and Agriculture. *Front Microbiol,* 9, 123.

Rao, S. S., Gomez, P., Mascola, J. R., Dang, V., Krivulka, G. R., Yu, F., Lord, C. I., Shen, L., Bailer, R., Nabel, G. J. and Letvin, N. L. (2006). Comparative evaluation of three different intramuscular delivery methods for DNA immunization in a nonhuman primate animal model. *Vaccine,* 24(3), 367-373.

Ray, R., Dos Santos, G., Buck, P. O., Claeys, C., Matias, G., Innis, B. L. and Bekkat-Berkani, R. (2017). A review of the value of quadrivalent influenza vaccines and their potential contribution to influenza control. *Hum Vaccin Immunother,* 13(7), 1640-1652.

Reimer, C. B., Baker, R. S., Newlin, T. E. and Havens, M. L. (1966). Influenza Virus Purification with the Zonal Ultracentrifuge. *Science,* 152(3727).

Reimer, C. B., Baker, R. S., Van Frank, R. M., Newlin, T. E., Cline, G. B. and Anderson, N. G. (1967). Purification of large quantities of influenza virus by density gradient centrifugation. *Journal of virology,* 1(6), 1207-1216.

Research Starters: Worldwide Deaths in World War II. (2021). Retrieved from https://de.statista.com/statistik/daten/studie/1055110/umfrage/zahl-der-toten-nach-staaten-im-zweiten-weltkrieg/#professional. Access Date: 02.04.2021.

Riordan, W. T., Heilmann, S. M., Brorson, K., Seshadri, K. and Etzel, M. R. (2009a). Salt Tolerant Membrane Adsorbers for Robust Impurity Clearance. *Biotechnology Progress,* 25(6), 1695-1702.

Riordan, W. T., Heilmann, S. M., Brorson, K., Seshadri, K., He, Y. and Etzel, M. (2009b). Design of Salt-Tolerant Membrane Adsorbers for Viral Clearance. *Biotechnology and Bioengineering,* 103(5), 920-929.

Roberts, J. J. and Warwick, G. P. (1963). The reaction of Beta-propiolactone with guanosine, deoxyguanylic acid and RNA. *Biochem Pharmacol,* 12, 1441-1442.

Saade, F. and Petrovsky, N. (2012). Technologies for enhanced efficacy of DNA vaccines. *Expert Rev Vaccines,* 11(2), 189-209.

Sabbaghi, A., Miri, S. M., Keshavarz, M., Zargar, M. and Ghaemi, A. (2019). Inactivation methods for whole influenza vaccine production. *Rev Med Virol,* 29(6), e2074.

Sakoda, Y., Okamatsu, M., Isoda, N., Yamamoto, N., Ozaki, K., Umeda, Y., Aoyama, S. and Kida, H. (2012). Purification of human and avian influenza viruses using cellulose sulfate ester (Cellufine Sulfate) in the process of vaccine production. *Microbiol Immunol*, 56(7), 490-495.

Saletti, G., Gerlach, T. and Rimmelzwaan, G. F. (2018). Influenza vaccines: 'tailor-made' or 'one fits all'. *Curr Opin Immunol*, 53, 102-110.

Sartorius Stedim Biotech. (2011). Manufacturer's operating instructions: Sartobind STIC PA, 4mm bed height. Retrieved from https://www.Sartorius.com. Access Date: 03.04.2017.

Sastry, L., Xu, Y., Cooper, R., Pollok, K. and Cornetta, K. (2004). Evaluation of plasmid DNA removal from lentiviral vectors by benzonase treatment. *Human Gene Therapy*, 15(2), 221-226.

Schild, G. C., Oxford, J. S., de Jong, J. C. and Webster, R. G. (1983). Evidence for host-cell selection of influenza virus antigenic variants. *Nature*, 303(5919), 706-709.

Sedlackova, T., Repiska, G., Celec, P., Szemes, T. and Minarik, G. (2013). Fragmentation of DNA affects the accuracy of the DNA quantitation by the commonly used methods. *Biological Procedures Online*, 15, 5.

Senczuk, A. M., Klinke, R., Arakawa, T., Vedantham, G. and Yigzaw, Y. (2009). Hydrophobic Interaction Chromatography in Dual Salt System Increases Protein Binding Capacity. *Biotechnology and Bioengineering*, 103(5), 930-935.

Sheng-Fowler, L., Lewis, A. M., Jr. and Peden, K. (2009). Issues associated with residual cell-substrate DNA in viral vaccines. *Biologicals*, 37(3), 190-195.

Sheng, L., Cai, F., Zhu, Y., Pal, A., Athanasiou, M., Orrison, B., Blair, D. G., Hughes, S. H., Coffin, J. M., Lewis, A. M. and Peden, K. (2008). Oncogenicity of DNA in vivo: Tumor induction with expression plasmids for activated H-ras and c-myc. *Biologicals*, 36(3), 184-197.

Shukla, A. A., Etzel, M. R. and Gadam, S. (2006). *Process Scale Bioseparations for the Biopharmaceutical Industry*. New York, USA: CRC Press, pp. 179-522.

Sikorski, A. F. (1988). Interaction of Spectrin with Hydrophobic Agaroses. *Acta Biochimica Polonica*, 35(1), 19-27.

Singh, S. K. and Nema, S. (2010). Freezing and thawing of protein solutions. *Formulation and Process Development Strategies for Manufacturing Biopharmaceuticals*, 625-675.

Skowronski, D. M., Janjua, N. Z., De Serres, G., Sabaiduc, S., Eshaghi, A., Dickinson, J. A., Fonseca, K., Winter, A. L., Gubbay, J. B., Krajden, M., Petric, M., Charest, H., Bastien, N., Kwindt, T. L., Mahmud, S. M., Van Caeseele, P. and Li, Y. (2014). Low 2012-13 influenza vaccine effectiveness associated with mutation in the egg-adapted H3N2 vaccine strain not antigenic drift in circulating viruses. *PloS one*, 9(3), e92153.

Solomaier, T. (2013a). *Prozessentwicklung zur Aufreinigung von Influenzaviren.* (internship report), Max Planck Institute for Dynamics of Complex Magdeburg, Germany.

Solomaier, T. (2013b). *Prozessentwicklung zur Aufreinigung von Influenzaviren für die Impfstoffproduktion.* (Bachelor thesis), Otto-von-Guericke University Magdeburg, Magdeburg, Germany.

Sparrow, E., Wood, J. G., Chadwick, C., Newall, A. T., Torvaldsen, S., Moen, A. and Torelli, G. (2021). Global production capacity of seasonal and pandemic influenza vaccines in 2019. *Vaccine*, 39(3), 512-520.

Spektrum. (2020). Hofmeister-Serie. *Lexikon der Biochemie.* Retrieved from https://www.spektrum.de/lexikon/biochemie/hofmeister-serie/2892. Access Date: 06.02.2020.

Svetlikova, S. B., Pospelov, V. A. and Vorob'ev, V. I. (1979). Nucleosome packing in chromatin as revealed by nuclease digestion. *Nucleic Acids Research*, 6(1), 399-418.

Sviben, D., Forcic, D., Ivancic-Jelecki, J., Halassy, B. and Brgles, M. (2017). Recovery of infective virus particles in ion-exchange and hydrophobic interaction monolith chromatography is influenced by particle charge and total-to-infective particle ratio. *Journal of Chromatography B-Analytical Technologies in the Biomedical and Life Sciences,* 1054, 10-19.

Sycheva, A. L., Pogorelyy, M. V., Komech, E. A., Minervina, A. A., Zvyagin, I. V., Staroverov, D. B., Chudakov, D. M., Lebedev, Y. B. and Mamedov, I. Z. (2018). Quantitative profiling reveals minor changes of T cell receptor repertoire in response to subunit inactivated influenza vaccine. *Vaccine,* 36(12), 1599-1605.

Sylte, M. J. and Suarez, D. L. (2009). *Vaccines for Pandemic Influenza - Influenza Neuraminidase as a Vaccine Antigen*. Berlin, Heidelberg, Germany: Springer Berlin Heidelberg, pp. 227-241.

Szepesy, L. and Horváth, C. (1988). Specific salt effects in hydrophobic interaction chromatography of proteins. *Chromatographia,* 26(1), 13-18.

Szepesy, L. and Rippel, G. (1992). Comparison and evaluation of HIC columns of different hydrophobicity. *Chromatographia,* 34(5), 391-397.

Taubenberger, J. K. and Morens, D. M. (2006). 1918 Influenza: the mother of all pandemics. *Emerg Infect Dis,* 12(1), 15-22.

Taubenberger, J. K. and Morens, D. M. (2009). Pandemic influenza--including a risk assessment of H5N1. *Rev Sci Tech,* 28(1), 187-202.

Thacker, E. and Janke, B. (2008). Swine influenza virus: zoonotic potential and vaccination strategies for the control of avian and swine influenzas. *The Journal of infectious diseases,* 197 Suppl 1, S19-24.

Thielen, B. K., Friedlander, H., Bistodeau, S., Shu, B., Lynch, B., Martin, K., Bye, E., Como-Sabetti, K., Boxrud, D., Strain, A. K., Chaves, S. S., Steffens, A., Fowlkes, A. L., Lindstrom, S. and Lynfield, R. (2018). Detection of Influenza C Viruses Among Outpatients and Patients Hospitalized for Severe Acute Respiratory Infection, Minnesota, 2013-2016. *Clinical infectious diseases : an official publication of the Infectious Diseases Society of America,* 66(7), 1092-1098.

To, B. C. S. and Lenhoff, A. M. (2007). Hydrophobic interaction chromatography of proteins I. The effects of protein and adsorbent properties on retention and recovery. *Journal of Chromatography A,* 1141(2), 191-205.

Transfiguracion, J., Jorio, H., Meghrous, J., Jacob, D. and Kamen, A. (2007). High yield purification of functional baculovirus vectors by size exclusion chromatography. *Journal of Virological Methods,* 142(1-2), 21-28.

Tree, J. A., Richardson, C., Fooks, A. R., Clegg, J. C. and Looby, D. (2001). Comparison of large-scale mammalian cell culture systems with egg culture for the production of influenza virus A vaccine strains. *Vaccine,* 19(25-26), 3444-3450.

Tsanev, R. G., Russev, G., Pashev, I. and Zlatanova, J. S. (1992). *Replication and Transcription of Chromatin*. New York, USA: Taylor & Francis, pp. 8-221.

Tseng, Y.-F., Weng, T.-C., Lai, C.-C., Chen, P.-L., Lee, M.-S. and Hu, A. Y.-C. (2018). A fast and efficient purification platform for cell-based influenza viruses by flow-through chromatography. *Vaccine,* 36(22), 3146-3152.

Tsumoto, K., Ejima, D., Senczuk, A. M., Kita, Y. and Arakawa, T. (2007). Effects of salts on protein-surface interactions: Applications for column chromatography. *Journal of pharmaceutical sciences,* 96(7), 1677-1690.

Uittenbogaard, J. P., Zomer, B., Hoogerhout, P. and Metz, B. (2011). Reactions of beta-propiolactone with nucleobase analogues, nucleosides, and peptides: implications for the inactivation of viruses. *The Journal of biological chemistry,* 286(42), 36198-36214.

Ulmer, J. B., Mason, P. W., Geall, A. and Mandl, C. W. (2012). RNA-based vaccines. *Vaccine,* 30(30), 4414-4418.

Utsunomiya, H., Ichinose, M., Tsujimoto, K., Katsuyama, Y., Yamasaki, H., Koyama, A. H., Ejima, D. and Arakawa, T. (2009). Co-operative thermal inactivation of herpes simplex virus and influenza virus by arginine and NaCl. *International Journal of Pharmaceutics,* 366(1-2), 99-102.

Vijaykrishna, D., Holmes, E. C., Joseph, U., Fourment, M., Su, Y. C., Halpin, R., Lee, R. T., Deng, Y. M., Gunalan, V., Lin, X., Stockwell, T. B., Fedorova, N. B., Zhou, B., Spirason, N., Kuhnert, D., Boskova, V., Stadler, T., Costa, A. M., Dwyer, D. E., Huang, Q. S., Jennings, L. C., Rawlinson, W., Sullivan, S. G., Hurt, A. C., Maurer-Stroh, S., Wentworth, D. E., Smith, G. J. and Barr, I. G. (2015). The contrasting phylodynamics of human influenza B viruses. *Elife,* 4, e05055.

Voeten, J. T. M., Brands, R., Palache, A. M., van Scharrenburg, G. J. M., Rimmelzwaan, G. F., Osterhaus, A. D. M. E. and Claas, E. C. J. (1999). Characterization of high-growth reassortant influenza A viruses generated in MDCK cells cultured in serum-free medium. *Vaccine,* 17(15-16), 1942-1950.

Vyas, G. N., Stoddart, C. A., Killian, M. S., Brennan, T. V., Goldberg, T., Ziman, A. and Bryson, Y. (2012). Derivation of non-infectious envelope proteins from virions isolated from plasma negative for HIV antibodies. *Biologicals,* 40(1), 15-20.

Wang, W. (2000). Lyophilization and development of solid protein pharmaceuticals. *Int J Pharm,* 203(1-2), 1-60.

Weigel, T., Soliman, R., Wolff, M. W. and Reichl, U. (2019). Hydrophobic-interaction chromatography for purification of influenza A and B virus. *Journal of Chromatography B,* 1117, 103-117.

Weigel, T., Solomaier, T., Peuker, A., Pathapati, T., Wolff, M. W. and Reichl, U. (2014). A flow-through chromatography process for influenza A and B virus purification. *Journal of Virological Methods,* 207(0), 45-53.

Weigel, T., Solomaier, T., Wehmeyer, S., Peuker, A., Wolff, M. W. and Reichl, U. (2016). A membrane-based purification process for cell culture-derived influenza A virus. *Journal of Biotechnology,* 220, 12-20.

WHO. (2021). Influenza (seasonal) fact sheet. Retrieved from https://www.who.int/news-room/fact-sheets/detail/influenza-(seasonal). Access Date: 07.03.2021.

Wickramasinghe, S. R., Kalbfuss, B., Zimmermann, A., Thom, V. and Reichl, U. (2005). Tangential flow microfiltration and ultrafiltration for human influenza A virus concentration and purification. *Biotechnology and Bioengineering,* 92(2), 199-208.

Wilks, S., de Graaf, M., Smith, D. J. and Burke, D. F. (2012). A review of influenza haemagglutinin receptor binding as it relates to pandemic properties. *Vaccine,* 30(29), 4369-4376.

Wolf, J. J., Wong, L. and Wang, F. (2007). Application of PCR technology in vaccine product development. *Expert Review of Vaccines,* 6(4), 547-558.

Wolff M. W., R. U., Opitz L. (2008), *Method for the Preparation of Sulfated Cellulose Membranes and Sulfated Cellulose Membranes.*, WO 002008125361 A1.

Wolff, M. W. and Reichl, U. (2008). Downstream processing: From egg to cell culture-derived influenza virus particles. *Chemical Engineering & Technology,* 31(6), 846-857.

Wolff, M. W., Siewert, C., Hansen, S. P., Faber, R. and Reichl, U. (2010). Purification of Cell Culture-Derived Modified Vaccinia Ankara Virus by Pseudo-Affinity Membrane Adsorbers and Hydrophobic Interaction Chromatography. *Biotechnology and Bioengineering,* 107(2), 312-320.

Wong, S. S. and Webby, R. J. (2013a). Traditional and new influenza vaccines. *Clinical microbiology reviews,* 26(3), 476-492.

Wong, S. S. and Webby, R. J. (2013b). Traditional and new influenza vaccines. *Clinical microbiology reviews,* 26(3), 476-492.

Wood, J. M., Schild, G. C., Newman, R. W. and Seagroatt, V. (1977). An improved single-radial-immunodiffusion technique for the assay of influenza hemagglutinin antigen: application for potency determinations of inactivated whole virus and subunit vaccines. *Journal of Biological Standardization,* 5, 237-247.

World Health Organization. (1995). Cell culture as a substrate for the production of influenza vaccines: Memorandum from a WHO meeting: (Geneva, Switzerland on February 16, 1995). *Bulletin of the World Health Organization,* 73(4), 431-435.

Wu, S. L. and Karger, B. L. (1996). *Hydrophobic interaction chromatography of proteins*. San Diego: Academic Press Inc, pp. 27-47.

Zhang, Y. J. and Cremer, P. S. (2006). Interactions between macromolecules and ions: the Hofmeister series. *Current Opinion in Chemical Biology,* 10(6), 658-663.

Zhilinskaya, I. N., el-Saed, L. H., Ivanova, N. A., Golubev, D. E. and Sokolov, N. N. (1972). Isolation of A2-Singapore-57 influenza virus V and S antigens by isoelectric focusing. *Acta Virol,* 16(5), 436-439.

Zolodz, M. D., Herberg, J. T., Narepekha, H. E., Raleigh, E., Farber, M. R., Dufield, R. L. and Boyle, D. M. (2010). Separation by hydrophobic interaction chromatography and structural determination by mass spectrometry of mannosylated glycoforms of a recombinant transferrin-exendin-4 fusion protein from yeast. *Journal of Chromatography A,* 1217(2), 225-234.

8 Relevant first author publications

1) Weigel, T., Solomaier, T., Peuker, A., Pathapati, T., Wolff, M.W., Reichl, U., (2014). A flow-through chromatography process for influenza A and B virus purification. Journal of Virological Methods 207, 45–53.

2) Weigel, T., Solomaier, T., Wehmeyer, S., Peuker, A., Wolff, M.W., Reichl, U., (2016). A membrane-based purification process for cell culture-derived influenza A virus. Journal of Biotechnology 220, 12–20.

3) Weigel, T., Soliman, R., Wolff, M.W., Reichl, U., (2019). Hydrophobic-interaction chromatography for purification of influenza A and B virus. Journal of Chromatography B, 1117, 103–117.

9 Annex

9.1 Additional results

9.1.1 Process chromatograms

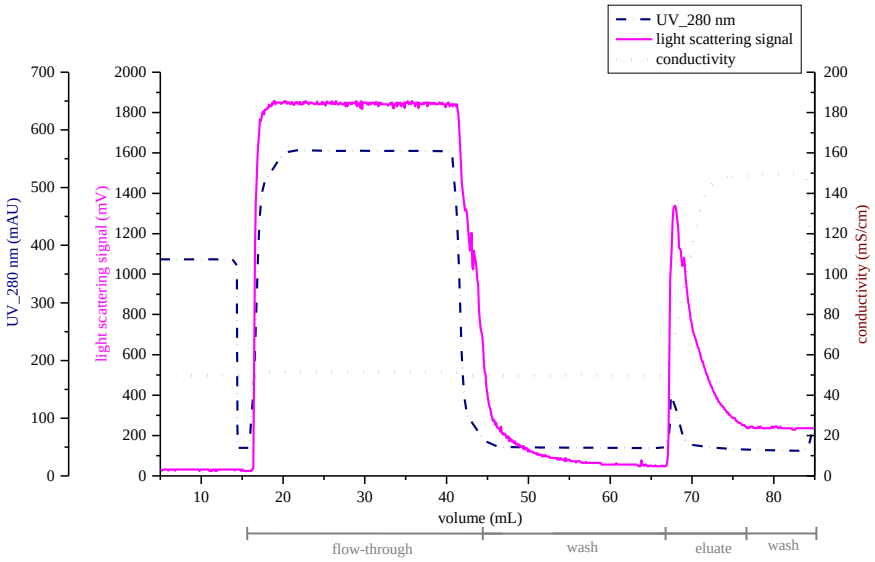

Figure 33: Chromatogram of a flow-through process: step 1 (AEC: Capto Q; representative). Shown are the UV-inline signal, the inline signal of the static light scattering detector and the conductivity-inline signal. The analyzed pooled fractions are shown at the bottom. Only the flow-through and the eluate fractions were incorporated into the process balance. Product fraction: flow-through fraction. IV strain: A/PR. For more data refer to the corresponding section 4.1.3.

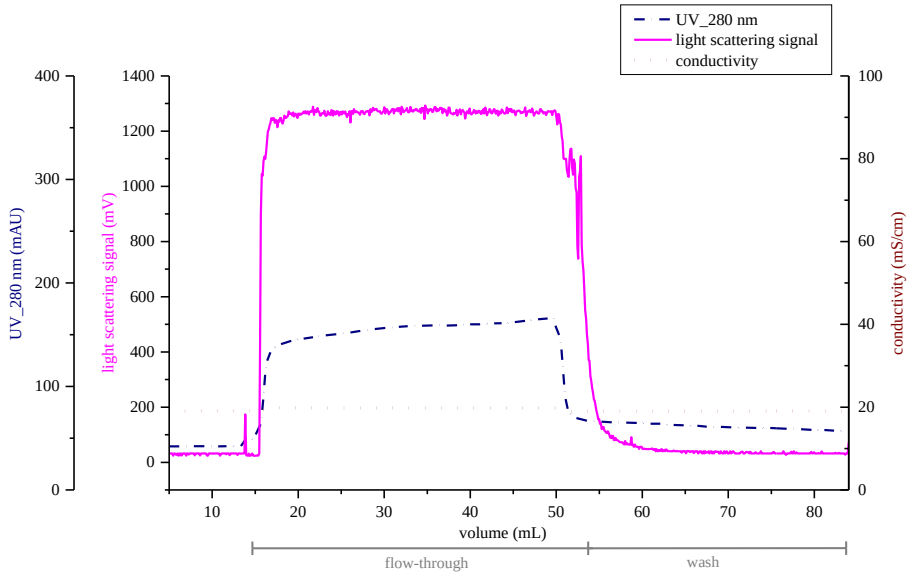

Figure 34: Chromatogram of a flow-through process: step 2 (LCC: Capto Core; representative). Shown are the UV-inline signal, the inline signal of the static light scattering detector and the conductivity-inline signal. The analyzed pooled fractions are shown at the bottom. Only the flow-through and the eluate fractions were incorporated into the process balance. Product fraction: flow-through fraction. IV strain: A/PR. For more data refer to the corresponding section 4.1.3.

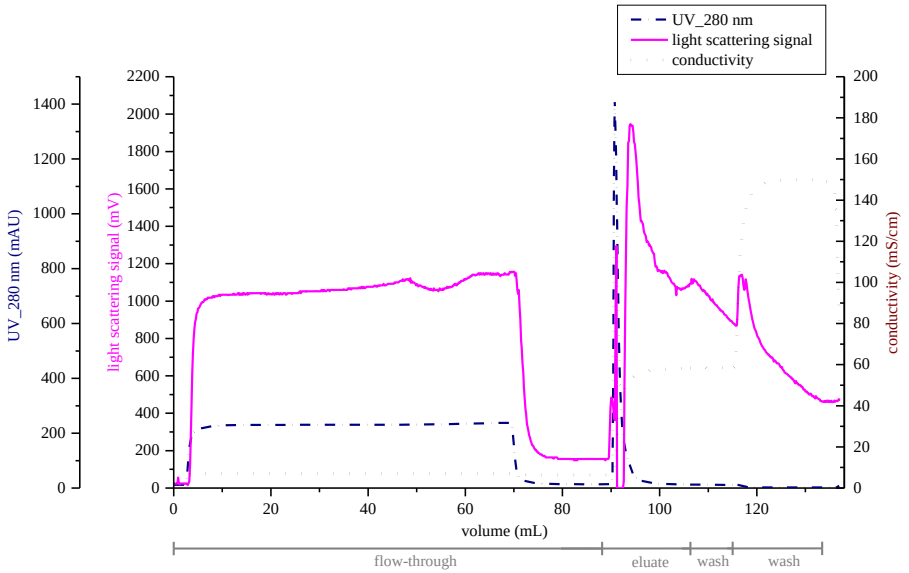

Figure 35: Chromatogram of a membrane-based process: step 1 (SCMA; capture step; representative). Shown are the UV-inline signal, the inline signal of the static light scattering detector and the conductivity-inline signal. The analyzed pooled fractions are shown at the bottom. Only the flow-through and the eluate fractions were incorporated into the process balance. Product fraction: eluate fraction. IV strain: A/PR. For more data refer to the corresponding section 4.2.3.

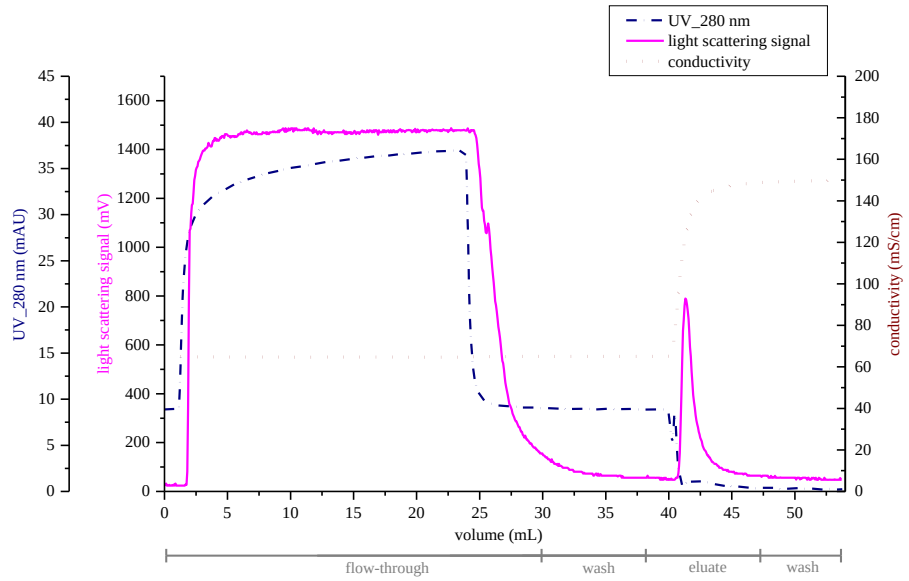

Figure 36: Chromatogram of a membrane-based process: step 2 (STMA; flow-through step; representative). Shown are the UV-inline signal, the inline signal of the static light scattering detector and the conductivity-inline signal. The analyzed pooled fractions are shown at the bottom. Only the flow-through and the eluate fractions were incorporated into the process balance. Product fraction: flow-through fraction. IV strain: A/PR. For more data refer to the corresponding section 4.2.3.

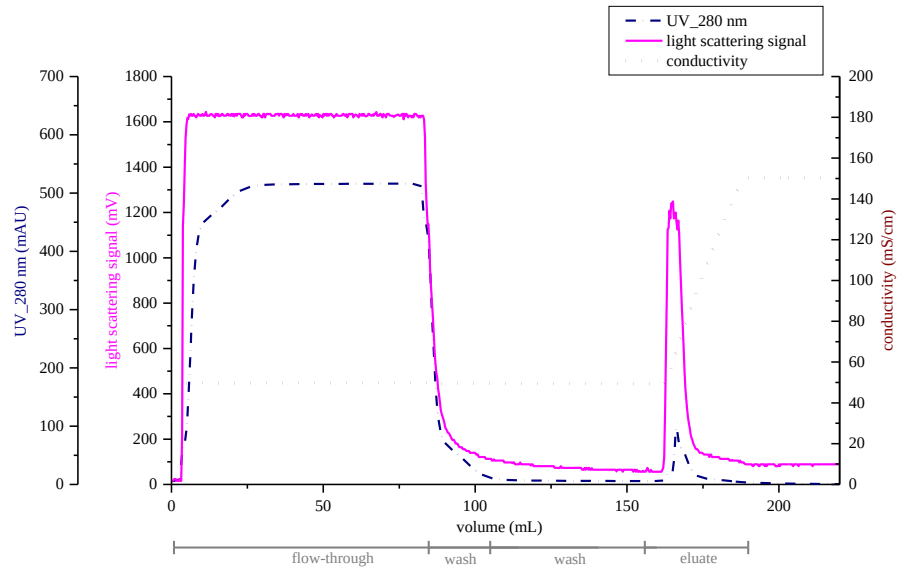

Figure 37: Chromatogram of an orthogonal process: step 1 (AEC: Capto Q; flow-through step; representative). Shown are the UV-inline signal, the inline signal of the static light scattering detector and the conductivity-inline signal. The analyzed pooled fractions are shown at the bottom. Only the flow-through and the eluate fractions were incorporated into the process balance. Product fraction: flow-through fraction. IV strain: A/PR. For more data refer to the corresponding section 4.3.3.

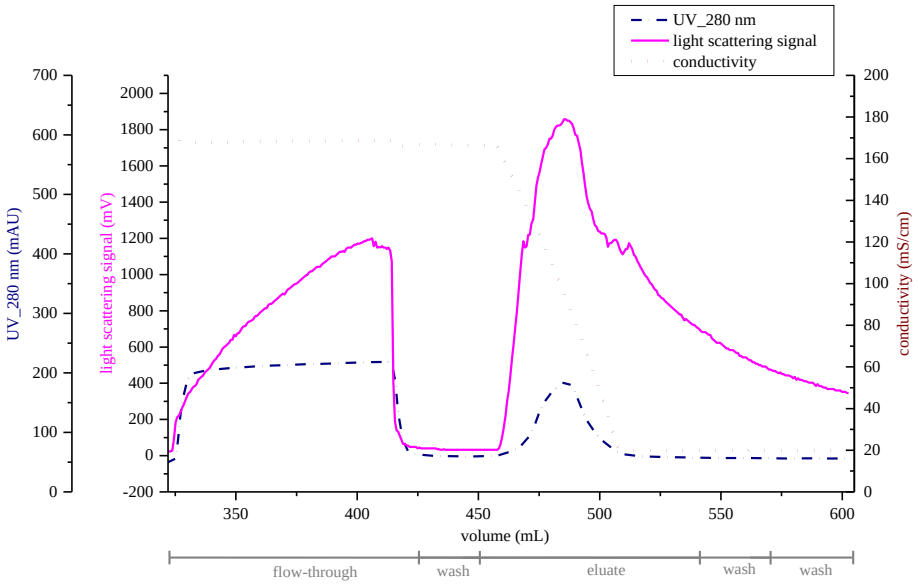

Figure 38: Chromatogram of an orthogonal process: step 2 (HIC: PPG; capture step; representative). Shown are the UV-inline signal, the inline signal of the static light scattering detector and the conductivity-inline signal. The analyzed pooled fractions are shown at the bottom. Only the flow-through and the eluate fractions were incorporated into the process balance. Product fraction: eluate fraction. IV strain: A/PR. For more data refer to the corresponding section 4.3.3.

9.1.2 Membrane-based process: Selection of process conditions

Table 22: The two-step membrane chromatography purification process with 100 mM Na_2HPO_4/NaH_2PO_4 instead of 150 mM Na_2HPO_4/NaH_2PO_4 for the STMA-step. All other process conditions are according to section 3.4.3. Shown are the step and final recoveries (%) for the product stream. The conditioning step represents the addition of buffer to adjust the Na_2HPO_4/NaH_2PO_4 concentration. IV strain: A/PR. Virus and DNA recoveries based on HA and PicoGreen® assay, respectively.

Steps	Step recoveries [%]		
	Virus	DNA	Total Protein
SCMA	86.8	2.4	29.8
Conditioning	78.1	106.0	96.3
STMA	83.9	15.0	82.5
	Final recovery [%]		
	56.8	0.39	23.6

9.1.3 Parameter estimation for mean particle size analysis

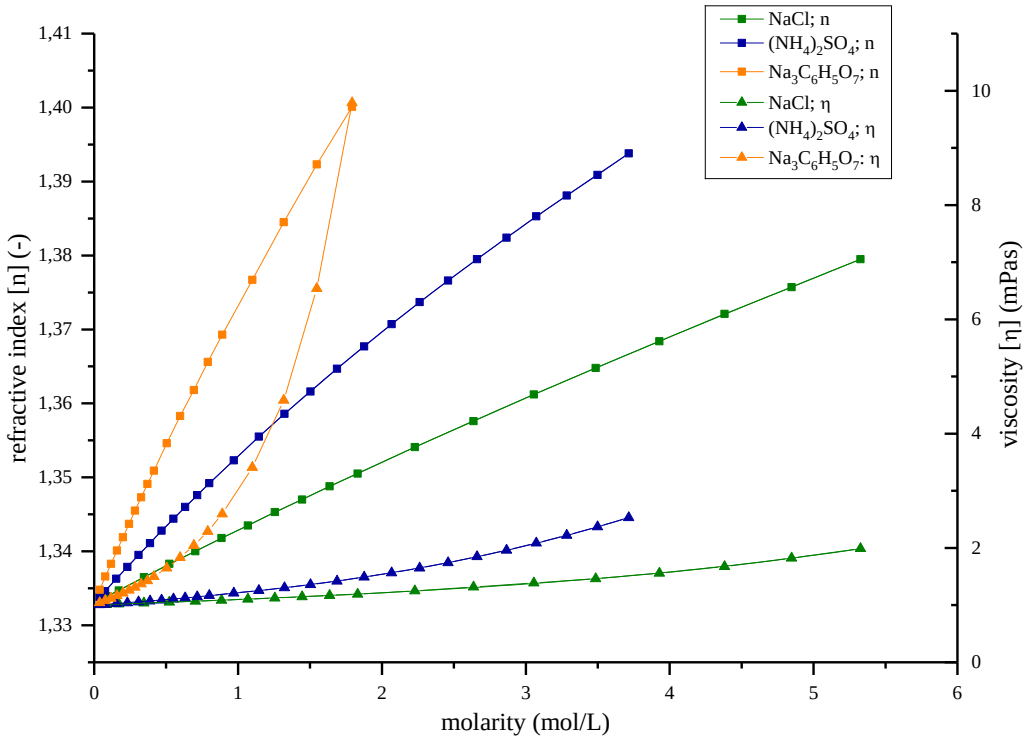

Figure 39: Approximation of refractive indexes and viscosities for different salts using reference data for salt-water-systems (Lide et al., 2009) and a polynomial fitting function. Data was used for setting the measurement parameters for the mean particle size analysis (section 3.6.7).

9.1.4 Proof-of-principle for "HIC – 96-well-plate screening for conditions" of section 4.3.2

A)

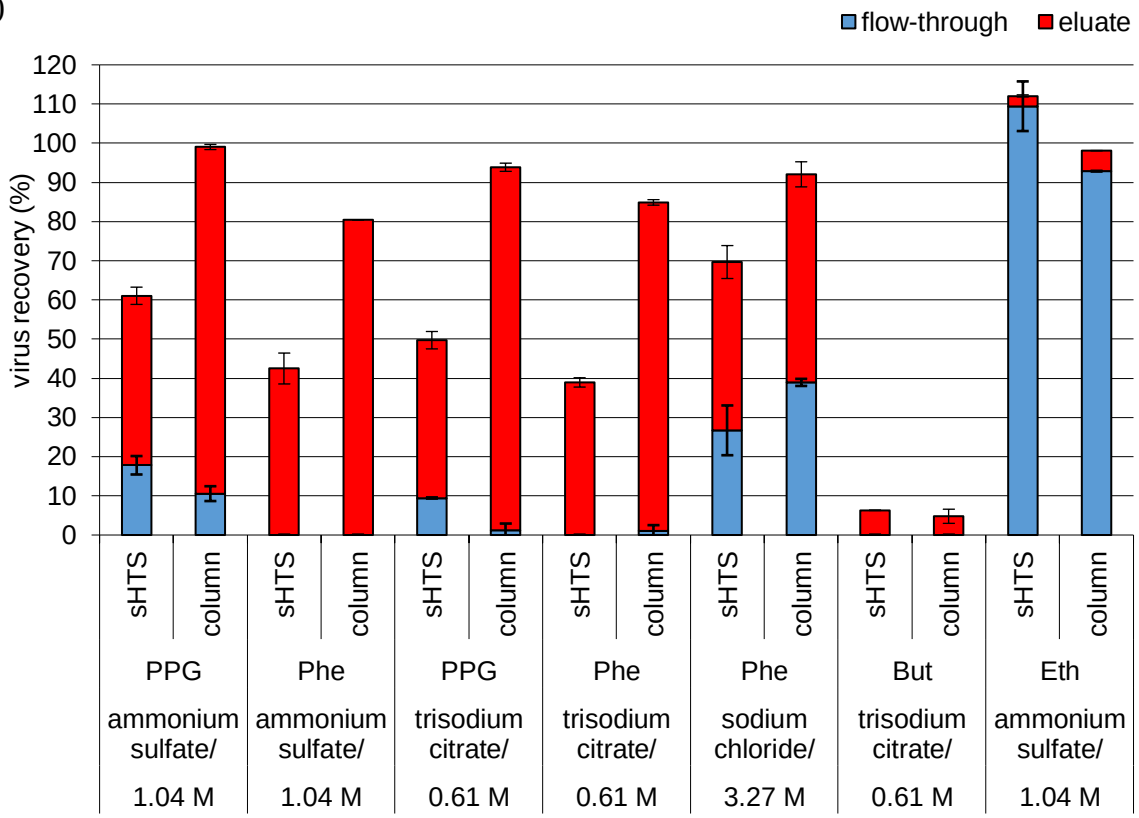

B)

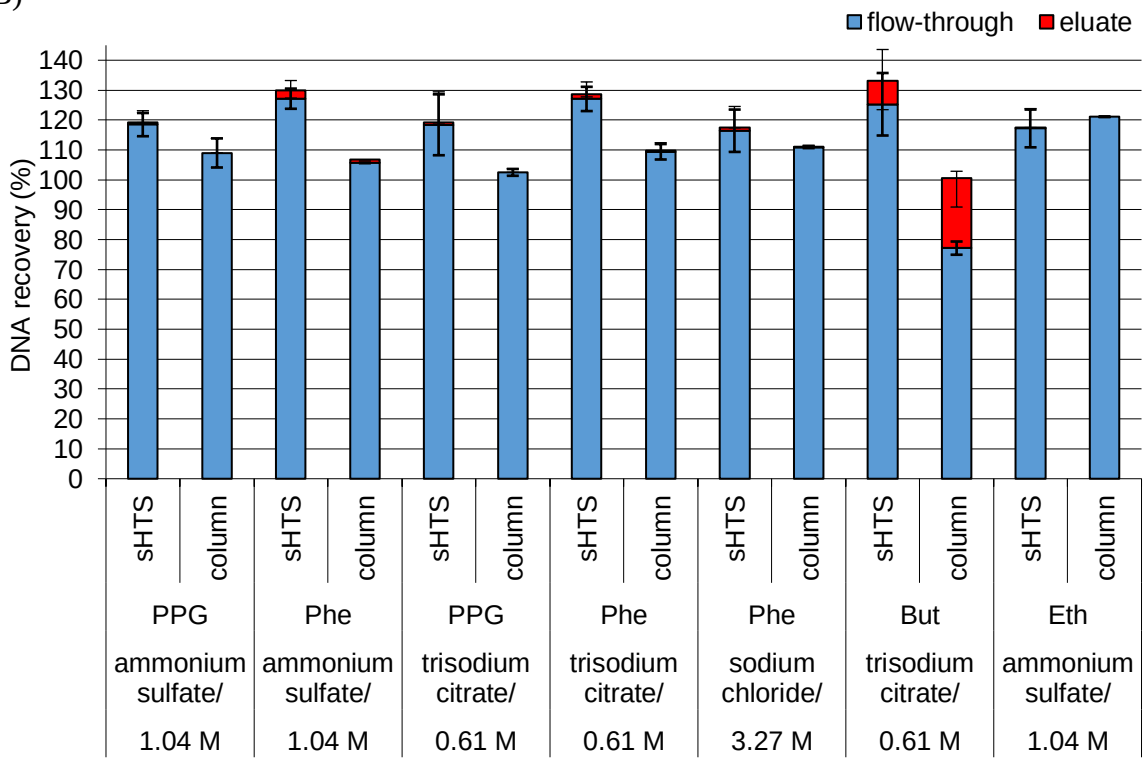

Figure 40 (A, B): Comparison of selected semi-high-throughput screening results (from Figure 23 – Figure 26) with chromatography results (preparative scale) at similar conditions (HIC resin/salting-out salt in the loading buffer/salting-out salt concentration) for each set. Shown are virus (A) and DNA (B) recoveries of flow-through and eluate fractions. Chromatography was performed with prepacked 1 mL chromatography columns (#21398, Tosoh, Japan) at 1 mL/min. Samples were conditioned 1:2 to achieve salt concentration of the loading buffer. Elutions were performed with 150 mM sodium chloride (NaCl), 20 mM Tris, pH 7.4 with a linear gradient. Samples were dialyzed according to the samples of the semi-high-throughput screening. Legend: resins: Eth: ether group, PPG: polypropylene glycol group, Phe: phenyl group, But: butyl group. Mean and standard deviation of technical replicates, n=2; except for: "column/But/trisodium citrate/0.61M", n=3. The experiments "column/Phe/ammonium sulfate/1.04M" and "column/Eth/ammonium sulfate/1.04M" were performed in simplex.

10 Index

10.1 Index of figures

10.2 Index of tables